www.oftalmoloji.org

E-ISSN: 2149-8709

TURKISH JOURNAL OF OPHTHALMOLOGY

TURKISH JOURNAL OF OPHTHALMOLOGY TJO

September
October 2023
53 Volume
Issue 5

galenos

TURKISH JOURNAL OF OPHTHALMOLOGY

TJO

www.oftalmoloji.org

Publishing House
Molla Gürani Mah. Kaçamak Sokak No: 21,
34093 Fındıkzade-İstanbul-Türkiye
Publisher Certificate Number: 14521
Phone: +90 (530) 177 30 97
E-mail: info@galenos.com.tr
Online Publishing Date: October 2023
International scientific journal published bimonthly.
E-ISSN: 2149-8709

The Turkish Journal of Ophthalmology is an official journal of the Turkish Ophthalmological Association.

On Behalf of the Turkish Ophthalmological Association Owner

Ziya KAPRAN
Private Practice, İstanbul, Türkiye

TURKISH JOURNAL OF OPHTHALMOLOGY

TJO

www.oftalmoloji.org

ABOUT US

The Turkish Journal of Ophthalmology is the only scientific periodical publication of the Turkish Ophthalmological Association and has been published since January 1929. The Journal was first published in Turkish and French in an effort to bring Turkish ophthalmological research to the international scientific audience. Despite temporary interruptions in publication over the intervening decades due to various challenges, the Turkish Journal of Ophthalmology has been published continually from 1971 to the present.

The Journal currently publishes articles in Turkish and English after an independent, unbiased double-blind peer review process. Issues are published electronically six times a year, with occasional special issues.

The aim of the Turkish Journal of Ophthalmology is to publish original research articles of the highest scientific and clinical value at an international level. It also features review articles, case reports, editorial commentary, letters to the editor, educational contributions, and congress/meeting announcements.

The target audience of the Turkish Journal of Ophthalmology includes physicians working in the various areas of ophthalmology and all other health professionals interested in these issues.

The Journal's publication policies are based on the Recommendations for the Conduct, Reporting, Editing, and Publication of Scholarly Work in Medical Journals from the International Committee of Medical Journal Editors (ICMJE) (2013, archived at http://www.icmje.org/).

The Turkish Journal of Ophthalmology is indexed in the **PubMed/MEDLINE, PubMed Central (PMC), Web of Science-Emerging Sources Citation Index (ESCI), Scopus, TÜBİTAK/ULAKBİM, Directory of Open Access Journals (DOAJ), EBSCO Database, Gale, CINAHL, Proquest, Embase, British Library, Index Copernicus, J-Gate, IdealOnline, Türk Medline, Hinari, GOALI, ARDI, OARE, AGORA, and Turkish Citation Index.**

Open Access Policy

This journal provides immediate open access to its content on the principle that making research freely available to the public supports a greater global exchange of knowledge.

Author(s) and copyright owner(s) grant access to all users for the articles published in the Turkish Journal of Ophthalmology as free of charge.

Open Access Policy is based on rules of Budapest Open Access Initiative (BOAI). By "open access" to [peer-reviewed research literature], we mean its free availability on the public internet, permitting any users to read, download, copy, distribute, print, search, or link to the full texts of these articles, crawl them for indexing, pass them as data to software, or use them for any other lawful purpose, without financial, legal, or technical barriers other than those inseparable from gaining access to the internet itself.

Copyright

Turkish Journal of Ophtalmology is an open access publication, and the journal's publication model is based on Budapest Open Access Initiative (BOAI) declaration.

All published content is available online, free of charge at www.oftalmoloji.org/.

Subscription Information

The full text of all issues of the Journal can be accessed free of charge at www.oftalmoloji.org.

Contact Information

Editor-in-Chief, Banu Bozkurt, MD, Professor of Ophthalmology
E-mail: drbanubozkurt@yahoo.com

Turkish Journal of Ophthalmology

Avrupa Konutları Kale, Maltepe Mah. Yedikule Çırpıcı Yolu Sk. 9. Blok No: 2 Kat:1 Ofis:1 Zeytinburnu-İstanbul-Türkiye

Secretary: Selvinaz Arslan
E-mail: dergi@oftalmoloji.org - sekreter@oftalmoloji.org
Phone: +90 212 801 44 36/37 **Fax:** +90 212 801 44 39
Website: www.oftalmoloji.org

Advertisement

Applications for advertisement should be addressed to the editorial office.

Publisher Contact Information

Galenos Publishing House, Ltd. Şti.
Address: Molla Gürani Mah. Kaçamak Sk. No: 21, 34093 Fındıkzade-İstanbul-Türkiye
Phone: +90 (530) 177 30 97
E-mail: info@galenos.com.tr

Information for Authors

Instructions for authors can be found on the Journal website and at www.oftalmoloji.org.

Material Disclaimer

The opinions and reports stated in all articles published in the Turkish Journal of Ophthalmology are the views of the author(s). They do not reflect the opinions of the Editor-in-Chief, editorial board, or publisher, and these parties accept no responsibility for these articles.

OPEN ACCESS

TURKISH JOURNAL OF OPHTHALMOLOGY

TJO

www.oftalmoloji.org

INSTRUCTIONS TO AUTHORS

The Turkish Journal of Ophthalmology is the official periodical of the Turkish Ophthalmological Association and accepts manuscripts written in Turkish and English. Each issue is published electronically in both Turkish and English. Manuscripts submitted in Turkish should be consistent with the Turkish Dictionary and Writing Guide ("Türkçe Sözlüğü ve Yazım Kılavuzu") of the Turkish Language Association, and care should be taken to use the Turkish forms of words. The Turkish Journal of Ophthalmology charges no submission or manuscript processing fee.

Contributions submitted to the Journal must be original and not published elsewhere or under consideration for publication by another journal.

Reviewed and accepted manuscripts are translated either from Turkish to English or from English to Turkish by the Journal through a professional translation service. Prior to publication, the translations are sent to the authors for approval or correction requests, to be returned within 3 days. If no response is received from the corresponding author within this period, the translation is checked and approved by the editorial board.

Turkish Journal of Ophthalmology is abbreviated as TJO, but should be denoted as Turk J Ophthalmol when referenced. In the international index and database, the journal is registered as Turkish Journal of Ophthalmology, abbreviated as Turk J Ophthalmol.

Scientific and ethical liability for a contribution remains with the author(s) and copyright is held by TJO. Authors are responsible for article contents and accuracy of the references. Manuscripts submitted for publication must be accompanied by the Copyright Transfer Form signed by all contributing authors. By submitting this form, the authors guarantee that the manuscript and the data therein are not previously published or being evaluated for publication elsewhere and declare their scientific contribution and liability.

All manuscripts submitted to TJO are screened for plagiarism using iThenticate. Results indicating plagiarism may result in manuscripts being returned or rejected.

Experimental, clinical and drug studies requiring approval by an ethics committee must be submitted to TJO with an ethics committee approval report confirming that the study was conducted in accordance with international agreements and the Helsinki Declaration (2013 revision) (https://www.wma.net/policies-post/wma-declaration-of-helsinki-ethical-principles-for-medical-research-involving-human-subjects). Information regarding ethical approval and patient informed consent for the study should be indicated in the Materials and Methods section. For experimental animal studies, the authors should include a statement confirming that the study procedures were in accordance with animal rights as per the Guide for the Care and Use of Laboratory Animals (http://oacu.od.nih.gov/regs/guide/guide.pdf) and that animal ethics committee approval was obtained.

If an article includes any direct or indirect commercial connections or if any institution provided material support for the research, authors must include a statement in the cover letter stating that they have no commercial relationship with the relevant product, drug, pharmaceutical company, etc. or specifying the nature of their relationship (consultant, other agreements).

All individuals and organizations from which the authors received any form of assistance and other support should be declared, and the Conflicts of Interest Form should be used to explain any conflicts of interest.

All contributions are evaluated by the editor-in-chief, associate editors, and independent referees.

The Turkish Journal of Ophthalmology uses an independent, unbiased, double-blind peer review process. Manuscripts are received and reviewed by the editor-in-chief, who directs them to the appropriate section editor. The section editor sends the manuscript to three independent referees. Referees are selected by the editorial board from among national and international experts in the area relevant to the study. The referees accept or reject the invitation to review the manuscript within two weeks. If they accept, they are expected to return their decision within 21 days. The associate editor reviews the referees' decisions, adds their own feedback, and returns the manuscript to the editor-in-chief, who makes the final decision. In case of disagreement among referees, the editor can assign a new referee.

The editor-in-chief, associate editors, biostatistics consultant, and English language editor may make minor changes to accepted manuscripts before publication, provided they do not fundamentally change the text.

In case of a potential scientific error or suspicion/allegation of ethical infringement in research submitted for evaluation, the Journal reserves the right to submit the manuscript to the supporting institutions or other authorities for investigation. The Journal accepts the responsibility of properly following-up on the issue but does not undertake any responsibility for the actual investigation or any power of decision regarding errors.

The editorial policies and general guidelines for manuscript preparation specified below are based on the "Recommendations for the Conduct, Reporting, Editing, and Publication of Scholarly Work in Medical Journals" from the International Committee of Medical Journal Editors (ICMJE) (2013, archived at http://www.icmje.org/).

Research articles, systematic reviews, and meta-analyses should be prepared according to the relevant guidelines:

CONSORT statement for randomized controlled trials (Moher D, Schultz KF, Altman D, for the CONSORT Group. The CONSORT statement revised recommendations for improving the quality of reports of parallel group randomized trials. JAMA 2001; 285: 1987-91) (http://www.consort-statement.org/);

PRISMA statement of preferred reporting items for systematic reviews and meta-analyses (Moher D, Liberati A, Tetzlaff J, Altman DG, The PRISMA Group. Preferred Reporting Items for Systematic Reviews and Meta-Analyses: The PRISMA Statement. PLoS Med 2009; 6(7): e1000097.) (http://www.prisma-statement.org/);

STARD checklist for the reporting of studies of diagnostic accuracy (Bossuyt PM, Reitsma JB, Bruns DE, Gatsonis CA, Glasziou PP, Irwig LM, et al., for the STARD Group. Towards complete and accurate reporting of studies of diagnostic accuracy: the STARD initiative. Ann Intern Med 2003;138:40-4.) (http://www.stard-statement.org/);

STROBE statement, a checklist of items that should be included in reports of observational studies (http://www.strobe-statement.org/);

MOOSE guidelines for meta-analysis and systemic reviews of observational studies (Stroup DF, Berlin JA, Morton SC, et al. Meta-analysis of observational studies in epidemiology: a proposal for reporting Meta-analysis of observational Studies in Epidemiology (MOOSE) group. JAMA 2000; 283: 2008-12).

GENERAL GUIDELINES

All submissions to TJO are made electronically through the Journal Agent website (http://journalagent.com/tjo/). After creating an account, authors can use this system for the online submission and review process. Manuscripts collected in the system are archived according to the rules of the ICMJE, Index Medicus (Medline/PubMed) and Ulakbim-Turkish Medicine Index.

Format: Manuscripts should be prepared using Microsoft Word, size A4 with 2.5 cm margins on all sides, 12 pt Arial font, and 1.5 line spacing.

Abbreviations: Abbreviations should be defined at first mention and used consistently throughout the text thereafter. Internationally accepted abbreviations should be used; refer to scientific writing guides as necessary.

Cover letter: The cover letter should include the manuscript type, a statement confirming that the article is not under consideration for publication by another journal, declaration of all sources of funding and equipment (if applicable) and a conflict of interest statement. In addition, the authors should confirm that articles submitted in English have undergone language editing and that original research articles have been reviewed by a biostatistician.

REFERENCES

Authors are solely responsible for the accuracy of all references.

In-text citations: References should be indicated as a superscript immediately after the period/full stop of the relevant sentence. If the author(s) of a reference is/are indicated at the beginning of the sentence, this reference should be written in superscript immediately after the author's name. Relevant research conducted in Türkiye or by Turkish investigators should be cited when possible.

Citing presentations given at scientific meetings, unpublished manuscripts, theses, Internet addresses, and personal interviews or experiences should be avoided. If such references are used, they should be indicated in parentheses at the end of the relevant sentence in the text, without a reference number and written in full, in order to clarify their nature.

References section: References should be numbered consecutively in the order in which they are first mentioned in the text. All authors should be listed regardless of number. The titles of journals should be abbreviated according to the style used in the Index Medicus.

Reference Format

Journal: Last name(s) of the author(s) and initials, article title, publication title and its original abbreviation, publication date, volume, the inclusive page numbers.

Example:

Collin JR, Rathbun JE. Involutional entropion: a review with evaluation of a procedure. Arch Ophthalmol. 1978;96:1058-1064.

Book: Last name(s) of the author(s) and initials, chapter title, book editors, book title, edition, place of publication, date of publication and inclusive page numbers of the extract cited.

TURKISH JOURNAL OF OPHTHALMOLOGY

TJO

www.oftalmoloji.org

INSTRUCTIONS TO AUTHORS

Example: Herbert L. The Infectious Diseases (1st ed). Philadelphia; Mosby Harcourt; 1999:11;1-8.
Book Chapter: Last name(s) of the author(s) and initials, chapter title, book editors, book title, edition, place of publication, date of publication and inclusive page numbers of the cited piece. Example:
O'Brien TP, Green WR. Periocular Infections. In: Feigin RD, Cherry JD, eds. Textbook of Pediatric Infectious Diseases (4th ed). Philadelphia; W.B. Saunders Company;1998:1273-1278.
Books in which the editor and author are the same person: Last name(s) of the author(s) and initials, chapter title, book editors, book title, edition, place of publication, date of publication and inclusive page numbers of the cited piece.
Example: Solcia E, Capella C, Kloppel G. Tumors of the exocrine pancreas. In: Solcia E, Capella C, Kloppel G, eds. Tumors of the Pancreas. 2nd ed. Washington: Armed Forces Institute of Pathology; 1997:145-210.
FIGURES, TABLES, GRAPHICS, AND IMAGES
All visual materials together with their legends should be located on separate pages following the main text.
Images:
Images (pictures) should be numbered and include a brief title. Permission to reproduce pictures that were published elsewhere must be included. All pictures should be of the highest quality possible, in JPEG format, and at a minimum resolution of 300 dpi.
Tables, Graphics, Figures: All tables, graphics or figures should be enumerated according to their sequence within the text and a brief descriptive caption should be written. Any abbreviations used should be defined in the accompanying legend. Tables in particular should be explanatory and facilitate readers' understanding of the manuscript, and should not repeat data presented in the main text.

BIOSTATISTICS

To ensure controllability of research findings, the study design, study sample, and methodological approaches and practices should be explained with appropriate sources referenced.
The "p" value defined as the limit of significance along with appropriate indicators of measurement error and uncertainty (confidence interval, etc.) should be specified. Statistical terms, abbreviations, and symbols used in the article should be described and the software used should be stated. Statistical terminology (random, significant, correlation, etc.) should not be used in non-statistical contexts.
All data and analysis results should be presented as tables and figures and summarized in the text of the Results section. Details of the biostatistical methods and procedures used should be presented in the Materials and Methods section or under a separate Statistics heading before the Results section.

MANUSCRIPT TYPES

Original Research Articles

Includes clinical studies, clinical observations, new techniques, and experimental and in vitro studies. Original research articles should include a title, structured abstract, keywords relevant to the content of the article, and introduction, materials and methods, results, discussion, study limitations, conclusion, references, tables/figures/images, and acknowledgements sections. The main text should not exceed 3000 words, excluding references.The title, abstract, and keywords should be written in both Turkish and English.
Title Page: This page should include the manuscript title, short title, and author name(s) and affiliation(s). The following descriptions should be stated in the given order:
1. Title of the manuscript (Turkish and English), as concise and explanatory as possible, including no abbreviations, up to 135 characters
2. Short title (Turkish and English), up to 60 characters
3. The authors should express the word number of the article on the title page in one sentence.
4. Each author's full name (without abbreviations and academic titles) and affiliation
5. The corresponding author's name, postal address, e-mail address, and phone and fax numbers
6. If the study was presented at a congress and its abstract was published in the congress abstract book, please provide the date and location of the relevant scientific meeting.
7. The online access link and date should be given for the articles that have been published in preprint repositories.
8. The total number of words in the main text, excluding abstract and references
9. The number of tables and figures
Abstract: The article should be summarized in a Turkish abstract not exceeding 250 words and a corresponding English abstract up to 285 words in length. References should not be cited in the abstract. The use of abbreviations should be avoided as much as possible; any abbreviations in the abstract should be defined and used independently of those used in the main text. For original research articles, the structured abstract should include the following 5 subheadings:
Objectives: The aim of the study should be clearly stated.
Materials and Methods: The study should be described, including selection criteria, design (randomized, retrospective/prospective, etc.), and statistical methods applied, if applicable.
Results: The main results of the study should be stated and the statistical significance level should be indicated.
Conclusion: The results of the study should be summarized and the clinical applicability of the results should be defined.
Keywords: The abstract should be followed by 3 to 5 keywords. Keywords in English should be consistent with the Medical Subject Headings (MESH) terms (www.nlm.nih.gov/mesh/MBrowser.html). Turkish keywords should be direct translations of MESH terms.
The main text of the article should include the following headings:
Introduction: Should consist of a brief background to the subject and the study objective(s), supported by information from the literature.
Materials and Methods: The study plan should be clearly described, including whether the study was randomized and retrospective or prospective, the inclusion and exclusion criteria applied, the patient/sample number and characteristics, and statistical methods used.
Results: The results of the study should be stated, with tables/figures given in numerical order; the results should be evaluated according to the statistical analysis methods applied. See the Tables, Graphics, Figures, And Images section of the General Guidelines for details about the preparation of visual material.
Discussion: The study results should be discussed in terms of their favorable and unfavorable aspects and they should be compared with the literature. The conclusion of the study should be highlighted.
Study Limitations: This section should state which data and analyses could not be included in the study, discuss limitations of the study, and give recommendations for future studies.
Conclusion: Highlights the results obtained and conclusions that can be drawn from the study.
Acknowledgements: Any technical or financial support or editorial contributions (statistical analysis, English/Turkish evaluation) towards the study should appear at the end of the article.
References: Authors are responsible for the accuracy of the references. See the General Guidelines for details about the usage and formatting required.

Case Reports

Case reports should present cases which are rarely seen, feature novelty in diagnosis and treatment, and contribute to our current knowledge. The first page should include the title in Turkish and English, an unstructured Turkish summary up to 150 words in length and a corresponding English abstract not exceeding 175 words, and keywords in both languages. The main text should include the introduction, case presentation, discussion, and references. The main text should not exceed 1500 words, excluding references. For case series of 3 or more, the main text should not exceed 2000 words, excluding references.

Review Articles

Review articles can address any aspect of clinical or basic ophthalmology and should be written in a format that describes, discusses, and analyzes the current state of knowledge or clinical use based on the latest evidence and offers directions for future research. Most review articles are invited, but uninvited review submissions are also welcome. Contacting the section editor is recommended before submitting a review.
Reviews articles analyze topics in depth, independently, and without bias. The first section should include Turkish and English titles, unstructured summaries, and keywords. All cited literature should be referenced. The main text should not exceed 5000 words, excluding references.

Letters to the Editor

Letters to the Editor should be short commentaries related to current developments in ophthalmology and their scientific and social aspects, or may ask questions or offer further contributions in response to articles published in the Journal. Letters do not include a title or an abstract, should not exceed 500 words, and can have up to 5 references.

CORRESPONDENCE

All correspondence should be directed to the Journal's secretariat:
Post: Turkish Ophthalmological Association
Avrupa Konutları Kale, Maltepe Mah. Yedikule Çırpıcı Yolu Sk. 9. Blok No: 2 Kat:1 Ofis:1 Zeytinburnu-İstanbul-Türkiye
Phone: +90 212 801 44 36/37 Fax: +90 212 801 44 39
Web Page: www.oftalmoloji.org
E-mail: dergi@oftalmoloji.org / sekreter@oftalmoloji.org

TURKISH JOURNAL OF OPHTHALMOLOGY

TJO

www.oftalmoloji.org

CONTENTS

TURKISH JOURNAL OF OPHTHALMOLOGY

TJO

www.oftalmoloji.org

AT A GLANCE

2023 Issue 5 at a Glance:

Esteemed colleagues,

In the fifth issue of 2023, the Turkish Journal of Ophthalmology features 6 original articles, 1 review, 2 case reports, and a letter to the editor.

An article by Dericioğlu et al. titled "Predictive Factors of Complications and Visual Outcomes after Pediatric Cataract Surgery" from Marmara University Hospital, a referral center in Türkiye, reports a study including 80 eyes of 50 patients treated for pediatric cataract between 2010 and 2020 with an average follow-up time of 60 months. In this detailed retrospective analysis, it was determined that total/mature cataract morphology and the presence of any complication negatively affected final visual acuity, and the presence of congenital cataract and intraoperative anterior hyaloid membrane rupture increased the risk of postoperative complications (See pages 267-274).

Çeper et al. conducted a study titled "Multimodal Imaging of Reticular Pseudodrusen in Turkish Patients" at Ege University Hospital and showed that the most sensitive imaging methods that can be used in the diagnosis of reticular pseudodrusen are infrared imaging, which had a 95% detection rate, followed by spectral domain optical coherence tomography (SD-OCT) with a rate of 91.6%. Despite their lower sensitivity rates, red-free photography, fundus autofluorescence, and blue reflectance imaging were recommended as auxiliary modalities due to their specificity rates of 100%, 100%, and 99.6%, respectively (See pages 275-280).

A pilot study by Kandarakis et al. titled "Combining Perfluorobutylpentane (F_4H_5) with Glaucoma Drainage Device Implantation for Silicone Oil-Induced Glaucoma" comes from our neighbor's capital, Athens, Greece. The study included 8 patients who had pars plana vitrectomy surgery with silicone oil tamponade and later underwent F_4H_5 washout to remove residual silicone oil with concurrent glaucoma drainage device (GDD) implantation to treat refractory glaucoma. They achieved a 60.9% reduction in mean intraocular pressure within 12 months after surgery and a decrease in the need for glaucoma medication from 4 drugs preoperatively to 0.75±0.89 drugs postoperatively. Based on these findings, the authors concluded that F_4H_5 is an effective emulsifier for silicone oil removal and can be used safely in combination with GDD implantation to control intraocular pressure in eyes with silicone oil-induced glaucoma (See pages 281-288).

In their study titled "Evaluation of Agreement Between Sweep Visual Evoked Potential Testing and Subjective Visual Acuity" including 49 subjects, Polat et al. concluded that the results of sweep visual evoked potential measurements and subjective visual acuity measurements did not show statistical agreement and that it would not be correct to use them interchangeably (See pages 289-293).

A study by Kaplan et al. titled "Clinical Findings and Optical Coherence Tomography Measurements of Pediatric Patients with Papilledema and Pseudopapilledema" included 58 children with pseudopapilledema, 32 children with mild-to-moderate papilledema, and 40 healthy controls. The authors concluded that in the differential diagnosis of papilledema and pseudopapilledema, which differ greatly in terms of follow-up and prognosis, non-invasive methods such as newly developed OCT techniques can spare patients from the stress and financial burden of expensive, extensive, and invasive procedures (See pages 294-300).

In their study titled "Detection and Classification of Diabetic Macular Edema with a Desktop-Based Code-Free Machine Learning Tool," Kırık et al. investigated the effectiveness of the Lobe program, a personal computer-based machine learning tool that requires no coding knowledge, in the recognition and classification of diabetic macular edema (DME) in SD-OCT images. The study included 695 cross-sectional images of 336 patients with DME and images from 200 healthy controls. The developed model was found to have 99.28% sensitivity and 100% specificity for DME detection independent of class. Sensitivity and specificity according to label were 87.80% and 98.57% for diffuse retinal edema, 96.43% and 99.29% for cystoid macular edema, and 95.71% and 95.41% for cystoid macular degeneration, respectively (See pages 301-306).

In this issue, Anderson and Akduman's article titled "Management of Myopic Maculopathy: A Review" addresses the diagnosis, clinical features, and treatment of myopic maculopathy, emphasizing the latest advances in the surgical treatment of myopic traction maculopathy. The comprehensive article discusses the possible advantages of using macular buckling in myopic maculopathy as well as the commercially available macular buckling materials, and reviews the new myopic traction maculopathy staging system and its role in the surgical management of these complex cases (See pages 307-312).

TURKISH
JOURNAL OF
OPHTHALMOLOGY

TJO

www.oftalmoloji.org

AT A GLANCE

In their case report titled "Epithelial Inoculation After Small-Incision Lenticule Extraction (SMILE): A Case Report," Ahmet et al. reported that immediate irrigation of the interface seemed to be a safe and effective treatment when epithelial inoculation is observed early after SMILE surgery, which has been performed since 2008 (See pages 313-317).

In another case report titled "Tractional Retinal Detachment Related to Hemoglobin C Trait Retinopathy: A Case Report," Garrell-Salat et al. describe a patient they treated with vitrectomy. They authors stated that because Hemoglobin C disease can threaten vision due to retinal proliferation, similar to sickle cell retinopathy, these patients should be followed up regularly and emphasized that ultra-wide angiography is a useful method to detect peripheral ischemia in the earlier stages (See pages 318-321).

In their letter to the editor, Ali et al. shared their experience in the Department of Ophthalmology of Te Whatu Ora, referring to the article titled "Bacillary Layer Detachment in Acute Vogt-Koyanagi-Harada Disease" by Ataş et al. They emphasized that their own observations support those of Ataş et al. in terms of obtaining good visual outcome despite the presence of bacillary layer detachment, and that further studies are needed to evaluate other OCT characteristics associated with poor prognosis, increased complications (such as choroidal neovascular membrane), or recurrence (See pages 322-323).

We believe that this issue, which blends together original research findings, striking case reports, and a review penned by authors who are also innovators in the field, will be of considerable interest to our colleagues.

Respectfully on behalf of the Editorial Board,
Sait Eğrilmez, MD

Original Article

Predictive Factors of Complications and Visual Outcomes after Pediatric Cataract Surgery: A Single Referral Center Study from Türkiye

Volkan Dericioğlu, Mehmet Orkun Sevik, Elif Bağatur Vurgun, Eren Çerman

Marmara University Faculty of Medicine, Department of Ophthalmology, İstanbul, Türkiye

Abstract

Objectives: To evaluate the predictive factors of complications and visual acuity outcomes in pediatric cataract patients.

Materials and Methods: This retrospective, observational clinical study included 80 eyes of 50 patients treated for pediatric cataracts between 2010 and 2020. The eyes were divided into Group I (congenital cataracts, n=38) and Group II (developmental cataracts, n=42). Group II was also divided into Group IIA (aphakic, n=21) and Group IIB (pseudophakic, n=21). The effects of the age, laterality, cataract morphology, intraocular lens implantation, preoperative nystagmus/strabismus, and intraoperative anterior hyaloid rupture on complications and final best-corrected visual acuity (BCVA; logMAR) were evaluated.

Results: The median (interquartile range) age and follow-up time were 28 (5-79) months and 60 (29-84) months, respectively. There was a significant difference in mean final BCVA between Group I (0.79±0.46) and Group II (0.57±0.51) (p=0.047); however, no difference was observed between Group IIA and Group IIB (p=0.541). Having congenital cataract (p=0.045), preoperative nystagmus/strabismus (p=0.042), total/mature cataract (p<0.001), and postoperative complications (p=0.07) were significantly associated with final BCVA. However, in multivariate analysis, only total/mature cataract (β: 0.52, p<0.001) and having any complication (β: 0.24, p=0.018) were associated with final BCVA. Congenital cataract and intraoperative anterior hyaloid rupture were the only significant risk factors of postoperative complications on univariate (p=0.027 and p=0.003, respectively) and binary logistic regression analysis (odds ratio [OR]: 2.95 [95% confidence interval: 1.07-8.15], p=0.036 and OR: 4.28 [95% confidence interval: 1.55-11.77], p=0.005, respectively).

Conclusion: Total/mature cataract and the presence of any postoperative complication adversely affected the final BCVA. Having a congenital cataract and intraoperative anterior hyaloid membrane rupture increased the risk of complications.

Keywords: Pediatric cataract, congenital cataract, developmental cataract, surgery, complication, visual outcomes

Introduction

The factors affecting the long-term outcomes of congenital and developmental pediatric cataracts are frequently studied in the literature, with the most commonly investigated parameters being age at surgery, bilaterality, and intraocular lens (IOL) implantation.[1,2,3] Although congenital and unilateral cataracts were generally accepted as affecting visual outcomes, recent long-term studies with IOL implantation and aphakic treatment resulted in comparable success rates in final visual acuity.[1,2,3] However, it is difficult to make prospective observations or definite conclusions about all factors influencing final visual acuity, such as cataract morphology, preoperative nystagmus or strabismus, and occlusion therapy compliance.

The most common complications after pediatric cataract surgeries are inflammatory reactions in the anterior chamber and visual axis opacifications (VAO), and one of the most severe complications is secondary glaucoma.[4,5,6,7] As complications after pediatric cataract surgeries result in worse visual outcomes, it is essential to recognize and manage the factors associated with complication development.[1,8] For this purpose, the most commonly investigated parameters are age at diagnosis, anterior vitrectomy, IOL implantation, and techniques of IOL implantation.[9,10,11,12,13,14]

The present study aimed to evaluate the effects of age at diagnosis, laterality, cataract morphology, preoperative nystagmus or strabismus, IOL implantation, and unintentional intraoperative anterior hyaloid rupture on complication rates

Cite this article as: Dericioğlu V, Sevik MO, Bağatur Vurgun E, Çerman E. Predictive Factors of Complications and Visual Outcomes after Pediatric Cataract Surgery: A Single Referral Center Study from Türkiye. Turk J Ophthalmol 2023;53:267-274

Address for Correspondence: Eren Çerman, Marmara University Faculty of Medicine, Department of Ophthalmology, İstanbul, Türkiye
E-mail: erencerman@yahoo.com **ORCID-ID:** orcid.org/0000-0002-8681-9214
Received: 13.06.2022 **Accepted:** 26.02.2023

DOI: 10.4274/tjo.galenos.2023.50951

and best-corrected visual acuities (BCVA) after pediatric cataract surgeries.

Materials and Methods

Study Design and Patients

This single-center, retrospective, observational study included congenital and developmental pediatric cataract patients who presented to the Pediatric Ophthalmology and Strabismus Unit of the Department of Ophthalmology at Marmara University Faculty of Medicine Hospital in Pendik, İstanbul between January 2010 and January 2020. The Institutional Review Board of Marmara University Faculty of Medicine approved the study protocol (decision no: 09.2020.1169, date: 06.11.2020), and the study was conducted following the principles of the Declaration of Helsinki. All patients' legal guardians routinely provided written informed consent about using their medical information in the study analysis at their first presentation and before the individual interventions.

The records of patients diagnosed with congenital and developmental cataracts were retrospectively reviewed, and eligible patients were included in the study. The exclusion criteria were: traumatic or uveitic cataracts, not having undergone cataract surgery, having cataract surgery at another center, having ocular comorbidities, having a secondary IOL implantation, lack of consistent or adequate medical records, having a follow-up time <1 year, and inability to obtain final visual acuity. Demographic and clinical characteristics of the patients such as sex, laterality (unilateral or bilateral), cataract morphology (lamellar-cortical, total/mature, posterior polar, posterior subcapsular, anterior polar, nuclear, and oil drop), age at diagnosis (months), age at surgery (months), time from diagnosis to surgery (months), and follow-up time (months) were recorded.

Surgical Indication and Technique

All patients underwent a comprehensive preoperative ophthalmologic examination including evaluation of best-corrected visual acuity (BCVA) with the HOTV, Snellen, or Tumbling "E" charts if possible, intraocular pressure (IOP) with TONO-PEN XL (Hagg-Streit, Koeniz, Switzerland) or Goldmann applanation tonometry depending on the patient's age, dilated fundus examination, retinoscopy with cycloplegia, keratometry, and B-scan ultrasonography if indicated. Any visually significant cataracts with a risk of deprivation amblyopia were considered an indication for cataract surgery.

All surgeries were performed under general anesthesia by the same experienced surgeon (E.Ç.). Two side port incisions were made at 2 and 10 clock hours, and the anterior chamber was filled with a cohesive ophthalmic viscoelastic device (OVD). A 5- to 5.5-mm anterior continuous curvilinear capsulorhexis (CCC) was made with micro-forceps. Then, lenticular material was aspirated by bimanual irrigation/aspiration. After clearance of the lenticular material, a small incision was made at the posterior capsule with a cystotomy cannula. Next, the Berger space was filled with dispersive OVD to prevent anterior hyaloid membrane rupture, and posterior CCC was completed with micro-forceps. Finally, a 23-gauge anterior vitrectomy was performed if the anterior hyaloid was ruptured unintentionally during the surgery with any vitreous prolapse into the anterior chamber.

A three-piece hydrophobic acrylic IOL was implanted in the capsular bag or sulcus through a 2.4-mm main incision as primary IOL implantation only if the patient was over 12 months old and the caregivers thought that using contact lenses or glasses would be problematic due to socio-economic difficulties. Otherwise, the patients were left aphakic.

All incisions were then sutured with 10-0 nylon or vicryl sutures. Postoperative therapy included topical moxifloxacin hydrochloride (Vigamox 0.5%, Alcon Laboratories, Inc., Texas, USA) and prednisolone acetate (Pred-forte 1%, Allergan Pharmaceutical, Westport/Co. Mayo, Ireland) four times a day for one month.

Postoperative Complications and Visual Acuity

Follow-up examinations were performed at 1 day, 1 week, 1 month, and 3 months after the surgery and then at intervals of 3 to 6 months. All follow-up visits included BCVA assessment (if possible), IOP measurement, slit-lamp biomicroscopy, retinoscopy, and dilated fundus examinations. The patients' final BCVA in decimal or Snellen values were converted to the logarithm of the minimum angle of resolution (logMAR) for statistical analysis. The appropriate contact lens corrections for the aphakic patients and spectacle corrections for the pseudophakic patients were prescribed at postoperative 1 week and monitored by regular retinoscopy at 3- to 6-month intervals. In addition, occlusion therapy was applied for all unilateral cases and the bilateral cases with significant anisometropia.

Postoperative complications noted were as follows: posterior synechia (defined as an adhesion between the iris and IOL or IOL capsule preventing iris dilation), VAO (capsular or anterior vitreous opacification obscuring retinal examination), fibrinous membrane (a membrane covering the pupil), IOP spike (an elevation in IOP within the first postoperative week requiring medication), and secondary glaucoma (determined according to The British Infantile and Childhood Glaucoma Eye Study criteria).[15] A second surgery was performed in patients with any complication obscuring the visual axis that can cause amblyopia and in secondary glaucoma unresponsive to medical treatment.

The possible predictive factors for postoperative complications and final BCVA were determined as age at surgery, laterality (unilateral or bilateral), IOL implantation, cataract morphology, preoperative nystagmus or strabismus, and unintentional intraoperative anterior hyaloid rupture.

To better present the effects of age and intraoperative IOL implantation on complication rates and final BCVA, the eyes were divided according to the patient's age at diagnosis and treatment into Group I (≤12 months; congenital cataracts) and Group II (>12 months; developmental cataracts). In addition, Group II was divided according to intraoperative IOL implantation into Group IIA (aphakic) and Group IIB (pseudophakic) subgroups.

Statistical Analysis

SPSS for Macintosh version 24.0 (IBM Corp., Armonk, NY, USA) was used to analyze the data. Data distributions were assessed with the Kolmogorov-Smirnov test and histogram graphs; descriptive data were presented as the median and interquartile range (IQR). However, despite a non-parametric distribution, BCVA values were given as mean ± standard deviation for better presentation of the data. Pearson's chi-square test and Bonferroni correction were used to compare categorical variables for two- or three-group comparisons. Cramer's V and point-biserial correlation tests were used to evaluate categorical-categorical and categorical-numerical correlations, respectively. Independent samples with two or more groups were compared with the Mann-Whitney U or Kruskal-Wallis test, respectively. Pairwise comparisons were used for post-hoc tests. A linear regression analysis, including variables significant at the 0.1 level in univariate analysis, was employed to evaluate the most effective predictive factors for BCVA. For factors correlated at the level of 0.4 or higher, only the most significantly affected one was included in the regression analysis. Cohen's d and phi coefficient tests were used to determine the effect size for continuous and categorical data, respectively. A chi-square test was performed for univariate analysis of risk factors for complication development. Risk factors that were determined to be significant in these analyses were also evaluated by binary logistic regression analysis. Odds ratios (OR) and 95% confidence intervals (CI) were assessed to identify independent risk factors. A p value less than 0.05 was considered statistically significant.

Results

There were 99 patients (161 eyes) with pediatric cataracts during the study period. After excluding the non-eligible patients, 50 patients (80 eyes) were included in the study analysis (Figure 1). Of them, 22 patients (38 eyes) were diagnosed with congenital cataracts before the age of 12 months, underwent cataract extraction without IOL implantation, and received contact lenses for refractive correction (Group I). The other 28 patients (42 eyes) were diagnosed with developmental cataracts after the age of 12 months and treated with cataract extraction (Group II). Among the patients in Group II, 14 patients (21 eyes) were left aphakic and treated with contact lens correction (Group IIA), and 14 patients (21 eyes) had primary IOL implantation during the cataract surgery (Group IIB). The overall median follow-up time was 60 (IQR: 29-84) months. The demographical and clinical data of the groups are presented in Table 1.

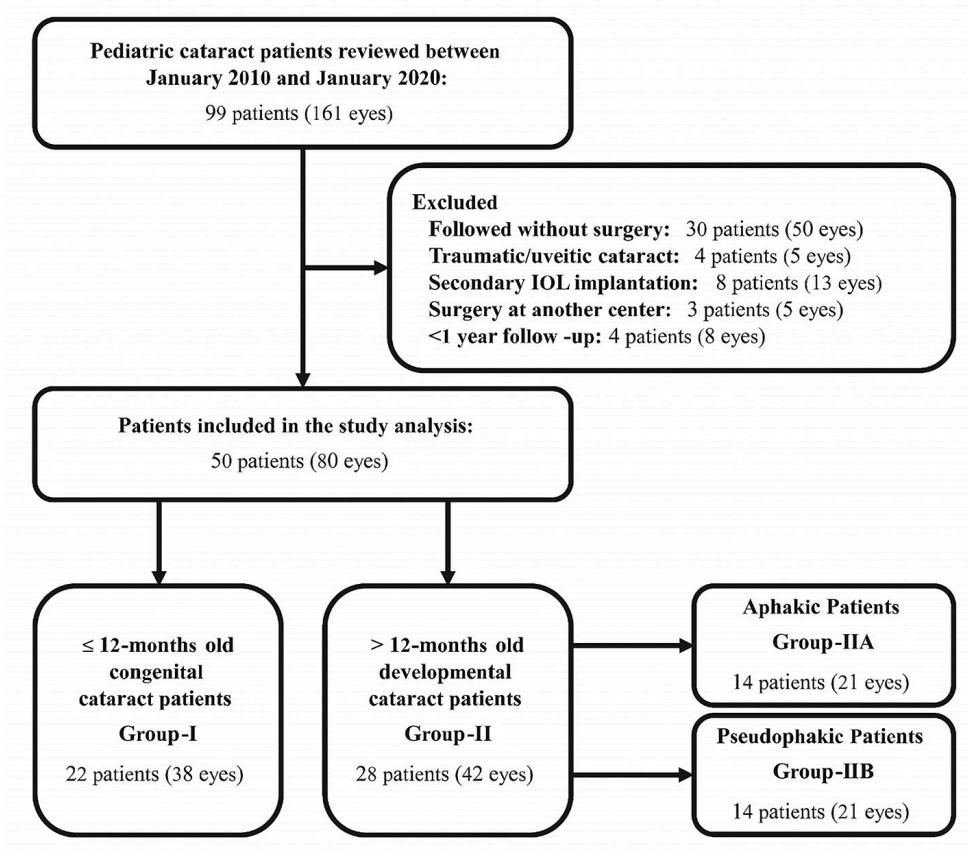

Figure 1. The flowchart of study enrollment
IOL: Intraocular lens

Table 1. Demographic and clinical characteristics of the patients

	Group I n=22 (38 eyes)	Group II			p values		
		Group II total n=28 (42 eyes)	Group IIA n=14 (21 eyes)	Group IIB n=14 (21 eyes)	p_1[a]	p_2[b]	Post-hoc test[c]
Sex, n (eyes) Female Male	 13 (20) 9 (18)	 12 (16) 16 (26)	 7 (11) 7 (10)	 5 (5) 9 (16)	0.192	0.076	NA
Age at diagnosis, months Median (IQR)	4 (2-5)	62 (36-80)	52 (43-72)	76 (32-94)	<0.001*	<0.001*	Group I vs. IIA, p<0.001* Group I vs. IIB, p<0.001*
Age at surgery, months Median (IQR)	5 (3-8)	74 (49-85)	52 (52-76)	80 (32-102)	<0.001*	<0.001*	Group I vs. IIA, p<0.001* Group I vs. IIB, p<0.001*
Time to surgery, months Median (IQR)	0.5 (0-2.5)	5 (0-12)	4 (0-6)	4 (0-12)	0.012*	0.020*	Group I vs. IIB, p=0.017*
Follow-up, months Median (IQR)	68 (46-102)	42 (18-72)	24 (12-54)	60 (32-93)	<0.001*	<0.001*	Group I vs. IIA, p<0.001* Group IIA vs. IIB, p=0.004*
Laterality, eyes (%) Bilateral Unilateral	 32 (84.2) 6 (15.8)	 28 (66.7) 14 (33.3)	 14 (66.7) 7 (33.3)	 14 (66.7) 7 (33.3)	0.123	0.194	NA
Cataract morphology, eyes (%) Lamellar-cortical Total/mature Posterior polar Posterior subcapsular Anterior polar Nuclear Oil drop	 12 (31.6) 12 (31.6) 9 (23.7) 2 (5.3) 2 (5.3) 0 (0.0) 1 (2.6)	 9 (21.4) 8 (19) 9 (21.4) 7 (16.7) 3 (7.1) 4 (9.5) 2 (4.8)	 0 (0.0) 6 (28.6) 5 (23.8) 3 (14.3) 3 (14.3) 2 (9.5) 2 (9.5)	 9 (42.9) 2 (9.5) 4 (19) 4 (19) 0 (0.0) 2 (9.5) 0 (0.0)	NA	NA	NA
Preoperative nystagmus or strabismus, eyes (%)	21 (65.8)	12 (28.6)	4 (19)	8 (38.1)	0.015*	0.024*	Group I vs. IIA, p=0.021*
Intraoperative anterior hyaloid rupture, eyes (%)	16 (42.1)	15 (35.7)	9 (42.9)	6 (28.6)	0.558	0.072	NA
Presence of any complication, eyes (%)	18 (47.4)	10 (23.8)	4 (19)	6 (28.6)	0.027*	0.071	NA
Final BCVA, logMAR Mean ± SD	0.79±0.46	0.57±0.51	0.65±0.59	0.49±0.40	0.020*	0.051	NA

p_1: Group I vs. II, p_2: Group I vs. IIA vs. IIB, [a]Mann-Whitney U test and chi-square test were used for continuous and categorical p_1 values, respectively, [b]Kruskal-Wallis test and chi-square test were used for continuous and categorical p_2 values, respectively. [c]Statistically significant p-values obtained from Kruskal-Wallis pairwise comparisons and chi-square test with Bonferroni correction for continuous and categorical variables, respectively. *Statistically significant.
BCVA: Best-corrected visual acuity, IQR: Interquartile range, logMAR: Logarithm of the minimum angle of resolution, NA: Not applicable, SD: Standard deviation

Final Visual Acuity

The final BCVA of Group II was significantly better than that of Group I (0.57±0.5 vs. 0.79±0.5 logMAR, p=0.020, Cohen's d=0.48). However, there was no significant difference in three-group comparisons (p=0.051).

Considering the predictive factors of final BCVA, a slight negative correlation was found between final BCVA and age at surgery (r=-0.280, p=0.012). The median age at diagnosis was significantly higher in unilateral cases (37 months, IQR: 7-75 months) than bilateral cases (9 months, IQR: 3-52 months) (p=0.035). However, there was no significant difference between unilateral and bilateral cases in terms of time from diagnosis to surgery (1.5 months, IQR: 0-12 vs. 1 month, IQR: 0-4, p=0.277) or final BCVA (0.73±0.35 vs. 0.66±0.54 logMAR, p=0.291, Cohen's d=0.14). Eyes with preoperative nystagmus or strabismus had significantly worse final BCVA than the other eyes (0.81±0.45 logMAR vs. 0.58±0.50 logMAR, p=0.020, Cohen's d=0.48).

Cataract morphology was lamellar-cortical in 21 (26.3%), total/mature in 20 (25%), posterior polar in 18 (22.5%), posterior subcapsular in 9 (11.3%), anterior polar in 5 (6.3%), nuclear in 4 (5%), and oil drop in 3 (3.8%) eyes. Although the median time from diagnosis to surgery was significantly shorter for total/mature cataracts than other cataract morphologies (0 [IQR: 0-1.5] months vs. 3 [IQR: 0-9] months, p=0.001), only total/mature cataract showed a moderate positive correlation with final BCVA (r=0.480, p<0.001). The mean final BCVA of eyes with total/mature cataract was 1.11±0.58 logMAR, which was significantly worse than with the other morphologies (0.53±0.37 logMAR, p<0.001, Cohen's d=1.17). Ninety percent (n=18) of the total/mature cataracts were bilateral, and there was no significant difference in the final BCVA of eyes with

total/mature cataract in Group I (1.15±0.53 logMAR, n=12) and Group II (1.05±0.69 logMAR, n=8) (p=0.295).

Considering the entire study population (Group I and II), pseudophakic eyes had a significantly better final BCVA than the aphakic eyes (0.49±0.40 vs. 0.65±0.59 logMAR, p=0.043, Cohen's d=0.55). However, there was no significant difference between pseudophakic and aphakic eyes in developmental cataract (Group II) (p=0.541).

The mean final BCVA of the eyes with anterior vitrectomy was 0.75±0.54 logMAR, and there was no significant difference with the eyes that had an intact hyaloid membrane (0.63±0.47 logMAR, p=0.263, Cohen's d=0.22).

Aphakic treatment was performed in 59 eyes, which had a mean final BCVA of 0.74±0.5 logMAR. There was no significant difference between aphakic congenital and developmental cataract patients in final BCVA (0.79±0.46 and 0.65±0.59 logMAR, respectively, p=0.153).

The univariate analysis showed that having congenital cataract (β: 0.226 [95% CI: 0.01, 0.44], p=0.044), presence of preoperative nystagmus or strabismus (β: 0.229 [95% CI: 0.01, 0.45], p=0.041), total/mature cataract morphology (β: 0.509 [95% CI: 0.28, 0.62], p<0.001), and development of any complication (β: 0.204 [95% CI: -0.02, 0.41], p=0.070) was significantly associated with final BCVA (Table 2). However, the multivariate analysis revealed that only total/mature cataract morphology (β: 0.59 [95% CI: 0.37, 0.81], p<0.001) and development of any complication (β: 0.243 [95% CI: 0.04, 0.45], p=0.018) was significantly associated with final BCVA (Table 2).

Complications

The complication rates of the groups are given in Table 3. There were significantly more complications in Group I (n=18; 47.4%) than in Group II (n=10, 23.8%) (p=0.028, phi-coefficient: -0.25). However, there was no significant difference in the three-group comparisons (Group I vs. Group IIA vs. Group IIB, p=0.118). A second surgery was required in 18 eyes (22.5%) with indications of VAO in 8 (44.4%), fibrinous membrane in 5 (27.7%), secondary glaucoma in 3 (16.7%), and posterior synechia in 2 (11.1%) eyes. The rest of the complications (n=10, 12.5%) were treated medically.

Considering the predictive factors separately, a slight negative correlation was found between the development of complications and age at surgery (r=-0.265, p=0.018). Complications occurred in 6 eyes (28.6%) with IOL implantation. Furthermore, complications were seen in 22 eyes (37.2%), and no statistical difference was observed between IOL implantation and aphakia in complication development (p=0.472, phi-coefficient: 0.47). Complications were seen in 17 eyes (54.8%) in which anterior hyaloid membrane unintentionally ruptured during surgery, and 9 (29%) of them required a second surgery. Intraoperative anterior hyaloid membrane rupture was significantly correlated with complication development (r=0.331, p=0.003), but not with a second surgery (r=0.124, p=0.271). However, there was no correlation with bilaterality (r=-0.121, p=0.285), primary IOL implantation (r=-0.08, p=0.478), or presence of preoperative nystagmus and strabismus (r=0.130, p=0.249).

Univariate analysis showed that having a congenital cataract (β: -0.247, 95% CI: -0.49, -0.03; p=0.027) and intraoperative anterior hyaloid rupture (β: 0.331, 95% CI: 0.12, 0.56; p=0.003) were significantly associated with the development of complications. Binary logistic regression analysis (Omnibus test: 0.0001, Nagelkerke R^2: 0.211) also showed that having a congenital cataract (OR: 2.95, 95% CI: 1.07, 8.15; p=0.036) and intraoperative anterior hyaloid rupture (OR: 4.28, 95%CI:

Table 2. Univariate analyses and linear regression analysis for predicting factors of postoperative visual outcomes

Variables[a]	Univariate analyses	Multivariate analysis				
	p	B	95% CI	β	t	p
Constant[b]		0.365	0.21, 0.52		4.81	<0.001*
Total cataract morphology	<0.001*	0.588	0.37, 0.81	0.52	5.40	<0.001*
Presence of any complication	0.070*	0.243	0.04, 0.45	0.24	2.40	0.018*
Nystagmus or strabismus	0.042*	0.130	-0.06, 0.32	1.30	1.33	0.187
Congenital cataract	0.045*	0.058	-0.14, 0.26	0.06	0.58	0.563

[a]Factors were ordered according to the significance level of linear regression analysis, [b]R^2_{Adj} = 0.318 (n=80, p<0.001); F [6, 75] = 10.214, p<0.001. *Statistical significance. CI: Confidence intervals for B, IOL: Intraocular lens

Table 3. Distribution of complications in the study groups and according to intraoperative anterior hyaloid status

Complications	Group I (n=38 eyes)	Group IIA (n=21 eyes)	Group IIB (n=21 eyes)	Intact anterior hyaloid (n=49 eyes)	Ruptured anterior hyaloid (n=31 eyes)	Total (n=80 eyes)
Posterior synechia, eyes (%)	6 (15.8)	1 (5.9%)	2 (9.5)	4 (8.9)	5 (16.1)	9 (11.3)
Capsular opacification, eyes (%)	4 (10.5)	0 (0.0)	4 (19.0)	4 (8.9)	4 (12.9)	8 (10)
Pupillary membrane, eyes (%)	4 (10.5)	1 (4.8)	0 (0.0)	1 (2.2)	4 (12.9)	5 (6.3)
Intraocular pressure spike, eyes (%)	1 (2.6)	2 (9.5)	0 (0.0)	1 (2.2)	2 (6.5)	3 (3.8)
Secondary glaucoma, eyes (%)	3 (7.9)	0 (0.0)	0 (0.0)	1 (2.2)	2 (6.5)	3 (3.8)

1.55, 11.77; p=0.005) increased the risk of development of complications.

Discussion

In this study, total/mature cataract morphology and development of postoperative complications were significantly associated with final BCVA after pediatric cataract surgery. In addition, having a congenital cataract and unintentional intraoperative anterior hyaloid rupture leading to anterior vitrectomy increased the risk of postoperative complication development.

Total/mature cataracts are among the most common pediatric cataracts, with a worse visual prognosis, and early surgical intervention is recommended to prevent deprivation amblyopia.[16,17,18,19] The overall final BCVA of the total/mature cataract eyes in our study (1.11±0.58 logMAR) was comparable with the mean BCVA in a study conducted by Zhang et al.[20] (1.07±0.53 logMAR, n=156 eyes), and slightly worse than in a study conducted by Lin et al.[21] (0.89±0.30 logMAR, n=88 eyes). Although we noted that total/mature cataracts had a significantly shorter time from diagnosis to surgery, regression analysis revealed that they were significantly associated with worse final BCVA. Among the eyes with a final BCVA worse than 1.0 logMAR, 54.8% (17/31) had total/mature cataract morphology, which was 85% (17/20) of the eyes with total/mature cataracts. That might have been a result of more severe obscuration of visual stimulus by total/mature cataracts than by other cataract morphologies, leading to profound deprivation amblyopia, which is generally more severe than strabismic or anisometropic amblyopia.[22]

In our study, the development of any complication was also associated with final BCVA, which supports the published literature.[1,8] In our study, the overall complication rate was 35% (28/80 eyes), with a 22.5% (n=18) second surgery rate. These rates are comparable with the Pediatric Eye Disease Investigator Group study, which had a complication rate of 33.6% excluding amblyopia and a second surgery rate of 17% in 1132 eyes.[23] We found that having a congenital cataract diagnosed and treated before 12 months of age was a significant risk factor for complications. Studies in the literature also report that younger age is associated with an increased complication risk.[4,5] Studies have recently focused on the relationship between surgery at a younger age with or without primary IOL implantation and the development of secondary glaucoma.[24,25,26] Solmaz et al.[27] reported a significantly lower mean age at surgery in patients who developed glaucoma, but they did not observe a difference in glaucoma incidence between aphakic and pseudophakic cases. We observed secondary glaucoma in only 3 eyes (3.75%), all of which were in the aphakic congenital cataract group. Reported rates of secondary glaucoma vary between 2% and 58% in the literature.[28] Our relatively low rate was comparable with that reported in a multicenter study by Nagamoto et al.[29] (3.54%; 25/706 eyes), which also demonstrated a significantly higher rate in aphakic patients (p=0.003).

VAO occurred in a total of 8 eyes (10%) in our study, with comparable rates between the eyes that had only posterior CCC (n=4, 8.2%) and posterior CCC with anterior vitrectomy (n=4, 12.9%) (p=0.491). The incidence of VAO was reported to be 100% in eyes without posterior CCC and was reduced by performing posterior CCC and anterior vitrectomy.[18,30,31] Demirkılınç Biler et al.[32] reported that while VAO was seen in 34.3% of eyes (23/67) that underwent posterior capsulotomy and anterior vitrectomy, the prevalence was 76.4% (n=26/34) in eyes without posterior capsulotomy. Similarly, Batur et al.[33] found a 70% rate of posterior capsular opacification and 50% VAO in eyes without posterior CCC. A recent meta-analysis including 11 randomized controlled trials concluded that anterior vitrectomy minimizes the risk of VAO in pediatric cataracts.[9] However, in our study, the positive effect of adding anterior vitrectomy to posterior CCC on VAO could not be demonstrated as other previous studies.[10,11,12]

Hosal and Biglan[13] found that only age at surgery was significantly associated with membrane formation after pediatric cataract surgery, with a 4.74-fold increase in patients younger than one year of age. We also observed a higher rate of membrane formation in patients before the age of 12 months (Group I, congenital cataracts) (10.5% vs. 2.3%, compared to Group II, p=0.105). There was also a higher rate of membrane formation in eyes with intraoperative anterior hyaloid rupture leading to anterior vitrectomy compared to eyes with intact anterior hyaloid membrane (12.9% vs. 2.2%, p=0.051) in our study. In contrast, Hosal and Biglan[13] suggested that primary posterior CCC combined with a planned anterior vitrectomy was protective against secondary membrane formation. In a recent study that controlled for individual variations in inflammatory factors among patients by performing posterior CCC without anterior vitrectomy and posterior IOL capture in one eye and posterior CCC with anterior vitrectomy and in-the-bag IOL implantation in the fellow eye of the same patient, Kaur et al.[14] observed significantly more inflammatory complications in the anterior vitrectomy group (p=0.004). They hypothesized that anterior vitrectomy might contribute to fibrinous complications.[14] We think that uncontrolled rupture of the anterior hyaloid membrane might result in more interaction between the anterior vitreous and aqueous humor, causing more inflammatory and fibrinous reactions in the anterior chamber.

Study Limitations

The main limitations of our study are its retrospective nature and limited sample size. However, the effect sizes of statistical comparisons were given to determine the difference between factors regardless of the number of cases. Although the results are not sufficient to be generalized, they shed light on the factors associated with final visual acuity and the development of complications in pediatric cataract patients.

Conclusion

This retrospective, observational, single-center study revealed that total/mature cataract morphology and the presence

of any postoperative complications adversely affected the final visual acuity of pediatric cataract patients. Moreover, having a congenital cataract or intraoperative anterior hyaloid membrane rupture independently increased the risk of complications in these patients.

Ethics

Ethics Committee Approval: The Institutional Review Board of Marmara University Faculty of Medicine approved the study protocol (decision no: 09.2020.1169, date: 06.11.2020), and the study was conducted following the principles of the Declaration of Helsinki.

Informed Consent: Obtained.

Peer-review: Externally peer-reviewed.

Authorship Contributions

Surgical and Medical Practices: E.Ç., Concept: V.D., M.O.S., E.B.V., E.Ç., Design: V.D., M.O.S., E.B.V., E.Ç., Data Collection or Processing: V.D., E.B.V., Analysis or Interpretation: V.D, M.O.S., E.Ç., Literature Search: V.D., E.B.V., Writing: V.D.

Conflict of Interest: No conflict of interest was declared by the authors.

Financial Disclosure: The authors declared that this study received no financial support.

References

1. Chak M, Wade A, Rahi JS; British Congenital Cataract Interest Group. Long-term visual acuity and its predictors after surgery for congenital cataract: findings of the British congenital cataract study. Invest Ophthalmol Vis Sci. 2006;47:4262-4269.
2. Infant Aphakia Treatment Study Group; Lambert SR, Lynn MJ, Hartmann EE, DuBois L, Drews-Botsch C, Freedman SF, Plager DA, Buckley EG, Wilson ME. Comparison of contact lens and intraocular lens correction of monocular aphakia during infancy: a randomized clinical trial of HOTV optotype acuity at age 4.5 years and clinical findings at age 5 years. JAMA Ophthalmol. 2014;132:676-682.
3. Lambert SR, Cotsonis G, DuBois L, Nizam Ms A, Kruger SJ, Hartmann EE, Weakley DR Jr, Drews-Botsch C; Infant Aphakia Treatment Study Group. Long-term Effect of Intraocular Lens vs Contact Lens Correction on Visual Acuity After Cataract Surgery During Infancy: A Randomized Clinical Trial. JAMA Ophthalmol. 2020;138:365-372.
4. Kuhli-Hattenbach C, Lüchtenberg M, Kohnen T, Hattenbach LO. Risk factors for complications after congenital cataract surgery without intraocular lens implantation in the first 18 months of life. Am J Ophthalmol. 2008;146:1-7.
5. Keech RV, Tongue AC, Scott WE. Complications after surgery for congenital and infantile cataracts. Am J Ophthalmol. 1989;108:136-141.
6. Chen J, Chen Y, Zhong Y, Li J. Comparison of visual acuity and complications between primary IOL implantation and aphakia in patients with congenital cataract younger than 2 years: a meta-analysis. J Cataract Refract Surg. 2020;46:465-473.
7. Solebo AL, Rahi JS; British Congenital Cataract Interest Group. Glaucoma following cataract surgery in the first 2 years of life: frequency, risk factors and outcomes from IoLunder2. Br J Ophthalmol. 2020;104:967-973.
8. Congdon NG, Ruiz S, Suzuki M, Herrera V. Determinants of pediatric cataract program outcomes and follow-up in a large series in Mexico. J Cataract Refract Surg. 2007;33:1775-1780.
9. Cao K, Wang J, Zhang J, Yusufu M, Jin S, Hou S, Zhu G, Wang B, Xiong Y, Li J, Li X, Chai L, He H, Wan XH. Efficacy and safety of vitrectomy for congenital cataract surgery: a systematic review and meta-analysis based on randomized and controlled trials. Acta Ophthalmol. 2019;97:233-239.
10. Kim KH, Ahn K, Chung ES, Chung TY. Clinical outcomes of surgical techniques in congenital cataracts. Korean J Ophthalmol. 2008;22:87-91.
11. Müllner-Eidenböck A, Amon M, Moser E, Kruger A, Abela C, Schlemmer Y, Zidek T. Morphological and functional results of AcrySof intraocular lens implantation in children: prospective randomized study of age-related surgical management. J Cataract Refract Surg. 2003;29:285-293.
12. Raina UK, Mehta DK, Monga S, Arora R. Functional outcomes of acrylic intraocular lenses in pediatric cataract surgery. J Cataract Refract Surg. 2004;30:1082-1091.
13. Hosal BM, Biglan AW. Risk factors for secondary membrane formation after removal of pediatric cataract. J Cataract Refract Surg. 2002;28:302-309.
14. Kaur S, Sukhija J, Ram J. Comparison of posterior optic capture of intraocular lens without vitrectomy vs endocapsular implantation with anterior vitrectomy in congenital cataract surgery: A randomized prospective study. Indian J Ophthalmol. 2020;68:84-88.
15. Papadopoulos M, Cable N, Rahi J, Khaw PT; BIG Eye Study Investigators. The British Infantile and Childhood Glaucoma (BIG) Eye Study. Invest Ophthalmol Vis Sci. 2007;48:4100-4106.
16. Tartarella MB, Britez-Colombi GF, Milhomem S, Lopes MC, Fortes Filho JB. Pediatric cataracts: clinical aspects, frequency of strabismus and chronological, etiological, and morphological features. Arq Bras Oftalmol. 2014;77:143-147.
17. Wu X, Long E, Lin H, Liu Y. Prevalence and epidemiological characteristics of congenital cataract: a systematic review and meta-analysis. Sci Rep. 2016;6:28564.
18. Khanna RC, Foster A, Krishnaiah S, Mehta MK, Gogate PM. Visual outcomes of bilateral congenital and developmental cataracts in young children in south India and causes of poor outcome. Indian J Ophthalmol. 2013;61:65-70.
19. Zhang H, Xie L, Wu X, Tian J. Long-term results of pediatric cataract surgery after delayed diagnosis. J AAPOS. 2012;16:65-69.
20. Zhang L, Wu X, Lin D, Long E, Liu Z, Cao Q, Chen J, Li X, Lin Z, Luo L, Chen H, Xiang W, Liu J, Tan X, Qu B, Lin H, Chen W, Liu Y. Visual Outcome and Related Factors in Bilateral Total Congenital Cataract Patients: A Prospective Cohort Study. Sci Rep. 2016;6:31307.
21. Lin HT, Long EP, Chen JJ, Liu ZZ, Lin ZL, Cao QZ, Zhang XY, Wu XH, Wang QW, Lin DR, Li XY, Liu JC, Luo LX, Qu B, Chen WR, Liu YZ. Timing and approaches in congenital cataract surgery: a four-year, two-layer randomized controlled trial. Int J Ophthalmol. 2017;10:1835-1843.
22. Antonio-Santos A, Vedula SS, Hatt SR, Powell C. Occlusion for stimulus deprivation amblyopia. Cochrane Database Syst Rev. 2014;3:CD005136.
23. Writing Committee for the Pediatric Eye Disease Investigator Group (PEDIG); Repka MX, Dean TW, Kraker RT, Bothun ED, Morrison DG, Lambert SR, Stahl ED, Wallace DK. Visual Acuity and Ophthalmic Outcomes in the Year After Cataract Surgery Among Children Younger Than 13 Years. JAMA Ophthalmol. 2019;137:817-824.
24. Plager DA, Lynn MJ, Buckley EG, Wilson ME, Lambert SR; Infant Aphakia Treatment Study Group. Complications in the first 5 years following cataract surgery in infants with and without intraocular lens implantation in the Infant Aphakia Treatment Study. Am J Ophthalmol. 2014;158:892-898.
25. Solebo AL, Russell-Eggitt I, Cumberland PM, Rahi JS; British Isles Congenital Cataract Interest Group. Risks and outcomes associated with primary intraocular lens implantation in children under 2 years of age: the IoLunder2 cohort study. Br J Ophthalmol. 2015;99:1471-1476.
26. Balekudaru S, Agarkar S, Guha S, Mayee RC, Viswanathan N, Pandey A, Singh M, Lingam V, George R. Prospective analysis of the predictors of glaucoma following surgery for congenital and infantile cataract. Eye (Lond). 2019;33:796-803.
27. Solmaz U, Önder F, Ersoy Koca G. Development of Secondary Glaucoma After Congenital Cataract Surgery and the Underlying Risk Factors. Turk J Ophthalmol. 2011;41:358-363.
28. Swamy BN, Billson F, Martin F, Donaldson C, Hing S, Jamieson R, Grigg J, Smith JE. Secondary glaucoma after paediatric cataract surgery. Br J Ophthalmol. 2007;91:1627-1630.
29. Nagamoto T, Oshika T, Fujikado T, Ishibashi T, Sato M, Kondo M, Kurosaka D, Azuma N. Surgical outcomes of congenital and developmental cataracts in Japan. Jpn J Ophthalmol. 2016;60:127-134.

30. Fenton S, O'Keefe M. Primary posterior capsulorhexis without anterior vitrectomy in pediatric cataract surgery: longer-term outcome. J Cataract Refract Surg. 1999;25:763-767.
31. Sen P, Kshetrapal M, Shah C, Mohan A, Jain E, Sen A. Posterior capsule opacification rate after phacoemulsification in pediatric cataract: Hydrophilic versus hydrophobic intraocular lenses. J Cataract Refract Surg. 2019;45:1380-1385.
32. Demirkılınç Biler E, Yıldırım Ş, Üretmen Ö, Köse S. Long-term Results in Pediatric Developmental Cataract Surgery with Primary Intraocular Lens Implantation. Turk J Ophthalmol. 2018;48:1-5.
33. Batur M, Gül A, Seven E, Can E, Yaşar T. Posterior Capsular Opacification in Preschool- and School-Age Patients after Pediatric Cataract Surgery without Posterior Capsulotomy. Turk J Ophthalmol. 2016;46:205-208.

Original Article

Multimodal Imaging of Reticular Pseudodrusen in Turkish Patients

Serap Bilge Çeper*, Filiz Afrashi**, Cumali Değirmenci**, Jale Menteş**, Serhad Nalçacı**, Cezmi Akkın**

*Malatya Training and Research Hospital, Clinic of of Ophthalmology, Malatya, Türkiye
**Ege University Faculty of Medicine, Department of Ophthalmology, İzmir, Türkiye

Abstract

Objectives: To investigate the presence and prevalence of reticular pseudodrusen (RPD) in patients with age-related macular degeneration using multiple imaging modalities and to compare the sensitivity and specificity of these modalities in the detection of RPD.

Materials and Methods: Images from a total of 198 consecutive patients were analyzed prospectively. Color fundus photography, red-free imaging, spectral domain optical coherence tomography (SD-OCT), infrared and blue reflectance (BR) imaging, fundus autofluorescence (FAF), enhanced-depth imaging OCT (EDI-OCT), fundus fluorescein angiography (FFA) and indocyanine green angiography were performed. RPD was diagnosed in the presence of relevant findings in at least two of the imaging methods used.

Results: RPD were detected in 149 eyes (37.6%). In the detection of RPD, color fundus photography, red-free photography, SD-OCT, infrared, FAF, BR, and FFA imaging had sensitivity values of 50%, 57.7%, 91.6%, 95%, 74.6%, 65.7%, and 28.2% and specificity values of 99.6%, 100%, 98.4%, 94.6%, 100%, 99.6%, and 69.8%, respectively.

Conclusion: Infrared imaging had the highest sensitivity. SD-OCT combined with infrared imaging was the most sensitive imaging technique for detecting RPD. The high specificity of FAF, red-free, and BR imaging may be useful to confirm a diagnosis of RPD.

Keywords: Age-related macular degeneration, imaging methods, reticular pseudodrusen, Turkish patients

Cite this article as: Çeper SB, Afrashi F, Değirmenci C, Menteş J, Nalçacı S, Akkın C. Multimodal Imaging of Reticular Pseudodrusen in Turkish Patients. Turk J Ophthalmol 2023;53:275-280

Address for Correspondence: Cumali Değirmenci, Ege University Faculty of Medicine, Department of Ophthalmology, İzmir, Türkiye
E-mail: cudegirmenci@yahoo.com **ORCID-ID:** orcid.org/0000-0002-8268-536X

Received: 22.01.2022 **Accepted:** 17.03.2023

DOI: 10.4274/tjo.galenos.2023.85616

Introduction

Reticular pseudodrusen (RPD) were first described by Mimoun et al.[1] in 1990 as "les pseudodrusen visible en lumiere bleue," referring to extramacular yellow deposits with an average diameter of 100 µm which were arranged in an interwoven network pattern and did not fluoresce on fluorescein angiography but became more visible under blue light. Arnold et al.[2] later coined the term "reticular pseudodrusen" and the morphology of RPD was further investigated. Since then, the term RPD has become widely used. Zweifel et al.[3] examined these lesions using spectral domain optical coherence tomography (SD-OCT) and showed in 2010 that they were located between the retinal pigment epithelium (RPE) and the inner segment/outer segment junction (recently referred to as the ellipsoid zone) and called them subretinal drusenoid deposits.

The reported incidence and prevalence of RPD vary based on the stage of age-related macular degeneration (AMD) and the imaging modality used. Very low rates were reported in community-based epidemiological studies based on color fundus images.[4,5] However, the prevalence of RPD cannot be determined accurately because diagnosis is dependent on the imaging modality and they show atypical distribution, are mistaken for typical drusen, and may disappear over time. RPD is associated with poor prognosis in AMD, which is a major cause of irreversible blindness in the older population. Therefore, the ability to detect and evaluate RPD via imaging and to determine their prevalence is of clinical importance.[6,7] The aim of this study was to prospectively investigate and analyze the presence and prevalence of RPD in consecutive patients diagnosed with AMD using multiple imaging modalities.

Materials and Methods

Patients who presented for the first time to the outpatient clinic of the Ege University Medical Faculty Hospital, Department of Ophthalmology and were diagnosed with AMD between September 2015 and September 2016 were

prospectively evaluated. Cooperative patients with AMD who were over 50 years of age, consented to the imaging procedures, had no media opacities that prevented imaging, had not been previously treated for AMD, had no additional retinal pathology, had no contraindication for the imaging methods used in the study, and had no advanced renal or hepatic pathology were included in the study. Patients under 50 years of age, those with media opacity, high myopia (refractive error greater than -6.00 diopters [D]), additional retinal pathology such as pathological myopia, idiopathic choroidal neovascularization (CNV), ocular histoplasmosis, angioid streaks, central serous chorioretinopathy, or retinal macroaneurysm, those who had been previously treated for AMD at another center, and those with fluorescein allergy were excluded from the study.

The study was conducted in compliance with Declaration of Helsinki and was approved by the Ethics Committee of the Ege University Medical Faculty (decision no: 15-11.1/5, date: 18.12.2015). Written informed consent was obtained from all patients enrolled.

The patients underwent a complete ophthalmologic examination including best corrected visual acuity (BCVA, expressed as logarithm of the minimum angle of resolution [logMAR]) assessment, intraocular pressure measurement, slit-lamp anterior segment examination, and posterior segment examination with a 90-D lens. All patients were examined using color and red-free fundus photography, macular SD-OCT, and infrared (IR), fundus autofluorescence (FAF), blue reflectance (BR), and fundus fluorescein angiography (FFA) imaging. In addition, indocyanine green angiography (ICGA) was performed in 66 eyes of 33 patients. Color fundus (50°) and red-free images were acquired with a Topcon 3D OCT-2000 (Topcon Medical Systems, Tokyo, Japan). Multimodal images including IR, BR, FAF (excitation 488 nm, emission >500 nm), macular OCT, ICGA, and FFA were obtained using a confocal scanning laser ophthalmoscope (Spectralis HRA+OCT; Heidelberg Engineering, Heidelberg, Germany). IR images of the macula were obtained at a resolution of 768 x 768 pixels using an excitation wavelength of 820 nm on a 55° area centered on the macula, while BR images were obtained using an excitation wavelength of 488 nm. In OCT image acquisition, 50 horizontal B-scans were obtained from a 30° x 20° or 30° x 25° macular area, depending on the patient. Each acquired B-scan was a composite of 50 B-scans averaged automatically by the device software. Subfoveal choroidal thickness was measured in the enhanced depth imaging mode of SD-OCT using the distance between the choriosclera border and the outer edge of the hyperreflective RPE at the fovea. Patients were classified as early, intermediate, or advanced AMD according to the multicenter Age-Related Eye Disease Study (AREDS) classification for AMD published in 2000.[8] Color fundus, red-free, SD-OCT, IR, FAF, BR, FFA, and ICGA images from each eye were independently assessed by two retina specialists and RPD was diagnosed if both specialists detected relevant findings by at least two of the methods.

RPD were identified as multiple yellowish-white reticular patterns on colored fundus images, and reticular pattern was identified as a bright interwoven network about 125-250 µm in width on red-free images. In addition, reticular lesions were identified as subretinal hyperreflective granular deposits on the RPE in at least one B-scan on SD-OCT, as hyporeflective lesions on a base of slightly increased hyperreflectivity in IR imaging, and as 5 or more small, hypoautofluorescent, round/oval lesions with indistinct margins surrounded by hyperautofluorescence on FAF imaging. RPD were identified as interwoven, hyperreflective lesions on BR imaging, as hypofluorescent dots appearing in the mid-late phase in ICGA, and as hypofluorescent dots in the early phase of FFA. In addition, RPD distribution in the macula was assessed by quadrant based on the Early Treatment Diabetic Retinopathy Study (ETDRS) grid. The ETDRS grid consists of 3 concentric circles 1, 3, and 6 mm in diameter, with the central 1-mm circle showing foveal thickness. The inner ring lying between the 1- and 3-mm circles and the outer ring between the 3- and 6-mm circles are divided into 4 sectors (inferior, superior, nasal, temporal). Finally, RPD were divided in three stages as described by Zweifel et al.[3]

Statistical Analysis

Chi-square, Shapiro-Wilk normality test, and Mann-Whitney U test were used for statistical analyses. The limit for statistical significance was set as $p<0.05$. All statistical analyses were performed with SPSS for Windows version 22 (IBM Corp., Armonk, NY, USA) software.

Results

The study was carried out on 396 eyes of 198 consecutive patients who met the inclusion criteria. The mean age was 72.0±7.74 years (range, 51-96 years); 102 (51.5%) patients were female and 96 (48.5%) were male. Mean BCVA was 0.46±0.56 logMAR (range, 0-3.10 logMAR). Mean subfoveal choroidal thickness was 203.5±75.31 µm (range, 45-436 µm).

Grading with the AREDS classification resulted in 145 eyes (36.6%) with early AMD, 86 eyes (21.7%) with intermediate AMD and 165 eyes (41.7%) with advanced AMD. The mean ages in these groups were 71.06±8.3, 71.59±7.2, and 73.04±7.3 years, respectively. There was no statistically significant difference when the stages were compared in terms of mean age.

Color fundus photography, red-free photography, SD-OCT, IR, FAF, BR, and FFA imaging had sensitivity values of 50%, 57.7%, 91.6%, 95%, 74.6%, 65.7%, and 28.2% and specificity values of 99.6%, 100%, 98.4%, 94.6%, 100%, 99.6%, and 69.8%, respectively, in the detection of RPD (Figure 1, Table 1). IR imaging had the highest sensitivity (95%), followed by SD-OCT (91.6%); however, specificity was higher in SD-OCT compared to IR imaging. Specificity was highest in red-free (100%), color fundus (99.6%), and BR imaging (99.6%), but their sensitivity was lower compared to IR, SD-OCT, and FAF. FFA had the lowest sensitivity and specificity.

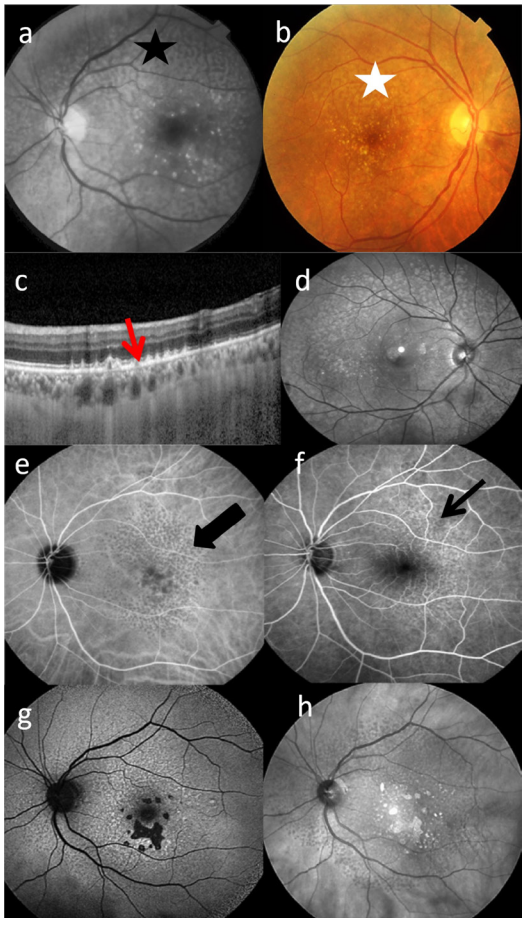

Figure 1. Appearance of reticular pseudodrusen on multimodal imaging. Appearance of the reticular pattern in red-free imaging (black star) (a) and color fundus photograph (white star) (b) Reticular pseudodrusen were identified as granular or triangular hyperreflective deposits located above the RPE in the subretinal space on SD-OCT imaging (red arrow) (c), a bright, interlacing network appearance on BR imaging (d), hypofluorescent dots on ICGA (bold black arrow) (e) and FFA (thin black arrow) (f), a grouping of hypofluorescent lesions with indistinct borders on a base of slightly increased autofluorescence on FAF imaging (g), and groups of hyporeflective lesions on a slightly hyperreflective background on IR imaging (h)

SD-OCT: Spectral domain optical coherence tomography, RPE: Retinal pigment epithelium, BR: Blue reflectance, ICGA: Indocyanine green angiography, FFA: Fundus fluorescein angiography, FAF: Fundus autofluorescence, IR: Infrared

Table 1. Sensitivity and specificity of imaging modalities in the detection of reticular pseudodrusen

Imaging method	Sensitivity (%)	Specificity (%)
Color fundus photography	50	99.6
Red-free photography	57.7	100
SD-OCT	91.6	98.4
Infrared imaging	95	94.6
FAF	74.6	100
BR imaging	65.7	99.6
FFA	28.2	69.8

SD-OCT: Spectral domain optical coherence tomography, FAF: Fundus autofluorescence, BR: Blue reflectance, FFA: Fundus fluorescein angiography

RPD were detected in at least two imaging methods in 149 (37.6%) of the eyes and were not detected in 247 eyes (62.4%). The prevalence of RPD detected in at least three imaging modalities was 30.5% (121 eyes). The mean age of patients with RPD was 73.98±7.33 years, which was significantly higher compared to the patients without RPD, whose mean age was 70.81±7.75 years (p<0.001). RPD were bilateral in 65 patients (77.4%) and unilateral in 19 patients (22.6%).

Forty-four (58.7%) of the patients with RPD were female and 31 (41.3%) were male. Statistical analysis showed RPD to be significantly more common among females. Of the patients without RPD, 58 were female and 65 were male. Statistical analysis revealed no significant sex difference between patients with and without RPD (p=0.038). Mean subfoveal choroid thickness was 167.94±62.7 µm in eyes with RPD and 224.83±74.3 µm among eyes without RPD. Eyes with RPD had significantly lower mean subfoveal choroidal thickness (p<0.001).

Mean BCVA was 0.42±0.49 logMAR in eyes with RPD and 0.48±0.6 logMAR in eyes without RPD. The difference in BCVA between eyes with and without RPD was not statistically significant (p=0.902).

One hundred eighteen eyes (29.8%) had neovascular AMD and 28 eyes (7.1%) had geographic atrophy. Of the 118 eyes with neovascular AMD, RPD was absent in 78 (66.1%) and present in 40 (33.9%). Of the 28 eyes with geographic atrophy, RPD was absent in 8 (28.6%) and present in 20 (71.4%). Among the 149 eyes with RPD, neovascular AMD (26.8%, 40 eyes) was significantly more common than geographic atrophy (13.4%, 20 eyes) (p<0.001). Of the 247 eyes without RPD, 97 had early AMD, 47 had intermediate AMD, and 103 had advanced AMD. Of the eyes with RPD, 48 had early AMD, 39 intermediate AMD and 62 advanced AMD. While RPD were more common in patients with advanced AMD, the difference did not reach statistical significance (p=0.178).

Analysis of the topographic distribution of macular RPD according to the ETDRS grid centered on the fovea showed that RPD was most common in the superior quadrant (100%), followed by the temporal quadrant (66%) (Figure 2). RPD were located nasal of the optic disc in 19.4% of eyes. In terms of area of distribution, RPD were located in at least 1 quadrant in 24

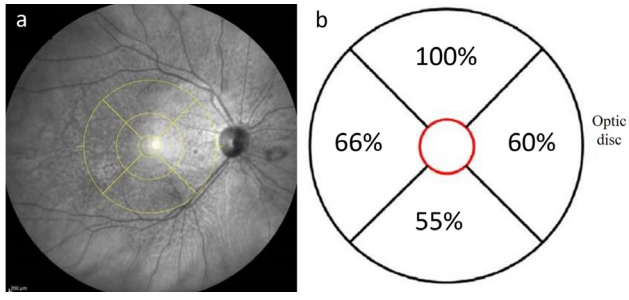

Figure 2. Illustration of the ETDRS grid used to determine the topographic distribution of RPD (a) and the prevalence of RPD in each quadrant (b)

ETDRS: Early Treatment Diabetic Retinopathy Study, RPD: Reticular pseudodrusen

eyes (17.6%), in at least 2 quadrants in 31 eyes (22.8%), in at least 3 quadrants in 32 eyes (23.5%), and in 4 quadrants in 49 eyes (39%). Progression of AMD stage was not associated with higher prevalence of RPD in the macula (p=0.779).

SD-OCT grading of RPD could not be done in 16 eyes because the RPD were located outside the OCT scanning area. Of the 133 eyes that had RPD in the macular area and could be staged, 77 (51.7%) did not exhibit stage 3 RPD, while 56 (37.6%) had stage 3 RPD in addition to stage 1 and stage 2 RPD. In other words, the "target" appearance corresponding to stage 3 was observed in 37.6% of the eyes. Presence of stage 3 RPD was not associated with more advanced AMD stage (p=0.058). ICGA was performed in 66 eyes of 33 patients. Of those 66 eyes, RPD were detected by other imaging modalities in 26 (39.4%) and ICGA was able to detect RPD in 25 eyes (96.2%).

Discussion

Although their clinical significance and pathophysiology are still not fully understood, RPD have been reported to be an early sign of the process leading to neovascular AMD and identified as a high-risk factor in many studies.[4,9,10,11,12] The incidence and prevalence of RPD vary in different studies based on AMD stage and the imaging modality used. Newer imaging modalities such as SD-OCT, IR imaging, FAF, and confocal scanning laser ophthalmoscopy have led to improvements in the diagnosis of RPD.[13] The higher sensitivity and specificity of some of these imaging methods have enabled a more accurate estimate of RPD prevalence based on multimodal imaging in more recent studies. Using blue fundus photography, IR, FAF, BR, ICGA, and SD-OCT, Ueda-Arakawa et al.[13] reported the prevalence of RPD as 20% in Japanese patients. Wilde et al.[14] determined a prevalence of 22.1% in their evaluation of 231 consecutive patients using OCT, color fundus photography, red-free photography, and FFA. Although Hogg et al.[10] concluded in 2014 that IR imaging was the modality that best visualizes RPD, this technique was not used in the study by Wilde et al.[14] In addition, it is reported that some patients may have had RPD prior to developing CNV, and that RPD regression or masking by hemorrhagic gliosis or fluid accumulation associated with CNV may result in a lower RPD detection rate. Ethnicity, sex, and age distribution may also play a role in the prevalence of RPD.[15] Using a wide variety of imaging techniques, we determined the prevalence of RPD to be 37.6% in our study. This high rate is also the result of using a wide SD-OCT scanning area as well as additional multimodal imaging techniques that display a larger area and allow the detection of RPD located outside the central macula. In a study conducted by De Bats et al.[16] using six imaging techniques, including color fundus photography, blue fundus photography, multicolor imaging, IR, FAF, and SD-OCT, RPD was detected in 149 eyes (61.3%) of 86 patients (68.8%). The high prevalence they reported compared to other studies may be attributed to the vast majority of their patients having late-stage AMD and the stronger association between RPD and advanced AMD.[16,17] The same group did not detect a statistical difference in RPD prevalence between the early and late stages of AMD. In our study, RPD were seen at every stage and were not statistically associated with a specific AREDS stage, which is consistent with previous studies.[18,19]

Significantly higher mean age and female preponderance were observed among the patients with RPD in our study. This is consistent with the literature. Lee et al.[15] found that the average age of those with RPD was significantly higher than that of patients without RPD. The same authors reported that the female sex predominated in the RPD patient group. Wilde et al.[14] reported in their study of 231 patients that RPD were more common in females, though they detected no age difference between those with and without RPD. While female sex is associated with a higher prevalence of systemic autoimmune inflammatory diseases, research is currently being conducted to determine whether there are inflammatory markers or pathogens associated with RPD. Although female sex and age were reported to be risk factors for RPD in various studies, other studies have not reported differences in age or sex between patients with and without RPD.[16,20]

Schmitz-Valckenberg et al.[21] reported that confocal scanning laser ophthalmoscopy imaging was superior to fundus photography for the detection of RPD and they recommended IR and FAF as optimal methods for the characterization of RPD. Ueda-Arakawa et al.[13] reported that color fundus photography, IR, FAF, near infrared-FAF, BR, ICGA, and SD-OCT had specificity of 100%, 91.8%, 95.0%, 95.3%, 100%, 100%, and 98.4% and sensitivity of 75.7%, 94.6%, 86.5%, 32.1%, 77.1%, 73.0%, and 94.6%, respectively, in the detection of RPD. In their study, SD-OCT was shown to have the highest sensitivity and specificity for detecting RPD. De Bats et al.[16] also reported that SD-OCT had the highest sensitivity and specificity in detecting RPD. In contrast, in a 2016 study by Gil et al.,[22] IR and FAF were the best imaging modalities for detecting RPD, followed by OCT. In the present study, eight imaging modalities (color fundus photography, red-free photography, BR imaging, IR imaging, FAF, SD-OCT, ICGA, and FFA) were used for a definitive RPD diagnosis. The sensitivity and specificity of ICGA could not be statistically evaluated because we were only able to perform ICGA on a small number of patients, as most of the patients could not purchase ICG stain. Therefore, sensitivity and specificity values were determined for seven imaging modalities. Sensitivity was highest in IR imaging (95%) and SD-OCT (91.6%), while SD-OCT had higher specificity compared to IR imaging. We found that FFA, red-free photography, and color fundus photography were inadequate for the detection of RPD. IR imaging was the most useful method for detecting RPD because it had the highest sensitivity and was less affected by media opacity, such as cataracts, than the other methods.[3] The sensitivity and specificity of SD-OCT were 91.6% and 98.4% in our study, which demonstrates the necessity of using this method when evaluating for RPD.

Because no imaging modality can detect RPD with 100% sensitivity, it is difficult to distinguish RPD from other changes

(soft/hard drusen) using a single imaging modality. Based on our study and others comparing different imaging techniques for visualizing RPD, it seems beneficial to use at least two imaging modalities to detect RPD and confirm the diagnosis, regardless of the techniques used.[13,16,23,24]

Several researchers have suggested a link between RPD and choroidal integrity. Switzer et al.[25] reported reduced subfoveal choroidal thickness in eyes with RPD. Although theories concerning the choroid vary greatly, they share choroidal thinning as an integral component in the appearance of RPD. In our study, subfoveal choroidal thickness was significantly lower in eyes with RPD. Querques et al.[26] found that the choroid was generally thinner in early AMD eyes with RPD compared to those without RPD. A hypothesis regarding the reduced subfoveal choroidal thickness in the presence of RPD and the choroidal etiology of RPD has not been fully clarified.[27] As RPD are associated with an increased risk of advanced AMD, choroidal thinning may be important to our understanding of the process underlying RPD and further research is needed on this topic.

While RPD are seen in every stage of AMD, neovascular AMD was more common than geographic atrophy among the eyes with RPD in our study. This may be related to the generally higher prevalence of CNV in cases of advanced AMD compared to geographic atrophy. The Beaver Dam Study found that eyes with RPD were at similar risk for both neovascular AMD (29%) and geographic atrophy (36%).[4] Smith et al.[23] also reported a high prevalence of both types of advanced AMD in patients with RPD. Although the relationship between RPD and late AMD is clear in the literature, the relative link between RPD and neovascular AMD and geographic atrophy remains uncertain. Lee et al.[15] detected bilateral RPD at a rate of 97.7%. This is higher than bilaterality rates reported in other studies, which range between 54.8% and 75.8%.[15,28] It was proposed that this finding was related to ethnic differences or the lower prevalence of neovascular AMD, which often causes RPD to disappear. In the present study, RPD were bilateral in 65 patients (77.4%) and unilateral in 19 patients (22.6%). Our bilaterality rate is also lower than that reported by Lee et al.,[15] which may be due to the higher prevalence of RPD among patients with neovascular AMD in our study.

In our analysis of the topographic distribution of macular RPD based on a fovea-centered ETDRS grid, RPD were most commonly found in the superior quadrant (100% of eyes), followed by the temporal quadrant (66% of eyes). There are a few other studies in which the topographic distribution of RPD has been analyzed using the ETDRS grid. In a study by Steinberg et al.,[29] RPD were found superior to the fovea in 100% of cases and nasal to the fovea in 81%. As confirmed by our results, RPD are most commonly located superior to the fovea.[4,26,30]

Conclusion

Considering the increasing importance of RPD, we investigated their prevalence in patients with AMD and determined the rate to be 37.6%. While IR imaging had the highest sensitivity of the 7 imaging modalities employed in our study, the combined use of SD-OCT and IR imaging may be beneficial in the detection of RPD. Due to the important prognostic information they provide, further research is needed regarding the detection and analysis of RPD.

Ethics

Ethics Committee Approval: The study was conducted in compliance with Declaration of Helsinki and was approved by the Ethics Committee of the Ege University Medical Faculty (decision no: 15-11.1/5, date: 18.12.2015).

Informed Consent: Obtained.

Peer-review: Externally peer-reviewed.

Authorship Contributions

Surgical and Medical Practices: S.B.Ç., F.A., J.M., C.A., Concept: S.B.Ç., F.A., C.D., S.N., Design: S.B.Ç., F.A., Data Collection or Processing: S.B.Ç., C.D., Analysis or Interpretation: S.B.Ç., F.A., C.D., S.N., J.M., C.A., Literature Search: S.B.Ç., Writing: S.B.Ç., C.D.

Conflict of Interest: No conflict of interest was declared by the authors.

Financial Disclosure: The authors declared that this study received no financial support.

References

1. Mimoun G, Soubrane G, Coscas G. Macular drusen. J Fr Ophtalmol. 1990;13:511-530.
2. Arnold JJ, Sarks SH, Killingsworth MC, Sarks JP. Reticular pseudodrusen. A risk factor in age-related maculopathy. Retina. 1995;15:183-191.
3. Zweifel SA, Spaide RF, Curcio CA, Malek G, Imamura Y. Reticular pseudodrusen are subretinal drusenoid deposits. Ophthalmology. 2010;117:303-312.
4. Klein R, Meuer SM, Knudtson MD, Iyengar SK, Klein BE. The epidemiology of retinal reticular drusen. Am J Ophthalmol. 2008;145:317-326.
5. Klein R, Klein BE, Jensen SC, Meuer SM. The five-year incidence and progression of age-related maculopathy: the Beaver Dam Eye Study. Ophthalmology. 1997;104:7-21.
6. Spaide RF, Curcio CA. Drusen characterization with multimodal imaging. Retina. 2010;30:1441-1454.
7. Zweifel SA, Imamura Y, Spaide TC, Fujiwara T, Spaide RF. Prevalence and significance of subretinal drusenoid deposits (reticular pseudodrusen) in age-related macular degeneration. Ophthalmology. 2010;117:1775-1781.
8. Ferris FL, Davis MD, Clemons TE, Lee LY, Chew EY, Lindblad AS, Milton RC, Bressler SB, Klein R; Age-Related Eye Disease Study (AREDS) Research Group. A simplified severity scale for age-related macular degeneration: AREDS Report No. 18. Arch Ophthalmol. 2005;123:1570-1574.
9. Joachim N, Mitchell P, Rochtchina E, Tan AG, Wang JJ. Incidence and progression of reticular drusen in age-related macular degeneration: findings from an older Australian cohort. Ophthalmology. 2014;121:917-925.
10. Hogg RE, Silva R, Staurenghi G, Murphy G, Santos AR, Rosina C, Chakravarthy U. Clinical characteristics of reticular pseudodrusen in the fellow eye of patients with unilateral neovascular age-related macular degeneration. Ophthalmology. 2014;121:1748-1755.
11. Sarks SH, Arnold JJ, Killingsworth MC, Sarks JP. Early drusen formation in the normal and aging eye and their relation to age related maculopathy: a clinicopathological study. Br J Ophthalmol. 1999;83:358-368.
12. Wu Z, Fletcher EL, Kumar H, Greferath U, Guymer RH. Reticular pseudodrusen: A critical phenotype in age-related macular degeneration. Prog Retin Eye Res. 2022;88:101017.

13. Ueda-Arakawa N, Ooto S, Tsujikawa A, Yamashiro K, Oishi A, Yoshimura N. Sensitivity and specificity of detecting reticular pseudodrusen in multimodal imaging in Japanese patients. Retina. 2013;33:490-497.
14. Wilde C, Patel M, Lakshmanan A, Morales MA, Dhar-Munshi S, Amoaku WM. Prevalence of reticular pseudodrusen in eyes with newly presenting neovascular age-related macular degeneration. Eur J Ophthalmol. 2016;26:128-134.
15. Lee MY, Yoon J, Ham DI. Clinical characteristics of reticular pseudodrusen in Korean patients. Am J Ophthalmol. 2012;153:530-535.
16. De Bats F, Mathis T, Mauget-Faÿsse M, Joubert F, Denis P, Kodjikian L. Prevelance of reticular pseudodrusen in age-related macular degeneration using multimodal imaging. Retina. 2016;36:46-52.
17. Finger RP, Wu Z, Luu CD, Kearney F, Ayton LN, Lucci LM, Hubbard WC, Hageman JL, Hageman GS, Guymer RH. Reticular pseudodrusen: a risk factor for geographic atrophy in fellow eyes of individuals with unilateral choroidal neovascularization. Ophthalmology. 2014;121:1252-1256.
18. Ueda-Arakawa N, Ooto S, Nakata I, Yamashiro K, Tsujikawa A, Oishi A, Yoshimura N. Prevalence and genomic association of reticular pseudodrusen in age-related macular degeneration. Am J Ophthalmol. 2013;155:260-269.
19. Farashi S, Ansell BRE, Wu Z, Abbott CJ, Pébay A, Fletcher EL, Guymer RH, Bahlo M. Genetics of reticular pseudodrusen in age-related macular degeneration. Trends Genet. 2022;38:312-316.
20. Boddu S, Lee MD, Marsiglia M, Marmor M, Freund KB, Smith RT. Risk factors associated with reticular pseudodrusen versus large soft drusen. Am J Ophthalmol. 2014;157:985-993.
21. Schmitz-Valckenberg S, Steinberg JS, Fleckenstein M, Visvalingam S, Brinkmann CK, Holz FG. Combined confocal scanning laser ophthalmoscopy and spectral-domain optical coherence tomography imaging of reticular drusen associated with age-related macular degeneration. Ophthalmology. 2010;117:1169-1176.
22. Gil JQ, Marques JP, Hogg R, Rosina C, Cachulo ML, Santos A, Staurenghi G, Chakravarthy U, Silva R. Clinical features and long-term progression of reticular pseudodrusen in age-related macular degeneration: findings from a multicenter cohort. Eye (Lond). 2017;31:364-371.
23. Smith RT, Sohrab MA, Busuioc M, Barile G. Reticular macular disease. Am J Ophthalmol. 2009;148:733-743.
24. Gliem M, Müller PL, Mangold E, Bolz HJ, Stöhr H, Weber BH, Holz FG, Charbel Issa P. Reticular Pseudodrusen in Sorsby Fundus Dystrophy. Ophthalmology. 2015;122:1555-1562.
25. Switzer DW, Engelbert M, Freund KB. Spectral domain optical coherence tomography macular cube scans and retinal pigment epithelium/drusen maps may fail to display subretinal drusenoid deposits (reticular pseudodrusen) in eyes with non-neovascular age-related macular degeneration. Eye (Lond). 2011;25:1379-1380.
26. Querques G, Querques L, Forte R, Massamba N, Coscas F, Souied EH. Choroidal changes associated with reticular pseudodrusen. Invest Ophthalmol Vis Sci. 2012;53:1258-1263.
27. Garg A, Oll M, Yzer S, Chang S, Barile GR, Merriam JC, Tsang SH, Bearelly S. Reticular pseudodrusen in early age-related macular degeneration are associated with choroidal thinning. Invest Ophthalmol Vis Sci. 2013;54:7075-7081.
28. Buitendijk GH, Hooghart AJ, Brussee C, de Jong PT, Hofman A, Vingerling JR, Klaver CC. Epidemiology of Reticular Pseudodrusen in Age-Related Macular Degeneration: The Rotterdam Study. Invest Ophthalmol Vis Sci. 2016;57:5593-5601.
29. Steinberg JS, Fleckenstein M, Holz FG, Schmitz-Valckenberg S. Foveal Sparing of Reticular Drusen in Eyes With Early and Intermediate Age-Related Macular Degeneration. Invest Ophthalmol Vis Sci. 2015;56:4267-4274.
30. Schmitz-Valckenberg S, Alten F, Steinberg JS, Jaffe GJ, Fleckenstein M, Mukesh BN, Hohman TC, Holz FG; Geographic Atrophy Progression (GAP) Study Group. Reticular drusen associated with geographic atrophy in age-related macular degeneration. Invest Ophthalmol Vis Sci. 2011;52:5009-5015.

Original Article

Combining Perfluorobutylpentane (F_4H_5) with Glaucoma Drainage Device Implantation for Silicone Oil-Induced Glaucoma: A Pilot Study

Stylianos A. Kandarakis*, Petros Petrou*, Spyridon Doumazos*, Konstantina Chronopoulou*, Leonidas Doumazos*, Ioannis Halkiadakis**, Ilias Georgalas*

*National and Kapodistrian University of Athens, G. Gennimatasgeneral Hospital, 1st Department of Ophthalmology, Athens, Greece
**Athens Eye Hospital, Ophthalmiatrion Athinon, Athens, Greece

Abstract

Objectives: Our aim was to perform a perfluorobutylpentane (F_4H_5) washout in conjunction with glaucoma drainage device (GDD) placement in patients with silicone oil (SO)-induced glaucoma. In this report we present our preliminary results concerning the effectiveness in clearing the SO and the safety of the procedure.
Materials and Methods: Eight patients who previously underwent pars plana vitrectomy with SO tamponade due to retinal detachment were selected. Removal of SO was performed on average 10 months after initial surgery. All patients developed glaucoma with evidence of SO remnants in the anterior chamber (AC) and angle. Removal of the remaining SO with F_4H_5 washout was performed in all cases with concomitant insertion of a GDD to treat the refractory glaucoma. Intraocular pressure (IOP), SO remnants, endothelial cell count, and need for glaucoma medications were evaluated up to 12 months after the surgical procedure.
Results: All patients had uneventful surgery with no major complications 12 months postoperatively. A marked reduction of SO remnants in the AC and angle was observed in all cases after surgery. There was a 60.9% decrease in mean IOP 12 months postoperatively ($p<0.05$) and the need for glaucoma medication was lower in all patients (mean topical medicines: 4 preoperatively vs. 0.75±0.89 postoperatively; $p<0.05$). Endothelial cell density showed no significant change (mean 2012±129 cells/mm^2 preoperatively vs. 1985±134 cells/mm^2 postoperatively; $p>0.05$), and there were no signs of corneal edema.
Conclusion: F_4H_5 is an effective emulsifier for removing SO remnants and may be safely used in conjunction with GDD placement in order to control IOP in eyes with silicone oil-induced glaucoma.

Keywords: Glaucoma drainage devices, silicon oil-induced glaucoma, silicon oil remnants, silicon oil removal, perfluorobutylpentane (F_4H_5)

Cite this article as: Kandarakis SA, Petrou P, Doumazos S, Chronopoulou K, Doumazos L, Halkiadakis I, Georgalas I. Combining Perfluorobutylpentane (F_4H_5) with Glaucoma Drainage Device Implantation for Silicone Oil-Induced Glaucoma: A Pilot Study. Turk J Ophthalmol 2023;53:281-288

Address for Correspondence: Stylianos A. Kandarakis, National and Kapodistrian University of Athens, G. Gennimatasgeneral Hospital, 1st Department of Ophthalmology, Athens, Greece
E-mail: s.kandarakis@gmail.com **ORCID-ID:** orcid.org/0000-0003-2912-7438
Received: 29.10.2022 **Accepted:** 14.02.2023

DOI: 10.4274/tjo.galenos.2023.95825

Introduction

The use of silicone oil (SO) in conjunction with pars plana vitrectomy (PPV) is strongly recommended in some complex vitreoretinal cases.[1] A great variety of vitreoretinal surgeries, including but not limited to proliferative vitreoretinopathy, trauma, recurrent retinal detachment, and retinitis, require the use of SO as an endotamponade medium.[2] Although SO is used to improve the final outcome and to reduce chances of relapse, complications may still occur. The most common complications of PPV with SO include cataract formation, endophthalmitis, retinal detachment, cystoid macular edema, hypotony, and ocular hypertension.[1,3,4] As far as ocular hypertension is concerned, it has been abundantly reported that there is increased risk of developing glaucoma or high intraocular pressure (IOP) following vitrectomy.[5] The overall incidence of glaucoma after uncomplicated PPV has been shown to range between 11.6% and 20%, and the prevalence increases up to 56% when SO is used as an endotamponade agent.[6,7,8,9] This highlights the fact that additional pathophysiologic mechanisms may attribute to acute or chronic IOP elevation secondary to SO use.[10] In a recent retrospective study including 196 patients, Lyssek-Boroń et al.[11] estimated the risk of developing chronic elevated IOP to be 4.7 times higher when SO was used with PPV.

Following restoration of the retinal anatomy after PPV + SO filling, removal of the SO is usually indicated to allow for potential improvement in visual acuity and to establish a normal range of IOP. However, normalization of IOP is not always achieved and patients may require medical treatment or even surgical intervention.[12,13] The incidence of surgical intervention in patients that have undergone PPV + SO filling varies in the literature.[12,14] Trabeculectomy has a low success rate after PPV, especially in SO-filled eyes, which have high rates of failure compared to glaucoma drainage device (GDD) implantation.[9,15,16] The success rate of Ahmed glaucoma valve

insertion to control IOP after PPV is reportedly high (80.7% at 5 years).[17] However, Gupta et al.[16] demonstrated more limited success (37% at 5 years) in PPV + SO-filled eyes.

Furthermore, SO has a propensity to emulsify into smaller droplets which can enter the anterior chamber (AC) and be detected via gonioscopy, appearing like "fish eggs" (shown in Figure 1B) or in more severe cases as an "inverse hypopyon."[18] These SO remnants in the AC can directly block the trabeculum and eventually cause elevation of IOP or even complicate a previous GDD implantation by blocking the drainage tube or leaking into the subconjunctival space.[19,20,21,22]

The complications caused by emulsified SO droplets can be prevented by removing them. A semifluorinated alkane (SFA) solvent can be used to solubilize the SO and enable its removal.[23] Perfluorohexyloctane was the first solvent used, but it yielded suboptimal results because it induced inflammation and was less effective in removing SO remnants.[23] Another solvent, perfluorobutylpentane (F_4H_5) has shown some promising results in washing out SO remnants more efficiently without causing inflammation.[23,24] Stalmans et al.[24] showed that F_4H_5 washout is safe and efficient in reducing SO remnants and seems to reduce postoperative SO-related complications.

In this report we present, to our knowledge for the first time, our preliminary results after combining F_4H_5 washout with GDD implantation in eyes that had uncontrolled IOP and SO remnants in the AC and angle after SO removal.

Materials and Methods

Eight patients were selected as candidates to use F_4H_5 washout in conjunction with GDD insertion (4 male and 4 female, mean age 66.5 years). All patients previously underwent a 23-gauge PPV with SO (5700 centistokes) tamponade for retinal detachment. SO removal was performed after a mean of 10 months (range 8-14 months) with concurrent phacoemulsification and intraocular lens (IOL) implantation. All the vitreoretinal surgeries were uncomplicated. All patients had signs of glaucomatous optical neuropathy with increased cup-to-disc ratio varying from 0.6 to 0.8. The average mean deviation in visual field was -9.3 decibels (±2.1) (Humphrey Field Analyzer 3, Carl Zeiss Meditec AG, Jena, Germany) and the mean retinal nerve fiber layer thickness on optical coherence tomography was 65 µm (±5 µm) (Heidelberg Spectralis, Heidelberg Engineering, Heidelberg Baden-Wurttemberg, Germany). Preoperative and postoperative visual acuity for each patient is shown in Table 1. After the vitreoretinal and phacoemulsification procedures, all patients exhibited high IOP which was not controlled by a maximum medical regimen, making them candidates for GDD insertion. In addition, it was observed (gonioscopy + photography) that SO remnants in the AC may be causing the increased IOP by blocking the trabecular meshwork (Figure 1A, B, Figure 2A, and Figure 3A). This fact made these patients ideal candidates for F_4H_5 washout to remove the SO remnants combined with GDD placement to manage IOP.

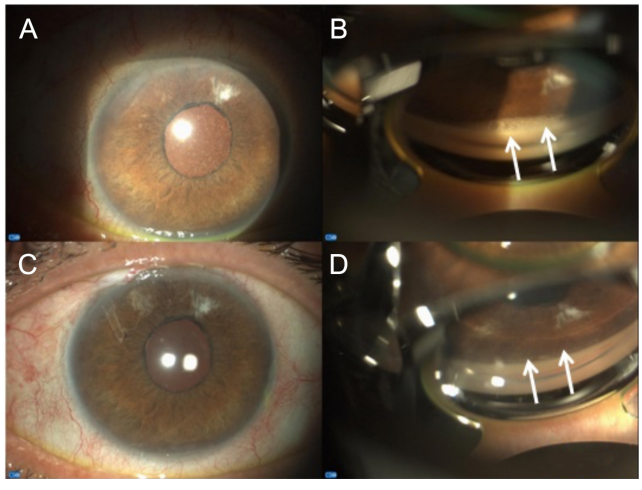

Figure 1. Patient 1: (A) Evidence of silicone oil (SO) remnants in the anterior chamber after SO removal. (B) Evidence of SO remnants (white arrows) in the superior aspect of the angle after SO removal possibly contributing to elevated intraocular pressure. (C) Anterior chamber 12 months after perfluorobutylpentane (F_4H_5) washout with concomitant Baerveldt 350-mm^2 implantation. (D) Superior angle 12 months after F_4H_5 washout with concomitant Baerveldt 350-mm^2 implantation, showing significantly fewer SO droplets present (white arrows)

All procedures were approved by the Ethics Committee of the G. Gennimatas Hospital in Athens (decision no: RN:#12042021004, date: 12/04/2021) and were conducted in accordance with the Declaration of Helsinki. Written consent was obtained from all patients both for the procedure and publication of their images. All patients underwent the same washout procedure of the AC with F_4H_5 (F_4H_5® WashOut, FLUORON GmbH, Germany) and concurrent GDD placement. Five patients received a 350-mm^2 103 Baerveldt implant (BAERVELDT® BG 103-250, Johnson & Johnson Surgical Vision, Inc., New Brunswick, New Jersey, United States) while 3 patients received an Ahmed valve implant (Ahmed® Glaucoma Valve FP7, Rancho Cucamonga, California, United States). Specifically, under sub-Tenon's anesthesia, a conjunctival peritomy was performed in the superotemporal quadrant followed by extensive conjunctival dissection. After identifying the superior and lateral rectus muscles, a 350-mm^2 Baerveldt implant was secured under the muscles using 10-0 nylon sutures. In eyes that received an Ahmed valve, after appropriate priming, the valve was secured in the superotemporal quadrant between the superior and lateral rectus muscles using 9-0 nylon sutures. Cautious cautery was used when necessary. Before tube insertion into the AC, a 2.4-mm corneal incision and paracentesis incision were created and a 27-gauge cannula was used to inject 2 mL of F_4H_5 into the AC for 5 min. The irrigation was performed towards the angle (360 degrees) and towards the pupil and IOL. Irrigation/aspiration (I/A) was then performed using a coaxial I/A metallic tip. A second irrigation of F_4H_5 was performed using the same procedure, followed by I/A. A small amount of cohesive viscoelastic was injected into the AC and the incisions were hydrated.

Tube insertion was performed using a 23-gauge cannula extending approximately 2 mm into the AC. The entry site

was posterior to Schwalbe's line and parallel to the iris as per standard technique. The tube was then secured to the sclera using 10-0 nylon sutures. In eyes that received a 350-mm^2 Baerveldt drainage device, the following additional steps were performed: a 4-0 Prolene (polypropylene) suture was inserted into the lumen of the tube, an 8-0 Vicryl (polyglactin 910) suture was used to securely watertight the lumen, and temporary fenestrations were made using a 30-gauge needle. For all GDDs, an alcohol-preserved scleral graft 2.5 mm x 2.5 mm was used to cover the tube at the entry site and was secured with nylon sutures. Finally, the conjunctiva was closed using 8-0 Vicryl sutures.

Clinical and photographic documentation was performed preoperatively (Figure 1A, B, Figure 2A, Figure 3A), at postoperative day 1, and at 1, 6, and 12 months postoperatively (Figure 1C, D, Figure 2B, Figure 3C). During the follow-up period, the patients were checked for IOP (Goldmann applanation tonometry), complications, SO remnants in AC, specifically

Table 1. Pre- and postoperative intraocular pressure (mmHg) and visual acuity (Snellen) values and postoperative medical treatment

			Preoperative			Postoperative				
Patient	Age (y)/sex	Eye	VA	IOP	GDD	IOP at 1 month	IOP at 6 months	IOP at 12 months	Topical Medicines	VA
#1	65/M	Right	8/10	38	Baerveldt	18	13	13	β-blocker	8/10
#2	63/F	Left	9/10	35	Baerveldt	15	9	9	None	9/10
#3	67/F	Right	7/10	28	Baerveldt	12	14	13	β-blocker	7/10
#4	68/M	Right	8/10	27	Baerveldt	10	12	15	None	8/10
#5	66/M	Left	7/10	46	Ahmed	14	16	17	β-blocker + CAI	7/10
#6	70/M	Right	6/10	29	Ahmed	8	10	9	None	7/10
#7	65/F	Left	8/10	35	Ahmed	11	9.5	14	β-blocker + CAI	8/10
#8	68/F	Left	9/10	28	Baerveldt	22	15	14	None	9/10
Mean ± SD			33.3±6.58		13.8±4.56	12.3±2.63	13±2.78	0.75±0.89		

VA: Visual acuity, IOP: Intraocular pressure, GDD: Glaucoma drainage device, M: Male, F: Female, SD: Standard deviation

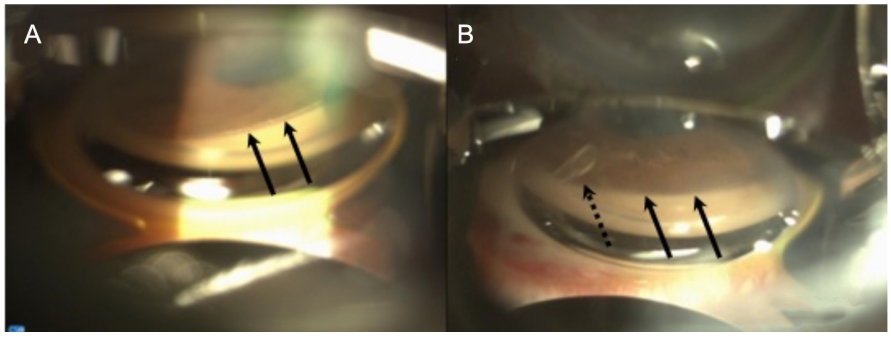

Figure 2. Patient 2: (A) Emulsified silicone oil droplets in the superior angle resembling "fish eggs" (black arrows). (B) Postoperative gonioscopy in the same patient, showing absence of silicone oil (black arrows) and appropriately placed tube (dashed arrow)

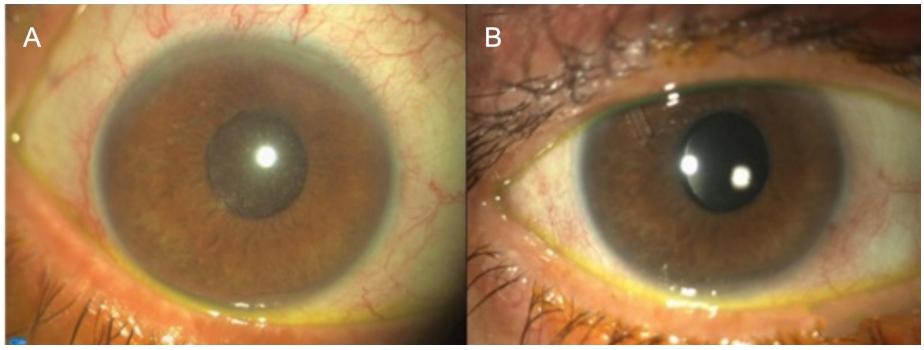

Figure 3. Patient 3: Anterior chamber with circulating silicone oil droplets prior to perfluorobutylpentane (F_4H_5) washout (A) and after F_4H_5 washout and Baerveldt 350-mm^2 placement (B)

at the angle (gonioscopy), and postoperative endothelial cell density (ECD) (CellChek X™ Specular Microscope; Konan Medical, Irvine, CA, USA). All glaucoma surgical procedures were performed by the same surgeon (S.K.) at the 1st Department of Ophthalmology of the National and Kapodistrian University of Athens at the G. Gennimatas General Hospital. IOP measurements were performed by two separate residents and mean IOP was used for documentation. If there was a difference of more than 3 mmHg between the two measurements, a third was taken by a consultant and that value was used.

Statistical Analysis

Microsoft Excel was utilized to collect the data and statistical calculations were performed using statistical software R (version 3.5.1, Foundation for Statistical Computing, Vienna, Austria). Descriptive statistics of the study population are reported as mean ± standard deviation for continuous variables. IOP differences at all postoperative visits, differences in the number of glaucoma medications and differences in ECD at 12-month follow-up were assessed using paired t-tests. All statistical tests were two-sided and p values less than 0.05 were considered statistically significant.

Results

All patients underwent successful F_4H_5 washout in conjunction with either Baerveldt 350 mm^2 or Ahmed valve implantation in the superior quadrant. None of the patients who received a Baerveldt 350 mm^2 implant required removal of the 4-0 Prolene intraluminal suture and no significant complications were observed.

The patients' mean preoperative IOP was 33.25 mmHg (±6.58) with maximum topical therapy and oral carbonic anhydrase inhibitor (CAI) therapy (250 mg twice daily, Acetazolamide 250 mg, Crescent Pharma Ltd, Basingstoke, England). The mean IOP was decreased by 60.9% at postoperative 12 months, reaching 13 mmHg (±2.78) ($p<0.05$). At 1-month follow-up, the mean IOP fell significantly to 13.75 mmHg (±4.56), a 58.6% drop compared to preoperative levels ($p<0.05$), while at 6 months after surgery the mean IOP was 12.3 mmHg (±2.63) (Figure 4). These results indicate a sustained low IOP for at least 12 months postoperatively.

The amount of topical therapy also decreased significantly after F_4H_5 washout with GDD implantation. The number of topical medicines prescribed was 4 per patient preoperatively and fell significantly to a mean of 0.75 (±0.89) postoperatively (81.3% reduction) ($p<0.05$). Specifically, patients 1 and 3 required a topical β-blocker drop (twice daily, Temserin 0.25%, Vianex, Athens, Greece) to maintain the low IOP, while patients 5 and 7 required both topical β-blocker (twice daily) and CAI drops (twice daily). The remaining 4 patients did not require any postoperative medical treatment for at least the duration of our maximum follow up period. Pre- and postoperative IOP results and postoperative treatments are presented in Table 1.

ECD quantified before and after the procedure showed no significant change in any of the patients. The mean ECD was 2012.38 cells/mm^2 (±129) preoperatively and 1985.13 cells/mm^2 (±134) postoperatively ($p>0.05$). No signs of corneal edema were evident in any of the patients. The patients' ECD values are presented in Table 2.

In all patients, there was a marked reduction in residual SO droplets in the AC and angle as evaluated by a masked ophthalmologist (D.P.) and evidenced in their postoperative photographs (Figure 1A, D, Figure 2A, B, Figure 3A, C).

Discussion

Combining PPV with SO filling remains a common surgical approach for patients with multiple retinal pathologies.[1] Removal of the SO usually follows and is sometimes combined with phacoemulsification and IOL implantation.[1] While acute IOP

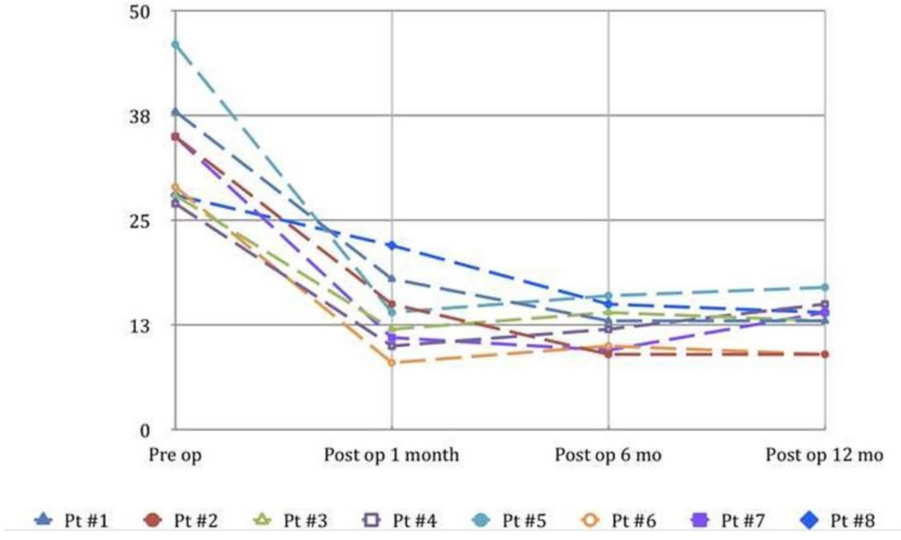

Figure 4. Graphical representation of intraocular pressure measurements of each patient preoperatively (preop) and during the postoperative (postop) follow-up period at 1 month, 6 months, and 12 months

Table 2. Pre- and postoperative epithelial cell density (ECD) values (cells/mm²)		
Patient	**Preoperative ECD**	**Postoperative ECD**
1	1947	1902
2	2159	2120
3	1983	2050
4	1826	1751
5	1902	1899
6	2205	2167
7	2090	1997
8	1987	1995
Mean ± SD	2012±129	1985±134
SD: Standard deviation		

rise is frequently due to SO overfilling, aqueous misdirection, iris-lens diaphragm shifting, and AC inflammation, chronic IOP elevation is commonly associated with angle synechiae, neovascularization, and emulsified SO droplets in the AC infiltrating the trabeculum.[2,5,21]

Potential mechanisms of SO-induced glaucoma mainly include the migration of emulsified SO particles into the AC, which can cause mechanical blockage or inflammation of the trabecular meshwork, impairing aqueous humor outflow.[9,10,18,21] Reported rates of late-onset glaucoma in eyes that received SO varies widely, from 2.2% to 56%.[9] Risk factors include preexisting glaucoma, diabetes mellitus, and aphakia, while the role of cataract extraction in postoperative IOP remains uncertain.[6,7,8] It has been hypothesized that the natural lens has a protective role against oxidative stress, which could potentially cause alterations in the trabecular meshwork and impair aqueous outflow.[6] On the other hand, some reports dispute the assumption that vitrectomy increases the risk of glaucoma or that the lens has a protective role.[25,26]

Emulsification of SO occurs due to factors that decrease its surface tension within a medium, causing it to initially disperse and subsequently emulsify.[27] These proteins or other molecules are surface acting particles (surfactants) which are usually present in inflammatory, infectious, or hemorrhagic conditions. These are often the complex and challenging conditions for which SO use is usually indicated, thus increasing the chances of emulsification.[21,28] However, the crucial factor affecting SO emulsification is the duration of SO tamponade in the eye. Some studies have shown that initial signs of SO emulsification occurred on average at 13.2 months of SO tamponade, while others indicated that emulsification can occur as early as 5 months after SO injection in some cases.[21,27,28] Although higher viscosity SO has been shown to be more resistant to deformation and thus less likely to disperse and eventually emulsify, it is also more difficult to remove, especially using small-gauge cannulas (sub-25 gauge).[21]

In our study, all patients included underwent SO removal combined with cataract extraction on average 10 months after the initial SO injection and developed refractory glaucoma. Whether lens removal contributed to the postoperative IOP rise remains unclear, although in all cases SO remnants were evident in the AC and the angle, thus identifying a well-documented cause for IOP elevation.[9,10,21,29,30,31,32] Since all patients had inadequate IOP control despite maximum medical treatment, GDD implantation was indicated.

However, the presence of SO remnants after SO removal represents a great challenge for glaucoma surgeons who are asked to surgically reduce IOP, given the potential risk of SO blockage of the tube lumen when a GDD is implanted.[14,19] Interestingly, cases where SO has migrated under the conjunctiva through the tube have also been described, highlighting the problem even further.[19,22,31,32,33]

According to the literature, there is no gold standard method on how a surgeon should approach these cases, including only SO removal, GDD implantation, or a combination of both. Honavar et al.[29] in a retrospective analysis of 150 eyes showed that adequate IOP control was not achieved in any of the cases by SO removal alone, but there was an overall 45.5% success rate when additional antiglaucoma medication was used. In contrast, Nguyen et al.[30] showed that 8 out of 14 eyes (57%) had IOP control after performing SO removal alone.

On the other hand, according to Chan et al.,[28] evidence of emulsified SO particles in the AC seen on slit-lamp biomicroscopy only partially reflects the magnitude of the emulsified SO and indicates the presence of many more small emulsified droplets which may be associated with complications such as open-angle glaucoma. In addition, electron microscopy of enucleated eyes previously filled with SO showed evidence of tiny emulsified SO droplets within the trabecular meshwork, suggesting that simply removing the visible bulk of SO does not necessary mean that the trabecular meshwork is free of SO and that IOP will drop.[34] Budenz et al.[13] argued that SO removal alone to control IOP tends to result in uncontrolled IOP with an increased need for glaucoma surgery. Furthermore, Moisseiev et al.[12] reported that after SO removal alone, IOP control could not be achieved in their patients even after glaucoma surgery was performed.

To reduce the aforementioned potential side effects of SO remnants, F_4H_5 has successfully and safely been used previously as a rinse in routine SO removal.[24] Specifically, F_4H_5 is a liquid SFA which is a colorless, physically and chemically inert

compound with a low density. In addition, it has excellent properties of low interface and surface tension, as well as being amphiphilic. Its chemical formula is $C_4F_9C_5H_{11}$ and it has an RFRH configuration. The RF segment gives the lipophobic properties of the compound while the RH segment (alkane) provides its lipophilic properties. Thus, lipophobia increases with the length of the RF segment while lipophilia increases with the length of the RH segment. F_4H_5 as well as other SFA are efficient and biocompatible solvents of SO. According to the general properties of SFAs, the longer the RH group and lower the viscosity of the SO, the better their solubility in each other.[35] However, F_4H_5 is able to dissolve SO more efficiently than other SFAs, as both *in vitro* and *in vivo* studies have previously shown.[23,36] Specifically, its superiority lies in the fact that admixtures of SO and F_4H_5 do not demonstrate phase separation (oil-in-water effect), and at room temperature these substances are mixable at every ratio, producing a transparent and homogenous solution.[23,35]

In our study, we evaluated the efficacy of SO remnant removal using F_4H_5 as a washout solution with simultaneous glaucoma valve implantation to maximize IOP lowering and avoid complications associated with SO remnants in the AC. To our knowledge, this is the first time published in the literature that F_4H_5 washout was performed in combination with GDD implantation in eyes that underwent SO removal and still had evident SO remnants in the angle and AC as well as glaucoma while under maximum medical treatment.

Our preliminary results, although limited, show that F_4H_5 washout may be successfully combined with either a Baerveldt 350-mm^2 or an Ahmed valve implantation. Overall, the postoperative course was uneventful, with no complications. IOP was significantly lower and remained under control for at least 12 months in all patients, with an average reduction in IOP of 60.9% after 12 months ($p<0.05$). Additionally, the need for IOP-lowering medications was significantly less than preoperatively, as we went from maximum topical treatment (4 IOP-lowering drugs) to an average of 0.75 (±0.89) drugs per patient. Specifically, patient 5 had the highest initial IOP in our study before surgery (46 mmHg). After F_4H_5 washout and Ahmed valve implantation, this patient's IOP fell by 29 mmHg (63%) to 17 mmHg after 12 months, albeit with dual medical treatment (β-blocker + CAI twice daily). The smallest IOP reduction was observed in patient 4, whose IOP dropped 12 mmHg (44.4%) after the surgical procedure to reach 15 mmHg, although this was achieved without the need for medical treatment. The largest percentage drop in IOP after our washout procedure in combination with a Baerveldt implantation was observed in patient 2, who had a 74.3% drop in IOP from 35 to 9 mmHg. Interestingly, patients receiving an Ahmed valve had a higher percentage drop in IOP at the end of our follow-up period (63.6%) than patients receiving the Baerveldt drainage device (58.9%). However, patients receiving the Ahmed valve required an average of 1.3 topical medications to control IOP, whereas those who received a Baerveldt device required an average of only 0.4. Therefore, even from our preliminary data it is clear that we achieved the desired IOP-lowering effect while reducing the need for IOP-lowering medication.

Photographic documentation obtained before and after surgery demonstrated the level of SO remnants in the AC (Figure 1A, D, Figure 2A, B, Figure 3A, B). The presence of SO was significantly reduced in the AC and angle, while no signs of SO were evident under the conjunctiva or obstructing the tube in any of the patients, suggesting the high success of F_4H_5 in binding and dissolving small SO droplets. This was also confirmed by a masked ophthalmologist who independently examined the patients for the presence of SO remnants in the AC and angle before and after surgery.

Previous studies where an Ahmed glaucoma valve was placed in eyes filled with SO have shown favorable results.[37] Ishida et al.[37] published a 70.2% success rate after Ahmed valve implantation in SO-filled eyes while highlighting that eyes containing SO have increased risk of failure compared to eyes without SO. Notably, they reported that in 40% of eyes with SO there were SO droplets evident in the tube, 10% of which eventually failed. Eyes without SO had a success rate of 87.2%.[37] Another study showed similar success rates (76% at 1 year) after Ahmed valve placement in SO-filled eyes.[38] More comparable to our cases, Gupta et al.[16] reported a 59.3% success rate in IOP control after placing an Ahmed glaucoma valve in eyes after SO removal, achieving an average of 56.9% IOP reduction. As the reasons are multifactorial, we cannot safely conclude as to why the success rate of Gupta et al.[16] was lower than in cases without SO. However, one reason may be the direct effect of SO on the trabeculum, as well as SO remnants as in our cases. In addition, given our current results we cannot also assume that our washout technique was solely or primarily responsible for the success of the GDD in reducing IOP. However, according to the previous reports mentioned above together with our own experience, SO remnants can greatly affect the outcome of GDD placement. Even the procedure itself can affect the success, as the maneuvering and fluidics during tube placement can shift remaining SO to other parts of the trabeculum, negatively affecting IOP even further. We believe a safe, quick, and efficient wash of the AC with F_4H_5 may prove to be an essential step before glaucoma surgery in such patients.

Even though F_4H_5 has been shown to be biocompatible with no significant toxic effects on the eye, it has been suggested that SFA could have a potentially negative effect on the endothelial cells.[35,39,40] A study on porcine corneas by Wenzel et al.[40] showed that short-term exposure to F_4H_5 had no significant toxic effect on endothelial cells, while prolonged exposure (over 60 minutes) increased morphological changes. In the present study, ECD measured pre- and postoperatively showed no significant changes (Table 2). This indicates that a short F_4H_5 washout up to 10 minutes (5 min x 2) in duration is safe and effective in removing the residual SO particles from the AC and, as evidenced from the IOP results, it may also contribute to overall IOP control.

Study Limitations

The limitations of this study undoubtedly include the small sample size. However, due to our promising results, we presented our preliminary data in this report. In addition, this study was not multicentered and all surgical procedures were conducted by a single surgeon. The follow-up time was relatively short (12 months), but in our view this is sufficient to be able to draw some reasonable conclusions from this work.

Conclusion

In conclusion, F_4H_5 is an SFA that can be safely used in combination with GDD placement. An AC washout may be performed prior to conventional Baerveldt 350-mm^2 or Ahmed valve implantation to reduce SO presence in the AC and angle in an effort to reduce the risk of tube blockage and the general adverse effects of SO remnants. Randomized controlled studies with larger numbers of patients are needed in the future to enable definitive conclusions on the safety and efficacy of the technique.

Ethics

Ethics Committee Approval: The study was approved by the Ethics Committee of the G. Gennimatas Hospital in Athens (decision no: RN:#12042021004, date: 12/04/2021) and was conducted in accordance with the Declaration of Helsinki.

Informed Consent: Obtained.

Peer-review: Externally and internally peer-reviewed.

Authorship Contributions

Surgical and Medical Practices: S.A.K., P.P., Concept: I.G., Design: S.D., L.D., Data Collection or Processing: K.C., Analysis or Interpretation: I.H., I.G., Literature Search: K.C., S.D., L.D., Writing: S.A.K., S.D.

Conflict of Interest: No conflict of interest was declared by the authors.

Financial Disclosure: The authors declared that this study received no financial support.

References

1. Pollack JS, Sabherwal N. Small gauge vitrectomy: operative techniques. Curr Opin Ophthalmol. 2019;30:159-164.
2. Cornacel C, Dumitrescu OM, Zaharia AC, Pirvulescu RA, Munteanu M, Tataru CP, Istrate S. Surgical Treatment in Silicone Oil-Associated Glaucoma. Diagnostics (Basel). 2022;12:1005.
3. Stein JD, Zacks DN, Grossman D, Grabe H, Johnson MW, Sloan FA. Adverse events after pars plana vitrectomy among medicare beneficiaries. Arch Ophthalmol. 2009;127:1656-1663.
4. Day S, Grossman DS, Mruthyunjaya P, Sloan FA, Lee PP. One-year outcomes after retinal detachment surgery among medicare beneficiaries. Am J Ophthalmol. 2010;150:338-345.
5. Rossi T, Ripandelli G. Pars Plana Vitrectomy and the Risk of Ocular Hypertension and Glaucoma: Where Are We? J Clin Med. 2020;9:3994.
6. Chang S. LXII Edward Jackson lecture: open angle glaucoma after vitrectomy. Am J Ophthalmol. 2006;141:1033-1043.
7. Luk FO, Kwok AK, Lai TY, Lam DS. Presence of crystalline lens as a protective factor for the late development of open angle glaucoma after vitrectomy. Retina. 2009;29:218-224.
8. Koreen L, Yoshida N, Escariao P, Niziol LM, Koreen IV, Musch DC, Chang S. Incidence of, risk factors for, and combined mechanism of late-onset open-angle glaucoma after vitrectomy. Retina. 2012;32:160-167.
9. Kornmann HL, Gedde SJ. Glaucoma management after vitreoretinal surgeries. Curr Opin Ophthalmol. 2016;27:125-131.
10. Ichhpujani P, Jindal A, Jay Katz L. Silicone oil induced glaucoma: a review. Graefes Arch Clin Exp Ophthalmol. 2009;247:1585-1593.
11. Lyssek-Boroń A, Krysik K, Jankowska-Szmul J, Grabarek BO, Osuch M, Kijonka M, Dobrowolski D. Comparison of Methods of Endotamponade Used During 23-Gauge Pars Plana Vitrectomy and the Risk of Raised Intraocular Pressure During 24-Month Follow-Up: A Retrospective Study of 196 Patients. Med Sci Monit. 2019;25:9327-9334.
12. Moisseiev J, Barak A, Manaim T, Treister G. Removal of silicone oil in the management of glaucoma in eyes with emulsified silicone. Retina. 1993;13:290-295.
13. Budenz DL, Taba KE, Feuer WJ, Eliezer R, Cousins S, Henderer J, Flynn HW Jr. Surgical management of secondary glaucoma after pars plana vitrectomy and silicone oil injection for complex retinal detachment. Ophthalmology. 2001;108:1628-1632.
14. de Vries MM, Müskens RP, Renardel de Lavalette VW, Hooymans JM, Jansonius NM. Glaucoma drainage device surgery after vitreoretinal surgery: incidence and risk factors. Acta Ophthalmol. 2016;94:135-139.
15. Singh D, Chandra A, Sihota R, Kumar S, Gupta V. Long-term success of mitomycin-augmented trabeculectomy for glaucoma after vitreoretinal surgery with silicone oil insertion: a prospective case series. Retina. 2014;34:123-128.
16. Gupta S, Chaurasia AK, Chawla R, Kapoor KS, Mahalingam K, Swamy DR, Gupta V. Long-term outcomes of glaucoma drainage devices for glaucoma post-vitreoretinal surgery with silicone oil insertion: a prospective evaluation. Graefes Arch Clin Exp Ophthalmol. 2016;254:2449-2454.
17. Pandav SS, Thattaruthody F, Singh SR, Chandra KK, Seth NG, Kaur S, Kaushik S, Raj S. Long-term Outcome of Ahmed Glaucoma Valve Implantation in Eyes With Intractably Raised Intraocular Pressure Following Pars Plana Vitrectomy. J Glaucoma. 20211;30:362-367.
18. Mangouritsas G, Mourtzoukos S, Portaliou DM, Georgopoulos VI, Dimopoulou A, Feretis E. Glaucoma associated with the management of rhegmatogenous retinal detachment. Clin Ophthalmol. 2013;7:727-734.
19. Friberg TR, Fanous MM. Migration of intravitreal silicone oil through a Baerveldt tube into the subconjunctival space. Semin Ophthalmol. 2004;19:107-108.
20. Chan CK, Tarasewicz DG, Lin SG. Subconjunctival migration of silicone oil through a Baerveldt pars plana glaucoma implant. Br J Ophthalmol. 2005;89:240-241.
21. Miller JB, Papakostas TD, Vavvas DG. Complications of emulsified silicone oil after retinal detachment repair. Semin Ophthalmol. 2014;29:312-318.
22. Téllez J, Vela JI, Luna S, Delgado R. Massive Silicone Oil Migration into the Subconjunctival Space: A Leakage Mechanism Dilemma. Case Rep Ophthalmol. 2018;9:310-314.
23. Liang Y, Kociok N, Leszczuk M, Hiebl W, Theisinger B, Lux A, Joussen AM. A cleaning solution for silicone intraocular lenses: "sticky silicone oil". Br J Ophthalmol. 2008;92:1522-1527.
24. Stalmans P, Pinxten AM, Wong DS. Cohort Safety and Efficacy Study of Siluron2000 Emulsification-Resistant Silicone Oil and F4h5 in the Treatment of Full-Thickness Macular Hole. Retina. 2015;35:2558-2566.
25. Yu AL, Brummeisl W, Schaumberger M, Kampik A, Welge-Lussen U. Vitrectomy does not increase the risk of open-angle glaucoma or ocular hypertension--a 5-year follow-up. Graefes Arch Clin Exp Ophthalmol. 2010;248:1407-1414.
26. Lalezary M, Kim SJ, Jiramongkolchai K, Recchia FM, Agarwal A, Sternberg P Jr. Long-term trends in intraocular pressure after pars plana vitrectomy. Retina. 2011;31:679-685.
27. Toklu Y, Cakmak HB, Ergun SB, Yorgun MA, Simsek S. Time course of silicone oil emulsification. Retina. 2012;32:2039-2044.
28. Chan YK, Cheung N, Chan WS, Wong D. Quantifying silicone oil emulsification in patients: are we only seeing the tip of the iceberg? Graefes Arch Clin Exp Ophthalmol. 2015;253:1671-1675.

29. Honavar SG, Goyal M, Majji AB, Sen PK, Naduvilath T, Dandona L. Glaucoma after pars plana vitrectomy and silicone oil injection for complicated retinal detachments. Ophthalmology. 1999;106:169-177.
30. Nguyen QH, Lloyd MA, Heuer DK, Baerveldt G, Minckler DS, Lean JS, Liggett PE. Incidence and management of glaucoma after intravitreal silicone oil injection for complicated retinal detachments. Ophthalmology. 1992;99:1520-1526.
31. Nazemi PP, Chong LP, Varma R, Burnstine MA. Migration of intraocular silicone oil into the subconjunctival space and orbit through an Ahmed glaucoma valve. Am J Ophthalmol. 2001;132:929-931.
32. Morales J, Shami M, Craenen G, Wentlandt TF. Silicone oil egressing through an inferiorly implanted ahmed valve. Arch Ophthalmol. 2002;120:831-832.
33. Parwar BL, Coleman AL, Small KW. Silicone oil migration through an Ahmed valve. Retina. 2002;22:657-658.
34. Wickham L, Asaria RH, Alexander R, Luthert P, Charteris DG. Immunopathology of intraocular silicone oil: enucleated eyes. Br J Ophthalmol. 2007;91:253-257.
35. Meinert H, Roy T. Semifluorinated alkanes A new class of compounds with outstanding properties for use in ophthalmology. Eur J Ophthalmol. 2000;10:189-197.
36. Stappler T, Williams R, Wong D. F4H5: a novel substance for the removal of silicone oil from intraocular lenses. Br J Ophthalmol. 2010;94:364-367.
37. Ishida K, Ahmed II, Netland PA. Ahmed glaucoma valve surgical outcomes in eyes with and without silicone oil endotamponade. 2009;18:325-330.
38. Al-Jazzaf AM, Netland PA, Charles S. Incidence and management of elevated intraocular pressure after silicone oil injection. J Glaucoma. 2005;14:40-46.
39. Mackiewicz J, Mühling B, Hiebl W, Meinert H, Maaijwee K, Kociok N, Lüke C, Zagorski Z, Kirchhof B, Joussen AM. In vivo retinal tolerance of various heavy silicone oils. Invest Ophthalmol Vis Sci. 2007;48:1873-1883.
40. Wenzel DA, Kunzmann BC, Druchkiv V, Hellwinkel O, Spitzer MS, Schultheiss M. Effects of Perfluorobutylpentane (F4H5) on Corneal Endothelial Cells. Curr Eye Res. Curr Eye Res. 2019;44:823-831.

Original Article

Evaluation of Agreement Between Sweep Visual Evoked Potential Testing and Subjective Visual Acuity

Osman Ahmet Polat*, Hidayet Şener*, Zekeriya Çetinkaya**, Hatice Arda*

*Erciyes University Faculty of Medicine, Department of Ophthalmology, Kayseri, Türkiye
**Elbistan State Hospital, Clinic of Ophthalmology, Kahramanmaraş, Türkiye

Abstract

Objectives: The primary objective of this study was to evaluate the agreement of visual acuity (VA) obtained with the sweep visual evoked potential (sVEP) method with the VA obtained with the Snellen chart. The secondary objective was to examine the effect of age and gender on agreement.

Materials and Methods: Best corrected VAs of subjects were recorded with the Snellen chart, and sVEP testing was performed according to the recommendations of the International Society for Clinical Electrophysiology of Vision (ISCEV). Snellen VAs and sVEP measurements were analyzed using logMAR conversion for statistical analysis. Agreement was evaluated with Bland-Altman analysis.

Results: The study included 49 subjects with a mean age of 53.5±17.3 years (range: 19-75 years) and mean Snellen VA of 0.31±0.32 logMAR (range: 1.3-0.0 logMAR). In the Bland-Altman analysis, the mean differences between the VA and sVEP measurements (VA-sVEP) were significantly different and outside the limits of agreement (p=0.035). A significant proportional bias (p=0.0007) was found in the regression analysis performed between VA-sVEP and the mean VA. According to the Bland-Altman analysis of sex subgroups, there was a significant difference between VA and sVEP measurements in female subjects (p=0.006). The difference between VA and sVEP measurement increased significantly with older age (R^2: 0.306, p<0.001, β: 0.05 [0.03, 0.08]).

Conclusion: In conclusion, sVEP measurements and VAs did not show statistical agreement. Cranial anatomy and endocrine differences of the subjects may affect their sVEP measurements. The difference between the methods varies according to VA level. Directly using sVEP results instead of VA would not be appropriate.

Keywords: Visual evoked potentials, spatial frequency limits, Snellen, sweep VEP, pattern VEP

Cite this article as: Polat OA, Şener H, Çetinkaya Z, Arda H. Evaluation of Agreement Between Sweep Visual Evoked Potential Testing and Subjective Visual Acuity. Turk J Ophthalmol 2023;53:289-293

Address for Correspondence: Osman Ahmet Polat, Erciyes University Faculty of Medicine, Department of Ophthalmology, Kayseri, Türkiye
E-mail: osmanahmet@gmail.com **ORCID-ID:** orcid.org/0000-0002-3905-4941

Received: 29.03.2022 **Accepted:** 27.01.2023

DOI: 10.4274/tjo.galenos.2023.37622

Introduction

Visual acuity (VA) is the most commonly measured visual function and an important part of routine ophthalmology practice. Psychophysical VA is an important clinical assessment, typically measured using subjective tests such as naming, pointing, or matching letters or symbols on calibrated charts. However, an electrophysiological evaluation may be required for assessment in non-cooperative individuals (pediatric age group, individuals with intellectual disability, simulating or converting individuals).[1,2,3,4]

Sweep visual evoked potential (sVEP) is a type of VEP testing used for the evaluation of visual function. In the sVEP method, the stimulator generates a pattern stimulus that alternates at a high temporal frequency and produces a visual evoked response. To measure VA, the size of the pattern is rapidly reduced and the smallest pattern that produces a response is detected, and VA is determined by regression analysis.[5,6]

Some studies evaluating the agreement and relationship between sVEP measurements and psychophysical VA demonstrated a statistically significant difference between the two methods, while other studies found the two methods to be similar.[7,8,9,10] Disagreement between the two methods may be explained by the fact that VEPs arise from the fovea and perifovea and the test is dynamic, whereas psychophysical VA requires a small number of cones and is a static test.[11,12,13] Despite this, sVEP measurement may be the only safe method available for VA evaluation when the psychophysical method is not possible. In this study, our primary objective was to evaluate the agreement between VA measured by sVEP and psychophysical VA obtained with the Snellen chart. Our secondary objective was to examine the effect of age and sex on agreement.

Materials and Methods

All procedures performed in studies involving human participants followed the ethical standards of the 1964 Helsinki Declaration and its later amendments or comparable ethical standards. The study protocol was approved by the Erciyes University Local Ethics Committee (decision no: 2020/622, date: 16.12.2020). Informed consent was obtained from all individual participants included in the study.

Best corrected VAs of the subjects were recorded using the Snellen chart at a distance of six meters (ACP-700 auto chart projector, Unicos Co., Korea). Routine anterior and posterior segment examinations were performed for all subjects.

Forty-nine subjects with different vision levels (between 0.05 and 1.0 decimal) according to the Snellen chart were included in the study. Data from both eyes of each patient were recorded. One eye was analyzed for each participant by random selection using the www.randomizer.org website.

Sweep VEP (Metrovision HVM-MonPackOne, France) recordings were performed according to the recommendations of the International Society for Clinical Electrophysiology of Vision (ISCEV) for the VEP spatial frequency limit.[1,14] In order to measure VA, the size of the pattern was reduced rapidly. Twenty different pattern sizes (1.5-30 cycles per degree [cpd]) were presented in succession, within 11 seconds for each sweep. Recording parameters were as follows: stimulation frequency 12 Hz, analysis window 1.3 s, and checkerboard stimulus. Ganzfeld background mean luminance was approximately 50 cd/m^2 and spatial resolution was 1024 x 768. A discrete Fourier transform was performed on the recorded signals. While recording, the subjects were asked to look at the red fixation point in the middle of the screen. The active electrode was placed on the occipital midline (Oz), the reference electrode was placed on the frontal midline (Fz), and the neutral electrode was placed on the forehead. The fellow eye was covered with an eye patch. The necessary refraction correction was applied and the pupil was not dilated. The device software automatically determined VA as the smallest pattern size that produced a response.

Statistical Analysis

Psychophysical VAs and sVEP measurements were converted from decimal to logMAR for statistical analysis. All VA results in the text, tables, and graphs are presented in logMAR. Statistical analysis was performed using MedCalc version 20 and SPSS version 22. Descriptive statistics were calculated and agreement between psychophysical VAs and sVEP measurements was evaluated with Bland-Altman analysis. According to distribution normality, parametric (paired-samples t, independent-samples t) and non-parametric (Wilcoxon signed-rank, Mann-Whitney U) tests and Pearson or Spearman correlation analysis were performed. Linear regression analysis was performed between age and the difference between psychophysical VA and sVEP measurement.

Results

The subjects ranged in age from 19 to 75 years (53.5±17.3 years); 14 (28.6%) were male and 35 (71.4%) were female. The patients were heterogeneous in terms of visual impairments and etiologies (e.g., age-related macular degeneration, diabetic retinopathy, macular hole, glaucoma). Subgroup analysis was not performed because the number of patients was not sufficient. The mean best-corrected psychophysical VA was 0.31±0.32 logMAR (range: 1.3-0.0 logMAR). The mean sVEP measurement was 0.26±0.28 (range: 1.3-0.05 logMAR). There was a significant difference between the overall mean psychophysical logMAR VA and sVEP measurements (p=0.030). However, a strong correlation was found between individuals' psychophysical logMAR VA and sVEP measurements (r=0.815, p<0.001). Psychophysical logMAR VA and sVEP measurements were also compared within the sex subgroups. The results are presented in Table 1.

There was no significant difference in the ratios of right and left eyes between the male and female subgroups. There was also no significant difference in psychophysical logMAR VA between the male and female subgroups, although women had significantly higher sVEP measurements than men. Comparisons between the male and female subgroups are presented in Table 2.

In the Bland-Altman analysis, the mean differences between the psychophysical logMAR VA and sVEP measurements (VA-sVEP) were significantly different and outside the limits of agreement (p=0.035). There was a significant proportional bias (p=0.0007) in the regression analysis performed between the VA-sVEP and the mean psychophysical VA (logMAR). No fixed bias was found. The regression equation was sVEP= 0.24 [0.10, 0.38] Snellen - 0.02 [-0.08, 0.03]. There was a significant proportional bias in the female subgroup (p=0.0015). The Bland-Altman plots and table are presented in Figure 1

Table 1. Comparison of psychophysical visual acuity and sVEP measurements

	Psychophysical visual acuity	sVEP measurement	p
Entire group with random eye selection	0.31±0.32	0.26±0.38	0.030*
Male	0.41±0.37	0.40±0.31	0.767
Female	0.28±0.30	0.20±0.25	0.003*

Values are expressed as logMAR, mean ± standard deviation. *Statistically significant p value (<0.05, Wilcoxon test), sVEP: Sweep visual evoked potentials

Table 2. Comparison of psychophysical visual acuity and sVEP measurements by sex

Variables	Male	Female	p
Eye (right/left)	6/8	23/12	0.141
Psychophysical VA	0.41±0.37	0.28±0.30	0.200
sVEP measurement	0.40±0.31	0.20±0.25	0.028*

Values are expressed as logMAR, mean ± standard deviation. *Statistically significant p value (<0.05, Pearson chi-square and Mann-Whitney U tests), VA: Visual acuity, sVEP: Sweep visual evoked potentials

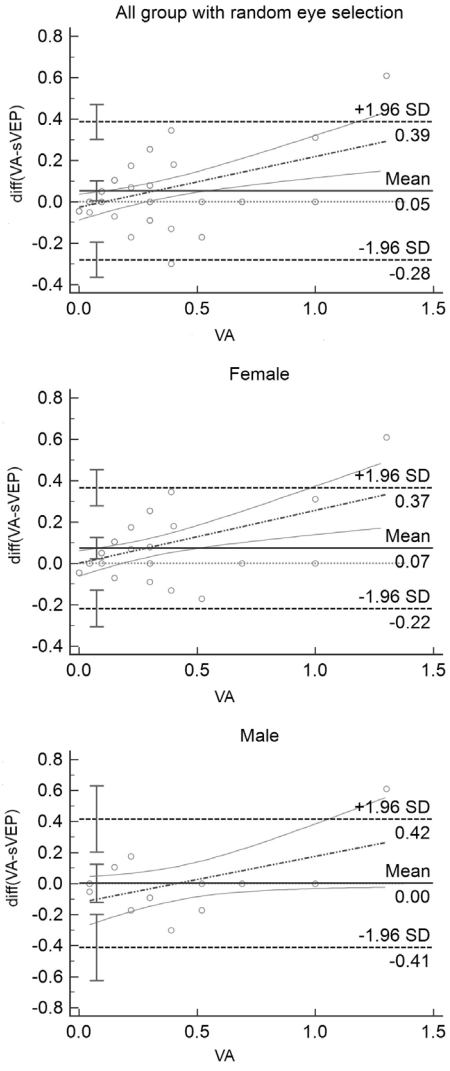

Figure 1. Bland-Altman plots of agreement between psychophysical (Snellen) visual acuity (VA) and sweep visual evoked potential (sVEP) values. Data were converted to logMAR values for the plots. There was a proportional bias for all subjects and female subjects. There was agreement between methods for male subjects

and Table 3. A correlation was found between age and VA-sVEP according to regression analysis (R^2: 0.306, p<0.001, β: 0.05 [0.03, 0.08]) and is presented in Figure 2.

Discussion

Our study showed that the psychophysical VAs (logMAR) and sVEP measurements (logMAR) were not statistically in agreement. The difference between the methods (VA-sVEP) varied according to level of visual acuity. At low vision levels, sVEP measurements were higher than psychophysical logMAR VA. We also found that VA-sVEP was moderately correlated with age. Finally, we found that the two methods showed poor agreement in female subjects.

The agreement between psychophysical VA and sVEP measurement depends on many factors, including the type of visual impairment (e.g., corneal, retinal, and optic nerve pathologies, cataract), non-identical optotypes (e.g., E chart, Landot C chart, and Snellen chart), non-identical stimuli (e.g., checkerboards and sinusoidal), the use of different techniques used to separate signal from noise, age, and other individual and technical factors.[4,7] In studies conducted with etiologically heterogeneous groups, it has been shown that sVEP measurement exceeds the psychophysical VA at low vision levels, which is consistent with our study.[4] In a study that evaluated psychophysical VA using different stimuli, it was stated that psychophysical VA was better than sVEP measurement, but contrary to our study, there was agreement between the methods in subjects with low vision and disagreement in subjects with high vision.[15] In a study evaluating the repeatability of psychophysical VA and sVEP measurement between visits and sessions, the intraclass correlation coefficient was 0.88 for psychophysical VA and 0.71 for sVEP, indicating that sVEP has slightly worse repeatability than psychophysical VA.[16] These results show that agreement between methods depends on the type of visual impairment, as well as temporal and methodological factors.

In our study, we found a correlation between age and VA-sVEP. sVEP measurements were lower than psychophysical VA before age 40 but higher after age 40. We could explain this situation by clustering people with low level of VA aged 40 years and older in our study group (Figure 2). When the literature is

Table 3. Analysis of agreement between psychophysical visual acuity and sVEP visual acuity

Variables		VA-sVEP [95% CI]	p (H_0: mean=0)	Lower limit [95% CI]	Upper limit [95% CI]
Entire group with random eye seleciton		0.052 [0.003, 0.100]	0.035*	-0.280 [-0.364, -0.196]	0.385 [0.301, 0.469]
	Reg. equation	sVEP = -0.025 [-0.086, 0.036] + **0.244 [0.108, 0.380]** Snellen			
Male		0.001 [-0.120, 0.123]	0.981	-0.412 [-0.626, -0.199]	0.415 [0.201, 0.629
Female		0.072 [0.021, 0.124]	0.006*	-0.219 [-0.307, -0.130]	0.365 [0.276, 0.453]
	Reg. equation	sVEP = -0.001 [-0.060, 0.062] + **0.255 [0.104, 0.406]** Snellen			

Values are expressed as logMAR. *Statistically significant p value (<0.05 Bland Altman test results), statistically significant confidence intervals (p value <0.05) shown in bold; VA, sVEP: Difference between psychophysical visual acuity and sweep visual evoked potential measurements, CI: Confidence interval; Reg.: Regression

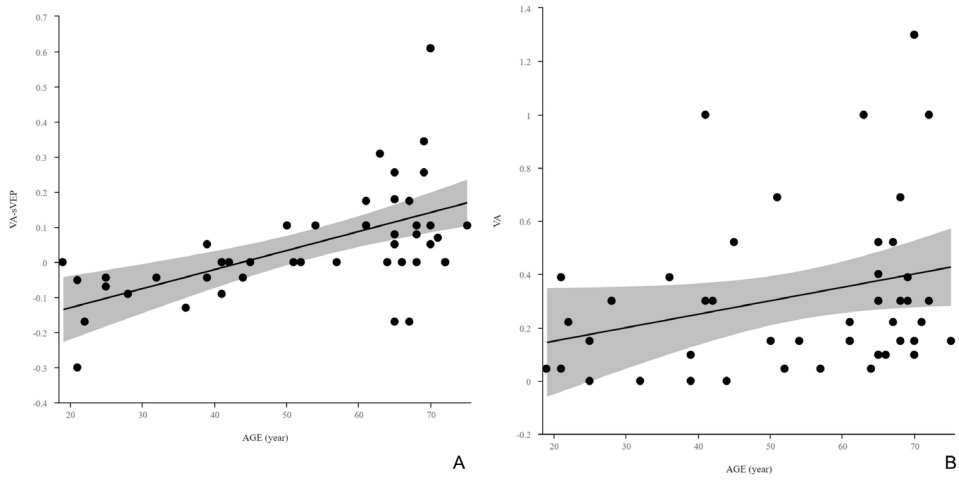

Figure 2. Scatter plots between age and the difference between Snellen visual acuity (VA) and sweep visual evoked potential (sVEP) values (VA-sVEP) (A) and VA (B). The difference between the two methods increased with age and was located outside the confidence interval in graph A. Subjects with low VA were more clustered in the older age group in graph B

reviewed, the opposite is expected, as age-related reduction in spatial frequency and reduced retinal illumination due to senile miosis are expected.[17,18] In the sex-based analysis, we found that sVEP measurement was higher than psychophysical VA in female subjects. This may be due to endocrine differences, and there are studies in the literature showing that female patients have higher VEP amplitudes and shorter implicit time.[19,20,21] When VEP parameters were evaluated in pregnant and non-pregnant women, a shortening of implicit time was observed in pregnant women. This difference was attributed to differences in circulating sex steroids, and it was suggested that this effect may be the main reason for the difference between the sexes.[22] Sex-related variations in the anatomical cranial structure may be another reason.[23,24]

A VEP is electrophysiological signals derived from electroencephalographic (EEG) activity and recorded from the visual cortex in the occipital region. Skull thickness has been reported as one of the factors affecting EEG responses.[25] The size, location, and spatial arrangement of human brain networks can vary between subjects.[26] The visual cortex can also show individual variations. Furthermore, it has been shown that VEP amplitude is higher and latency is shorter in dominant eyes compared to nondominant eyes.[27,28] Another factor to consider is binocular rivalry.[29] It has been suggested that rivalry underlies amplitude fluctuations in monocularly recorded VEP.[30,31] It has been reported that both eyes are not synchronized and there are fluctuations in VEP responses.[32] Psychophysical VA test also assesses cognitive function. However, sVEP assesses cellular electrical activity, not cognitive functions. In addition, sVEP is a dynamic test, there is no fixed target like Snellen, so it is more visible to the patient.[13] These may differ between subjects and may ultimately be the cause of differences between the two methods.

Study Limitations

Our study may have some limitations. The average age of the participants was relatively high, so our results may not provide information about the agreement between measurements in younger patients. Another limitation was the inability to include subjects in all age ranges and at every visual level for both sexes. Information on the etiology of low vision of the patients was not presented and could not be analyzed. Our last limitation is that we converted decimal VA to logMAR VA; we could not directly measure logMAR VA.

Conclusion

In conclusion, sVEP measurement and psychophysical VA did not have statistical agreement. When subjects were evaluated according to gender, psychophysical VA and sVEP measurements were not statistically congruent for female subjects. Individual cranial anatomy and endocrine-chemical differences may affect sVEP results. The difference between measurements varies according to the VA level. It would not be correct to use sVEP results directly instead of VA. It would be appropriate to detect the bias between sweep VEP and psychophysical VA and to correct the measurement values in clinical practice.

Ethics

Ethics Committee Approval: All procedures performed in studies involving human participants were in accordance with the ethical standards of the Erciyes University Local Ethics Committee (approval no: 2020/622, date: 16.12.2020) and with the 1964 Helsinki Declaration and its later amendments or comparable ethical standards.

Informed Consent: Informed consent was obtained from all individual participants included in the study.

Authorship Contributions

Concept: O.A.P., Z.Ç., H.A., Design: O.A.P., Z.Ç., H.A., Data Collection or Processing: O.A.P., H.Ş., Z.Ç., Analysis or Interpretation: O.A.P., H.Ş., Z.Ç., H.A., Literature Search: O.A.P., H.Ş., Writing: O.A.P., H.Ş.

Conflict of Interest: No conflict of interest was declared by the authors.

Financial Disclosure: The authors declared that this study received no financial support.

References

1. Hamilton R, Bach M, Heinrich SP, Hoffmann MB, Odom JV, McCulloch DL, Thompson DA. ISCEV extended protocol for VEP methods of estimation of visual acuity. Doc Ophthalmol. 2021;142:17-24.
2. Jeon J, Oh S, Kyung S. Assessment of visual disability using visual evoked potentials. BMC Ophthalmol. 2012;12:36.
3. Almoqbel F, Leat SJ, Irving E. The technique, validity and clinical use of the sweep VEP. Ophthalmic Physiol Opt. 2008;28:393-403.
4. Hamilton R, Bach M, Heinrich SP, Hoffmann MB, Odom JV, McCulloch DL, Thompson DA. VEP estimation of visual acuity: a systematic review. Doc Ophthalmol. 2021;142:25-74.
5. Campbell FW, Maffei L. Electrophysiological evidence for the existence of orientation and size detectors in the human visual system. J Physiol. 1970;207:635-652.
6. Harter MR, White CT. Evoked cortical responses to checkerboard patterns: effect of check-size as a function of visual acuity. Electroencephalogr Clin Neurophysiol. 1970;28:48-54.
7. Ridder WH, Waite BS, Melton TF. Comparing enfant and PowerDiva sweep visual evoked potential (sVEP) acuity estimates. Doc Ophthalmol. 2014;129:105-114.
8. Bach M, Maurer JP, Wolf ME. Visual evoked potential-based acuity assessment in normal vision, artificially degraded vision, and in patients. Br J Ophthalmol. 2008;92:396-403.
9. Chen SA, Wu LZ, Wu DZ. Objective measurement of contrast sensitivity using the steady-state visual evoked potential. Doc Ophthalmol. 1990;75:145-153.
10. Allen D, Norcia AM, Tyler CW. Comparative study of electrophysiological and psychophysical measurement of the contrast sensitivity function in humans. Am J Optom Physiol Opt. 1986;63:442-449.
11. Williams DR. Aliasing in human foveal vision. Vision Res. 1985;25:195-205.
12. Armington JC. The electroretinogram, the visual evoked potential, and the area-luminance relation. Vision Res. 1968;8:263-276.
13. Campbell FW, Maffei L. The influence of spatial frequency and contrast on the perception of moving patterns. Vision Res. 1981;21:713-721.
14. Odom JV, Bach M, Brigell M, Holder GE, McCulloch DL, Mizota A, Tormene AP; International Society for Clinical Electrophysiology of Vision. ISCEV standard for clinical visual evoked potentials: (2016 update). Doc Ophthalmol. 2016;133:1-9.
15. Ridder WH. A comparison of contrast sensitivity and sweep visual evoked potential (sVEP) acuity estimates in normal humans. Doc Ophthalmol. 2019;139:207-219.
16. Ridder WH, Tong A, Floresca T. Reliability of acuities determined with the sweep visual evoked potential (sVEP). Doc Ophthalmol. 2012;124:99-107.
17. Sokol S, Moskowitz A, Towle V. Age-related changes in the latency of the visual evoked potential: influences of check size. Electroencephalogr Clin Neurophysiol. 1981;51:559-562.
18. Wright CE, Williams DE, Drasdo N, Harding GF. The influence of age on the electroretinogram and visual evoked potential. Doc Ophthalmol. 1985;59:365-384.
19. Sharma R, Joshi S, Singh KD, Kumar A. Visual Evoked Potentials: Normative Values and Gender Differences. J Clin Diagn Res. 2015;9:12-15.
20. Steffensen SC, Ohran AJ, Shipp DN, Hales K, Stobbs SH, Fleming DE. Gender-selective effects of the P300 and N400 components of the visual evoked potential. Vision Res. 2008;48:917-925.
21. Ekayanti MS, Mahama CN, Ngantung DJ. Normative values of visual evoked potential in adults. Indian J Ophthalmol. 2021;69:2328-2332.
22. Marsh MS, Smith S. Differences in the pattern visual evoked potential between pregnant and non-pregnant women. Electroencephalogr Clin Neurophysiol. 1994;92:102-106.
23. Gregori B, Pro S, Bombelli F, La Riccia M, Accornero N. Vep latency: sex and head size. Clin Neurophysiol. 2006;117:1154-1157.
24. Dion LA, Muckle G, Bastien C, Jacobson SW, Jacobson JL, Saint-Amour D. Sex differences in visual evoked potentials in school-age children: what is the evidence beyond the checkerboard? Int J Psychophysiol. 2013;88:136-142.
25. Hagemann D, Hewig J, Walter C, Naumann E. Skull thickness and magnitude of EEG alpha activity. Clin Neurophysiol. 2008;119:1271-1280.
26. Anderson KM, Ge T, Kong R, Patrick LM, Spreng RN, Sabuncu MR, Yeo BTT, Holmes AJ. Heritability of individualized cortical network topography. Proc Natl Acad Sci U S A. 2021;118:e2016271118.
27. Strasser T, Nasser F, Langrová H, Zobor D, Lisowski Ł, Hillerkuss D, Sailer C, Kurtenbach A, Zrenner E. Objective assessment of visual acuity: a refined model for analyzing the sweep VEP. Doc Ophthalmol. 2019;138:97-116.
28. Shams L, Kamitani Y, Thompson S, Shimojo S. Sound alters visual evoked potentials in humans. Neuroreport. 2001;12:3849-3852.
29. Ellingham RB, Waldock A, Harrad RA. Visual disturbance of the uncovered eye in patients wearing an eye patch. Eye (Lond). 1993;7:775-778.
30. Petersen J. Amplitude fluctuations of the monocular checkerboard Ver caused by binocular rivalry. Visual electrodiagnosis in systemic diseases. Springer; 1980:245-248.
31. Lansing RW. Electroencephalographic correlates of binocular rivalry in man. Science. 1964;146:1325-1327.
32. Brown RJ, Norcia AM. A method for investigating binocular rivalry in real-time with the steady-state VEP. Vision Res. 1997;37:2401-2408.

Original Article

Clinical Findings and Optical Coherence Tomography Measurements of Pediatric Patients with Papilledema and Pseudopapilledema

Ayşin Tuba Kaplan*, Sibel Öskan Yalçın*, Safiye Güneş Sağer**

*University of Health Sciences Türkiye, Kartal Dr. Lütfi Kırdar City Hospital, Clinic of Ophthalmology, İstanbul, Türkiye
**University of Health Sciences Türkiye, Kartal Dr. Lütfi Kırdar City Hospital, Clinic of Pediatric Neurology, İstanbul, Türkiye

Abstract

Objectives: To compare the clinical findings and multimodal imaging of pediatric patients diagnosed with papilledema and pseudopapilledema with those of healthy individuals.

Materials and Methods: Ninety children (<18 years of age) referred for suspected papilledema were included in this study. All patients underwent optical coherence tomography (OCT) imaging and were compared with normal control subjects.

Results: Fifty-eight children diagnosed with pseudopapilledema, 32 children with mild-to-moderate papilledema, and 40 controls were evaluated. The average and all quadrants of retinal nerve fiber layer (RNFL) thickness were significantly higher in the papilledema group than in the pseudopapilledema and control groups ($p<0.001$). Bruch's membrane opening (BMO) measurements were similar in both groups ($p>0.05$). The average, nasal, and temporal RNFL thicknesses were significantly higher in the pseudopapilledema group compared with the controls ($p<0.001$). Area under the receiver operating characteristic (ROC) curve showed high diagnostic ability for RNFL thickness in all quadrants to differentiate papilledema from pseudopapilledema ($p<0.001$). In the pseudopapilledema group, average, temporal, and inferior RNFL thickness and BMO measurements were significantly higher in eyes with optic nerve head drusen (n=28) compared with those without drusen (n=88) ($p=0.035$, $p=0.022$, $p=0.040$ and, $p=0.047$ respectively).

Conclusion: Papilledema and pseudopapilledema show great differences in evaluation, follow-up, and prognosis. Using non-invasive methods such as newly developed OCT techniques in differential diagnosis can relieve patients with pseudopapilledema from the stress and financial burden of expensive, extensive, and invasive procedures.

Keywords: Optic nerve, drusen, papilledema, optical coherence tomography, tilted disc

Cite this article as: Kaplan AT, Öskan Yalçın S, Sağer SG. Clinical Findings and Optical Coherence Tomography Measurements of Pediatric Patients with Papilledema and Pseudopapilledema. Turk J Ophthalmol 2023;53:294-300

Address for Correspondence: Ayşin Tuba Kaplan, University of Health Sciences Türkiye, Kartal Dr. Lütfi Kırdar City Hospital, Clinic of Ophthalmology, İstanbul, Türkiye
E-mail: aysintuba@yahoo.com **ORCID-ID:** orcid.org/0000-0003-0793-5530
Received: 17.09.2022 **Accepted:** 15.02.2023
DOI: 10.4274/tjo.galenos.2023.81504

Introduction

Optic nerve head edema due to increased intracranial pressure is called papilledema. Pseudopapilledema is not true edema but is defined by the presence of blurring and swelling at the borders of the optic nerve head due to structural anomalies.[1] Especially in children, distinguishing the two diagnoses is vital. Misdiagnosis of papilledema as pseudopapilledema can be life-threatening, and conversely, diagnosis of pseudopapilledema as papilledema can lead to unnecessary, invasive, and expensive procedures and treatments.[1,2]

The prevalence of optic nerve head drusen (ONHD) is approximately 0.4% in children and 2.4% in adults. This difference is probably due to the smaller and deeper location of drusen in children.[3,4,5,6] High hypermetropia, crowded or congenitally anomalous optic nerves, and tilted optic discs may also cause a pseudopapilledema appearance in children.[7,8]

To diagnose true papilledema, neuroimaging (computed tomography [CT], magnetic resonance imaging [MRI]) and invasive procedures (lumbar puncture [LP]) are required. Performing these tests in children is not easy and may require sedation or general anesthesia. Non-invasive imaging modalities such as ocular ultrasonography (USG), fundus autofluorescence (FAF), and optical coherence tomography (OCT) can help diagnose true and pseudopapilledema.

The purpose of this study was to present the clinical data of our pediatric patients who were diagnosed as having pseudopapilledema or papilledema and to compare their OCT findings with healthy subjects.

Materials and Methods

Patients under 18 years of age who were diagnosed as having pseudopapilledema or mild papilledema and had at least 1 year of follow-up between 2018 and 2020 were included in the study. This study was approved by the Ethics Committee of University

of Health Sciences Türkiye, Kartal Dr. Lütfi Kırdar Şehir Hospital (decision no: 2022/514/236/15, date: 26.10.2022). All procedures and data collection were conducted in accordance with the Declaration of Helsinki. The children were referred to a tertiary hospital by pediatric neurologists for evaluation of suspected papilledema or by an ophthalmologist because of disc margin blurring detected in routine examinations.

One hundred sixteen eyes of 58 children in the pseudopapilledema group and 64 eyes of 32 children in the papilledema group were included in this retrospective study. Eighty eyes of 40 patients of similar age and sex were included as the control group. The participants in the control group had normal healthy eyes and had no visual field or retinal nerve fiber layer (RNFL) defects.

In patients with suspected papilledema on ophthalmologic examination, the presence of headache with characteristics indicating increased intracranial pressure and accompanying symptoms such as diplopia, vomiting, and visual symptoms are guides for further investigation. In such cases, our primary approach is to perform a neurologic examination and MRI. If there is no mass or other pathology that might cause papilledema on MRI, LP is performed. The presence of possible signs of high intracranial pressure (empty sella, flattening of the posterior globe, tortuosity of the optic nerve or increase in perioptic cerebrospinal fluid) on MRI strengthens the diagnosis of papilledema in the presence of suspicious optic disc appearance or certain symptoms.[2] Otherwise, if there is no sign of increased intracranial pressure on MRI or patients have no specific symptoms, patients are directed to advanced ophthalmologic examinations for the diagnosis of pseudopapilledema. These patients are followed up regularly for at least 6 months.

In cases of suspected pseudopapilledema, B-scan USG, FAF, fluorescein angiography (FA), and spectral domain (SD)-OCT scans were performed. The ocular examination included examinations of visual acuity, color vision (Ishihara color plate), light reflex, ocular motility, visual fields (Humphrey 30-2; Allergan, Irvine, CA, USA), anterior segment, and fundus. Optic nerve head swelling was graded according to the Frisen scale.[9] Grade III-IV papilledema patients were excluded from the study. Fundus images of all patients were obtained from the first examination to monitor changes. ONHD was defined as hyperechoic and posterior acoustic shadowing structures within or on the optic nerve surface on B-scan (E-Z Scan AB5500+; Sonomed, Lake Success, NY, USA), autofluorescence in the optic nerve on FAF imaging (Canon CX-1; Canon Inc., Tokyo, Japan), absence of dye leakage in FA (Canon CX-1; Canon Inc, Tokyo, Japan), or a hyporeflective core surrounded by hyperreflective margins on SD-OCT (Nidek RS-3000 Advance; Nidek Co., Aichi, Japan).[10] Enlargement of the optic nerve sheath with a hypoechogenic crescent sign surrounding the optic nerve, which may suggest papilledema, was assessed and measurements were made using A-scans in necessary cases.[11] Peripapillary hyperreflective ovoid mass-like structures (PHOMS) were defined as hyperreflective structures surrounding the optic nerve and were located subretinally above Bruch's membrane on OCT.[12,13]

The diagnosis of pseudopapilledema was defined as the presence of spontaneous venous pulsation and normal MRI, venography, or LP without specific symptoms evaluated by a pediatric neurologist, and stability of the optic nerve head on examination and imaging in at least three follow-up visits at 6-month intervals. After 1 year of follow-up, optic nerve appearances were stable and no change was observed in the diagnosis of our patients with pseudopapilledema.

The peripapillary RNFL thickness in all four quadrants, average RNFL thickness, and Bruch's membrane opening (BMO) were measured using SD-OCT. The RNFL thickness in each 90-degree quadrant (superior, inferior, temporal, and nasal) was calculated within a 3.45-mm diameter scan circle around the optic disc. The BMO was defined as the horizontal transverse diameter of the neural canal opening (in micrometers) at the level of the retinal pigment epithelium and Bruch's membrane.[14] BMO measurements were performed manually using the OCT software. The quality of all scans was evaluated and scans were excluded if they had artifacts or errors. Particular attention was paid to patients with high myopia (>6.0 diopters) and hyperopia (>6.0 diopters). In such patients, the errors that might arise from disc centration were noted and images with signal strength >5 were evaluated. Optic nerve examinations and images were evaluated by two experienced ophthalmologists, and SD-OCT measurements were analyzed by the same experienced technician.

Statistical Analysis

The data were evaluated in the IBM SPSS Statistics Standard Concurrent User V 26 (IBM Corp., Armonk, New York, USA) statistical package program. Descriptive statistics were given as the number of units (n), percentage (%), mean and standard deviation (mean ± SD), median (M), and interquartile range (IQR). The normal distribution of the data of numerical variables was evaluated using the Shapiro-Wilk test of normality. Homogeneity of variances was evaluated using Levene's test. The ages of the patients in the groups were compared using One-way analysis of variance (ANOVA), and Pearson's chi-square test was used for sex comparisons. Since the right and left eyes of the patients were evaluated together, comparisons between groups for OCT variables were made using linear mixed model analysis. Bonferroni correction was applied for multiple comparisons. A value of $p<0.05$ was considered statistically significant.

Results

The study included 116 eyes of 58 patients with pseudopapilledema, 64 eyes of 32 patients with mild-to-moderate papilledema, and 80 eyes of 40 healthy normal individuals. The mean ages of the children were 13.2±3.2 years in the pseudopapilledema group, 12.1±2.8 years in the papilledema group, and 12.0±3.3 years in the control group. The age and sex distributions of the groups were statistically similar (Table 1).

Of the 58 children in the pseudopapilledema group, 30 (52%) presented with headaches, 8 (14%) with blurred vision, and 20 (34%) children were completely asymptomatic and referred for

examination of the optic disc. In the papilledema group, the most common symptom was headache (50%) with visual symptoms, followed by double vision (21.8%), tinnitus (15.6%), and transient vision loss (12.5%). The etiologies of papilledema were idiopathic intracranial hypertension (IIH) (n=24, 75%), cerebral venous sinus thrombosis (n=5, 15.6%), and intracranial tumor (n=3, 9.4%). The mean visual acuity was 0.05±0.04 logarithm of the minimum angle of resolution (logMAR) in the pseudopapilledema group, 0.02±0.04 logMAR in the papilledema group, and 0.05±0.1 logMAR in the control group.

Of the patients diagnosed as having pseudopapilledema, 44 (76%) underwent MRI, 2 (3.4%) underwent CT, and 30 (52%) underwent LP. The mean opening pressure was 21.5±3.07 (range, 14-25) cm H_2O. Three children diagnosed as having pseudopapilledema were using acetazolamide for the misdiagnosis of IIH. The drug was discontinued when the diagnosis was revised. In a patient with optic disc drusen, IIH was also detected and treatment was initiated. Of the 116 eyes with pseudopapilledema, PHOMS were detected in 82 eyes (70.7%), ONHD in 28 eyes (24.1%), crowded discs in 25 eyes (21.6%), and tilted/torsioned discs in 13 eyes (11.2%). Only 2 eyes (7%) had visible ONHD and 26 eyes had buried ONHD (93%). The diagnosis of ONHD was confirmed using USG in 26 eyes, SD-OCT in 21 eyes, FAF in 11 eyes, and clinical examination in 2 eyes (Figure 1a, b, c). FA was used in 8 patients to diagnose pseudopapilledema.

In the papilledema group, grade 1 papilledema was detected in 19 (29.7%) eyes and grade 2 papilledema was detected in 45 (70.3%) eyes. PHOMS were also detected in 20 (31.2%) of these eyes (Figure 1c). MRI and LP were performed in all patients in the papilledema group. The mean opening pressure was 37.5±9.3 (range, 25-60) cm H_2O. Patients diagnosed as having papilledema were treated by pediatric neurology or neurosurgery and followed up ophthalmologically.

Table 2 gives the RNFL thickness and BMO measurements in both groups. The average and all quadrants of RNFL thickness were significantly higher in the papilledema group than in the pseudopapilledema and control groups ($p<0.001$). The BMO measurements were similar in both groups ($p>0.05$). The average, nasal, and temporal RNFL thicknesses were significantly higher in the pseudopapilledema group compared with the controls ($p<0.001$). Within the pseudopapilledema group, average, temporal, and inferior RNFL thickness and BMO measurements were significantly higher in eyes with ONHD compared to those without ONHD (p=0.035, p=0.022, p=0.040, and p=0.047, respectively) (Table 3).

Table 1. Comparison of sex and age by group

	Papilledema (n=32)	**Pseudopapilledema (n=58)**	**Control (n=40)**	**p value**
Sex, n (%) Boy/girl	8 (25.0)/24 (75.0)	20 (34.5)/38 (65.5)	14 (35.0)/26 (65.0)	0.632*
Age, years mean ± SD Median (min-max)	12.1±2.8 12 (6-16)	13.2±3.2 13 (5-18)	12.0±3.3 12 (7-18)	0.106**

*Pearson chi-square test, **One-way analysis of variance, SD: Standard deviation

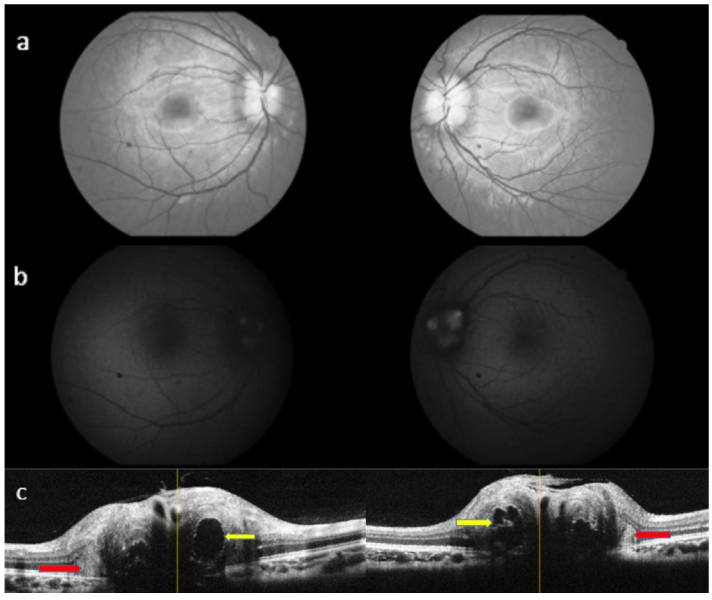

Figure 1. (a) Fundus red-free photo of a patient with visible optic nerve head drusen (ONHD); (b) fundus autofluorescence image of ONHD; (c) optical coherence tomography image of ONHD (yellow arrow) and peripapillary hyperreflective ovoid mass-like structures (red arrow) in the same patient

Table 4 gives the results of ROC analyses of RNFL thickness and BMO in differentiating papilledema from pseudopapilledema. Average RNFL thickness had the highest area under the curve (AUC), followed by temporal, nasal, superior, and inferior RNFL thickness. BMO had a smaller AUC, with a cutoff point of 1563 µm resulting in a sensitivity and specificity of 75% and 52.6%, respectively.

Discussion

In recent years, children's referrals to ophthalmology departments have increased due to suspected papilledema. Making the correct diagnosis is a difficult and stressful process for both the physician and patient. The misdiagnosis rate of papilledema in childhood has been reported as up to 76%.[15] Most of these children undergo unnecessary MRI, CT, or other imaging and several LPs.

Headache that occurs due to IIH increases especially in the morning and when lying down, and is sometimes associated with neck and shoulder pain due to stretching of the dural sheaths of spinal roots. Questioning the character of the headache and examining for accompanying additional symptoms such as transient visual obscurations, double vision, vomiting, and tinnitus are necessary for a detailed history and differential diagnosis. Headache was more common and was a non-specific symptom in most of the children in our study; however, MRI was performed in 76% of these children and LP was performed in 52%. Liu et al.[16] reported that children with pseudopapilledema referred for suspected papilledema over a

Table 2. Comparison of optical coherence tomography parameters by group

	Groups			Pairwise comparisons*		
	Papilledema (n=64 eyes) Mean ± SEM	Pseudopapilledema (n=116 eyes) Mean ± SEM	Control (n=80 eyes) Mean ± SEM	Papilledema vs. pseudopapilledema	Papilledema vs. control	Pseudopapilledema vs. control
RNFL	140.4±2.3	117.2±1.7	106.7±2.1	<0.001	<0.001	<0.001
Nasal RNFL	117.3±2.6	98.5±1.9	72.5±2.4	<0.001	<0.001	<0.001
Temporal RNFL	106.6±2.2	84.6±1.6	74.5±1.9	<0.001	<0.001	<0.001
Superior RNFL	161.7±3.5	137.8±3.6	136.7±3.3	<0.001	<0.001	0.999
Inferior RNFL	161.0±3.9	146.1±2.9	140.0±3.6	0.009	<0.001	0.559
BMO	1660.6±23.4	1596.1±17.3	1591.8±21.2	0.086	0.094	0.999

*Significant values based on linear mixed model, RNFL: Retinal nerve fiber layer, BMO: Bruch's membrane opening, SEM: Standard error of the mean

Table 3. Comparison of optical coherence tomography parameters according to the presence of drusen in the pseudopapilledema group

	No drusen (n=88) Mean ± SEM	Drusen (n=28) Mean ± SEM	p value*
Average RNFL	114.8±2.23	124.4±3.8	0.035
Nasal RNFL	97.1±2.3	102.3±4.0	0.260
Temporal RNFL	82.3±1.9	91.1±3.2	0.022
Superior RNFL	134.9±3.4	145.5±5.9	0.128
Inferior RNFL	141.8±4.2	159.4±7.2	0.040
BMO	1575.2±20.8	1658.8±35.4	0.047

*Significant values based on linear mixed model, RNFL: Retinal nerve fiber layer, BMO: Bruch's membrane opening, SEM: Standard error of the mean

Table 4. Results of receiver operating characteristic curve analysis of optical coherence tomography parameters in papilledema vs. pseudopapilledema

	Cut-off	AUC	95% CI	p value	Sens	Spec	PPV	NPV
Average RNFL	>125	0.868	0.809-0.914	<0.001	90.6	76.7	68.2	93.7
Nasal RNFL	>100	0.819	0.755-0.873	<0.001	82.8	75.9	65.4	88.9
Temporal RNFL	>96	0.862	0.802-0.908	<0.001	82.8	83.6	73.6	89.8
Superior RNFL	>137	0.797	0.731-0.853	<0.001	95.3	58.6	56.0	95.8
Inferior RNFL	>144	0.719	0.647-0.783	<0.001	82.8	56.0	51.0	85.5
BMO	>1563	0.632	0.557-0.703	0.002	75.0	52.6	46.6	79.2

RNFL: Retinal nerve fiber layer, BMO: Bruch's membrane opening, AUC: Area under the curve, CI: Confidence interval, Sens: Sensitivity, Spec: Specificity, PPV: Positive predictive value, NPV: Negative predictive value

6-year period underwent LP, MRI, and CT at rates of 53.8%, 73.1%, and 34.6%, respectively. They suggested that detailed histories and expert ophthalmologic examinations in the early period would prevent unnecessary tests and treatments.

It is very difficult to distinguish papilledema from pseudopapilledema in childhood. For instance, ONHD, the most common cause of pseudopapilledema, is buried deeper in children and mimics papilledema. Over time, it becomes more superficial and is easier to detect.[17] In addition, because ONHD is less calcified in children than in adults, it is difficult to diagnose it with USG, which is one of the traditional diagnostic methods.[18] Similarly, ONHD may not be detected with FAF and FA because it is hidden deep within the neural tissue.[17,18,19]

Although pseudopapilledema was diagnosed in 116 eyes in our study, we detected ONHD in only 28 eyes. In all of these patients, USG confirmed the diagnosis, and OCT helped in 21 eyes. It was not possible to detect buried and non-calcified drusen because the mean age of our patients was young (13.2±3.2 years). Previously, USG was considered the gold standard for diagnosing ONHD. However, ONHD is now more reliably diagnosed using enhanced depth imaging (EDI) OCT, which enables high-resolution visualization of the optic nerve head. In the pediatric population, this advantage is limited with increasing depth. Deeper ONHD has a lower resolution, often resulting in a poorer demarcation of their posterior borders.[20,21] Sim et al.[22] compared EDI-OCT, non-EDI-OCT, and FAF imaging in 28 children with definite ONHD confirmed using USG and determined that the three modalities revealed ONHD in 24, 21, and 18 eyes, respectively. In that study, EDI-OCT was not as successful as USG in detecting ONHD, unlike in adults. Similarly, the authors attributed this to a high incidence of buried ONHD in children.[22]

In our study, RNFL average and all quadrant thickness values were significantly higher in the papilledema group than in the pseudopapilledema and control groups ($p<0.001$) and the average, temporal, and inferior RNFL thickness values were significantly higher in the pseudopapilledema group with ONHD compared to those without ONHD ($p=0.035$, $p=0.022$, and $p=0.040$, respectively). Although OCT studies comparing papilledema and pseudopapilledema have been performed in recent years, no absolute values have been shown to be diagnostic for papilledema. In studies using SD-OCT, Lee et al.[23] reported significantly greater RNFL thickness in patients with papilledema than in patients with ONHD (174.1±53.5 µm vs. 119.2±20.2 µm), as well as higher average and temporal RNFL thickness in patients with pseudopapilledema compared to the control group. Aghsaei Fard et al.[24] determined that the average and all sectoral peripapillary RNFL thicknesses were higher in the papilledema group than in the other groups, and they reported an AUC of 0.82 for the ability of peripapillary RNFL to distinguish papilledema from pseudopapilledema. Swanson et al.[25] reported 79% sensitivity and 81% specificity in determining increased intracranial pressure due to craniosynostosis when the RNFL cut-off value was accepted as 208 µm. It is noteworthy that the cut-off value was quite high for mild and moderate papilledema. In our study the average RNLF had the highest AUC (0.868) with a cut-off value of 125 µm in papilledema compared to pseudopapilledema. Kulkarni et al.[26] found no significant difference between Frisen grade 2 mild papilledema and ONHD in terms of RNFL thickness. Chang et al.[27] was unable to make an accurate classification due to the overlap of RNFL thickness values in papilledema (mean: 142 µm, range: 91-199 µm) and ONHD (mean: 125 µm, range: 98-162 µm). In patients with pseudopapilledema, an increase in thickness has been demonstrated in different quadrants, which is not always consistent with healthy subjects and patients with mild papilledema. It has been suggested that the nasal quadrant in particular can provide important information in the differential diagnosis, and the nasal quadrant values seen in ONHD may be thinner.[23,28,29,30] This hypothesis is explained by the fact that the drusen are mostly located in the nasal quadrant, causing displacement and thinning of the nerve fibers over time. It has also been reported that there is a gradual enhancement in drusen size with age and the optic nerve size is smaller in children than in adults.[4,22,31] In line with previous studies, it was not possible to detect nasal RNFL thinning in children in the early period.[32]

Studies based on optic nerve imaging and OCT suggested that pseudopapilledema might originate from a narrow scleral canal and there could be stasis in the axoplasmic flow due to compression of the peripapillary nerves.[24,33,34] In some studies, as in our study, BMO was similar in the pseudopapilledema, mild papilledema, and control groups.[8,24] Thompson et al.[35] compared BMO in children with mild papilledema and pseudopapilledema and reported a larger mean BMO in the papilledema group than in the pseudopapilledema group and no significant difference between the pseudopapilledema and control groups. However, after the treatment of papilledema, the patients' mean BMO no longer differed significantly from the other groups. It has also been reported that BMO may enlarge in papilledema, non-arteritic ischemic optic neuropathy (NAION), or ONHD, and also shrink again after resolving the edema in the optic nerve.[35,36,37] García-Montesinos et al.[37] reported BMO enlargement in papilledema and NAION. They suggested that during optic nerve swelling, axonal fibers increased in volume and expanded the optic canal, then shrank again when the edema decreased. In another study using time-domain-OCT, it was reported that patients with ONHD and their first-degree relatives did not have narrow scleral canals, and both groups had a larger scleral canal area than the controls.[24] Similarly, Floyd et al.[38] studied 25 patients with ONHD and found larger scleral canals than in 17 control patients. In contrast, Malmqvist et al.[12] reported in their prospective study that children with ONHD had smaller scleral canals than those with normal optic nerves. In our study, BMO was similar in both groups but was higher in pseudopapilledema patients with ONHD than in those without ONHD, and the sensitivity and specificity of BMO in the differentiation of papilledema and pseudopapilledema were quite low. In light of similar studies, we thought that drusen may cause enlargement of the scleral canal over time, depending on their size and location. Significant differences in BMO

measurements between healthy individuals and patients with different optic nerve pathologies suggest that the clinical value of this OCT finding may be limited.

In recent years, the Optic Disc Drusen Studies Consortium has defined an optic nerve head lesion distinct from ONHD.[12] Formerly described as drusen-like or drusen precursors, they are now called PHOMS.[39,40,41,42] It is suggested that the presence of these structures should not be included as a diagnostic criterion for ONHD. Apart from drusen, it can be seen in various forms of optic disc edema and optic disc anomalies.[12,43,44] PHOMS was defined as the OCT finding corresponding to lateral herniation of retinal nerve fibers at the level of Bruch's membrane. They have the appearance of typical hyperreflective lesions surrounding the optic disc in the subretinal area but are neither hyperechogenic structures in B-scan images nor hyperautofluorescent on FAF images.[45]

In our study, PHOMS were detected using SD-OCT in 70.7% of eyes with pseudopapilledema and in 31.2% eyes with papilledema. Mezad-Koursh et al.[13] emphasized that PHOMS were the most common causes of pseudopapilledema in children and they characterized PHOMS in EDI-OCT, USG, FAF, and infrared images. They reported significant differences between PHOMS and ONHD, as in the study of Teixeira et al.[45] PHOMS are a new structure defined in the optic nerve head, and their development over the years is not clear. Malmqvist et al.[44] studied 5-year changes in children with ONHD and found that crowded disc and axonal distension resulting from the enlargement of optic nerve drusen were associated with PHOMS. It is important to follow up PHOMS because there are insufficient prospective studies about its change and progression, especially in children.

Study Limitations

Our study had some limitations. The number of patients was small and it was a retrospective study. Prospective studies with large series are needed to determine the gold standard methods in the differentiation of papilledema and pseudopapilledema in children.

Conclusion

In conclusion, a detailed history, complete ophthalmologic examination, and neurologic assessment can provide accurate diagnosis of papilledema or pseudopapilledema in most patients without invasive and expensive procedures. EDI-OCT appears to be an advanced technique with the potential to become the gold standard for identifying and monitoring PHOMS and ONHD in early childhood.

Ethics

Ethics Committee Approval: This study was approved by the Ethics Committee of University of Health Sciences Türkiye, Kartal Dr. Lütfi Kırdar Şehir Hospital (decision no: 2022/514/236/15, date: 26.10.2022).

Informed Consent: Obtained.

Peer-review: Externally peer-reviewed.

Authorship Contributions

Surgical and Medical Practices: A.T.K., S.Ö.Y., S.G.S., Concept: A.T.K., S.G.S., Design: A.T.K., Data Collection or Processing: A.T.K., S.Ö.Y., S.G.S., Analysis or Interpretation: A.T.K., S.Ö.Y., Literature Search: A.T.K., S.Ö.Y., Writing: A.T.K.

Conflict of Interest: No conflict of interest was declared by the authors.

Financial Disclosure: The authors declared that this study received no financial support.

References

1. Leon M, Hutchinson AK, Lenhart PD, Lambert SR. The cost-effectiveness of different strategies to evaluate optic disk drusen in children. J AAPOS. 2014;18:449-452.
2. Mishra A, Mordekar SR, Rennie IG, Baxter PS. False diagnosis of papilloedema and idiopathic intracranial hypertension. Eur J Paediatr Neurol. 2007;11:39-42.
3. Erkkila H. Clinical appearance of optic disc drusen in childhood. Albrecht Von Graefes Arch Klin Exp Ophthalmol. 1975;193:1-18.
4. Auw-Haedrich C, Staubach F, Witschel H. Optic disk drusen. Surv Ophthalmol. 2002;47:515-532.
5. Frisén L. Evolution of drusen of the optic nerve head over 23 years. Acta Ophthalmol. 2008;86:111-112.
6. Spencer TS, Katz BJ, Weber SW, Digre KB. Progression from anomalous optic discs to visible optic disc drusen. J Neuroophthalmol. 2004;24:297-298.
7. Davis PL, Jay WM. Optic nerve head drusen. Semin Ophthalmol. 2003;18:222-242.
8. Lam BL, Morais CG Jr, Pasol J. Drusen of the optic disc. Curr Neurol Neurosci Rep. 2008;8:404-408.
9. Frisen L. Swelling of the optic nerve head: a staging scheme. J Neurol Neurosurg Psychiatry. 1982;45:13-18.
10. Rebolleda G, Kawasaki A, de Juan V, Oblanca N, Muñoz-Negrete FJ. Optical Coherence Tomography to Differentiate Papilledema from Pseudopapilledema. Curr Neurol Neurosci Rep. 2017;17:74.
11. Neudorfer M, Ben-Haim MS, Leibovitch I, Kesler A. The efficacy of optic nerve ultrasonography for differentiating papilloedema from pseudopapilloedema in eyes with swollen optic discs. Acta Ophthalmol. 2013;91:376-380.
12. Malmqvist L, Bursztyn L, Costello F, Digre K, Fraser JA, Fraser C, Katz B, Lawlor M, Petzold A, Sibony P, Warner J, Wegener M, Wong S, Hamann S. The Optic Disc Drusen Studies Consortium Recommendations for Diagnosis of Optic Disc Drusen Using Optical Coherence Tomography. J Neuroophthalmol. 2018;38:299-307.
13. Mezad-Koursh D, Klein A, Rosenblatt A, Teper Roth S, Neudorfer M, Loewenstein A, Iglicki M, Zur D. Peripapillary hyperreflective ovoid mass-like structures-a novel entity as frequent cause of pseudopapilloedema in children. Eye (Lond). 2021;35:1228-1234.
14. Anand A, Pass A, Urfy MZ, Tang R, Cajavilca C, Calvillo E, Suarez JI, Venkatasubba Rao CP, Bershad EM. Optical coherence tomography of the optic nerve head detects acute changes in intracranial pressure. J Clin Neurosci. 2016;29:73-76.
15. Kovarik JJ, Doshi PN, Collinge JE, Plager DA. Outcome of pediatric patients referred for papilledema. J AAPOS. 2015;19:344-348.
16. Liu B, Murphy RK, Mercer D, Tychsen L, Smyth MD. Pseudopapilledema and association with idiopathic intracranial hypertension. Childs Nerv Syst. 2014;30:1197-1200.
17. Chang MY, Pineles SL. Optic disk drusen in children. Surv Ophthalmol. 2016;61:745-758.
18. Kurz-Levin MM, Landau K. A comparison of imaging techniques for diagnosing drusen of the optic nerve head. Arch Ophthalmol. 1999;117:1045-1049.
19. Pineles SL, Arnold AC. Fluorescein angiographic identification of optic disc drusen with and without optic disc edema. J Neuroophthalmol. 2012;32:17-22.

20. Yi K, Mujat M, Sun W, Burnes D, Latina MA, Lin DT, Deschler DG, Rubin PA, Park BH, de Boer JF, Chen TC. Imaging of optic nerve head drusen: improvements with spectral domain optical coherence tomography. J Glaucoma. 2009;18:373-378.
21. Wester ST, Fantes FE, Lam BL, Anderson DR, McSoley JJ, Knighton RW. Characteristics of optic nerve head drusen on optical coherence tomography images. Ophthalmic Surg Lasers Imaging. 2010;41:83-90.
22. Sim PY, Soomro H, Karampelas M, Barampouti F. Enhanced Depth Imaging Optical Coherence Tomography of Optic Nerve Head Drusen in Children. J Neuroophthalmol. 2020;40:498-503.
23. Lee KM, Woo SJ, Hwang JM. Differentiation of optic nerve head drusen and optic disc edema with spectral-domain optical coherence tomography. Ophthalmology. 2011;118:971977.
24. Aghsaei Fard M, Okhravi S, Moghimi S, Subramanian PS. Optic Nerve Head and Macular Optical Coherence Tomography Measurements in Papilledema Compared With Pseudopapilledema. J Neuroophthalmol. 2019;39:28-34.
25. Swanson JW, Xu W, Ying GS, Pan W, Lang SS, Heuer GG, Bartlett SP, Taylor JA. Intracranial pressure patterns in children with craniosynostosis utilizing optical coherence tomography. Childs Nerv Syst. 2020;36:535-544.
26. Kulkarni KM, Pasol J, Rosa PR, Lam BL. Differentiating mild papilledema and buried optic nerve head drusen using spectral domain optical coherence tomography. Ophthalmology. 2014;121:959-963.
27. Chang MY, Velez FG, Demer JL, Bonelli L, Quiros PA, Arnold AC, Sadun AA, Pineles SL. Accuracy of Diagnostic Imaging Modalities for Classifying Pediatric Eyes as Papilledema Versus Pseudopapilledema. Ophthalmology. 2017;124:1839-1848.
28. Johnson LN, Diehl ML, Hamm CW, Sommerville DN, Petroski GF. Differentiating optic disc edema from optic nerve head drusen on optical coherence tomography. Arch Ophthalmol. 2009;127:45-49.
29. Sarac O, Tasci YY, Gurdal C, Can I. Differentiation of optic disc edema from optic nerve head drusen with spectral-domain optical coherence tomography. J Neuroophthalmol. 2012;32:207-211.
30. Capo H. Don't Miss This! Red Flags in the Pediatric Eye Exam: Blurred Disc Margins. J Binocul Vis Ocul Motil. 2019;69:110-115.
31. Sato T, Mrejen S, Spaide RF. Multimodal imaging of optic disc drusen. Am J Ophthalmol. 2013;156:275-282.
32. Loo KG, Lim SA, Lim IL, Chan DW. Guiding follow-up of paediatric idiopathic intracranial hypertension with optical coherence tomography. BMJ Case Rep. 2016;2016:bcr2015213070.
33. Mullie MA, Sanders MD. Scleral canal size and optic nerve head drusen. Am J Ophthalmol. 1985;99:356-359.
34. Jonas JB, Gusek GC, Guggenmoos-Holzmann I, Naumann GO. Pseudopapilledema associated with abnormally small optic discs. Acta Ophthalmol (Copenh). 1988;66:190-193.
35. Thompson AC, Bhatti MT, El-Dairi MA. Bruch's membrane opening on optical coherence tomography in pediatric papilledema and pseudopapilledema. J AAPOS. 2018;22:38-43.
36. Rebolleda G, García-Montesinos J, De Dompablo E, Oblanca N, Muñoz-Negrete FJ, González-López JJ. Bruch's membrane opening changes and lamina cribrosa displacement in non-arteritic anterior ischaemic optic neuropathy. Br J Ophthalmol. 2017;101:143-149.
37. García-Montesinos J, Muñoz-Negrete FJ, de Juan V, Rebolleda G. Relationship between lamina cribrosa displacement and trans-laminar pressure difference in papilledema. Graefes Arch Clin Exp Ophthalmol. 2017;255:1237-1243.
38. Floyd MS, Katz BJ, Digre KB. Measurement of the scleral canal using optical coherence tomography in patients with optic nerve drusen. Am J Ophthalmol. 2005;139:664-669.
39. Sarkies NJ, Sanders MD. Optic disc drusen and episodic visual loss. Brit J Ophthalmol. 1987;71:537-539.
40. Savino PJ, Glaser JS, Rosenberg MA. A clinical analysis of pseudopapilledema. II. Visual field defects. Arch Ophthalmol. 1979;97:71-75.
41. Savino PJ, Guy JR, Trobe JD, McCrary JA, Smith CH, Chrousos GA, Thompson HS, Katz BJ, Brodsky MC, Goodwin JA, Atwell CW, and the Optic Neuritis Study Group. A randomized, controlled trial of corticosteroids in the treatment of acute optic neuritis. N Engl J Med. 1992;326:581-588.
42. Horwitz H, Friis T, Modvig S, Roed H, Tsakiri A, Laursen B, Frederiksen JL. Differential diagnoses to MS: experiences from an optic neuritis clinic. J Neurol. 2014;261:98-105.
43. Malmqvist L, Bursztyn L, Costello F, Digre K, Fraser JA, Fraser C, Katz B, Lawlor M, Petzold A, Sibony P, Warner J, Wegener M, Wong S, Hamann S. Peripapillary Hyperreflective Ovoid Mass-Like Structures: Is It Optic Disc Drusen or Not?: Response. J Neuroophthalmol. 2018;38:568-570.
44. Malmqvist L, Li XQ, Hansen MH, Thomsen AK, Skovgaard AM, Olsen EM, Larsen M, Munch IC, Hamann S. Progression Over 5 Years of Prelaminar Hyperreflective Lines to Optic Disc Drusen in the Copenhagen Child Cohort 2000 Eye Study. J Neuroophthalmol. 2020;40:315-321.
45. Teixeira FJ, Marques RE, Mano SS, Couceiro R, Pinto F. Optic disc drusen in children: morphologic features using EDI-OCT. Eye (Lond). 2020;34:1577-1584.

Original Article

Detection and Classification of Diabetic Macular Edema with a Desktop-Based Code-Free Machine Learning Tool

Furkan Kırık, Büşra Demirkıran, Cansu Ekinci Aslanoğlu, Arif Koytak, Hakan Özdemir

Bezmialem Vakif University Faculty of Medicine, Department of Ophthalmology, İstanbul, Türkiye

Abstract

Objectives: To evaluate the effectiveness of the Lobe application, a machine learning (ML) tool that can be used on a personal computer without requiring coding expertise, in the recognition and classification of diabetic macular edema (DME) in spectral-domain optical coherence tomography (SD-OCT) scans.

Materials and Methods: A total of 695 cross-sectional SD-OCT images from 336 patients with DME and 200 OCT images of 200 healthy controls were included. Images with DME were classified into three main types: diffuse retinal edema (DRE), cystoid macular edema (CME), and cystoid macular degeneration (CMD). To develop the ML model, we used the desktop-based code-free Lobe application, which includes a pre-trained ResNet-50 V2 convolutional neural network and is available free of charge. The performance of the trained model in recognizing and classifying DME was evaluated with 41 DRE, 28 CMD, 70 CME, and 40 normal SD-OCT images that were not used in the training.

Results: The developed model showed 99.28% sensitivity and 100% specificity for class-independent detection of DME. Sensitivity and specificity by labels were 87.80% and 98.57% for DRE, 96.43% and 99.29% for CME, and 95.71% and 95.41% for CMD, respectively.

Conclusion: To our knowledge, this is the first evaluation of the effectiveness of Lobe with ophthalmological images, and the results indicate that it can be used with high efficiency in the recognition and classification of DME from SD-OCT images by ophthalmologists without coding expertise.

Keywords: Artificial intelligence, code-free, machine learning, diabetic macular edema, optical coherence tomography

Cite this article as: Kırık F, Demirkıran B, Ekinci Aslanoğlu C, Koytak A, Özdemir H. Detection and Classification of Diabetic Macular Edema with a Desktop-Based Code-Free Machine Learning Tool. Turk J Ophthalmol 2023;53:301-306

Address for Correspondence: Furkan Kırık, Bezmialem Vakif University Faculty of Medicine, Department of Ophthalmology, İstanbul, Türkiye
E-mail: f.kirik21@gmail.com **ORCID-ID:** orcid.org/0000-0001-5846-8536

Received: 05.02.2023 **Accepted:** 08.04.2023

DOI: 10.4274/tjo.galenos.2023.92635

Introduction

Optical coherence tomography (OCT) provides physicians with non-invasive, rapid, and micron-level resolution images of the ocular tissues with near histological detail. It is widely used in diagnosis and follow-up of many retinal diseases, especially diabetic retinopathy.[1] Diabetic macular edema (DME), which is the main cause of visual impairment in patients with diabetic retinopathy, can also be successfully detected with OCT.[2] Various OCT-based DME classifications have been developed.[3,4,5,6,7] The most current of these classifications was reported by Arf et al.[7] and defines three main types of DME with different clinical and morphological features: diffuse retinal edema (DRE), cystoid macular edema (CME), and cystoid macular degeneration (CMD).

OCT has become more preferred for the development of artificial intelligence (AI) models compared to other imaging methods due to its widespread usage and superiority in terms of acquiring multiple retinal images, providing high-resolution retinal imaging of pathological lesions undetectable by standard color fundus photography or clinical examination, and revealing various biomarkers that can provide information about disease prognosis.[8,9] Although physicians' interest in AI has increased over time, many still have reservations about AI because earlier systems required a certain level of coding skills, and highly specialized computing resources were needed.[10]

With the web-, cloud-, or personal computer-based code-free AI platforms that have become available in recent years, physicians can develop their own AI models and perform classification and segmentation of medical images without the need for any coding expertise.[11] Lobe (www.lobe.ai, Lobe Artificial Intelligence, Microsoft, Inc.) is a free desktop-based no-code machine learning (ML) application that classifies images by using pre-trained ResNet-50 V2 and MobileNet V2 convolutional neural networks (CNN).[12] However, the effectiveness of Lobe in classifying ocular images is unknown.

The aim of this study was to evaluate the effectiveness of Lobe in the detection and classification of DME from cross-sectional spectral-domain (SD)-OCT scans.

Materials and Methods

Dataset Preparation and Image Labeling

Macular volumetric OCT scans of 336 patients with diabetic retinopathy and DME detected by Heidelberg Spectralis SD-OCT (Heidelberg Engineering, Inc., Heidelberg, Germany) between June 2019 and June 2021 were retrospectively analyzed. Cross-sectional OCT scans were evaluated by two ophthalmologists (H.O., F.K.) according to DME type, image quality, and the presence of additional retinal pathology. The classification defined by Arf et al.[7] was used to determine DME type. Accordingly, DRE was defined as DME characterized by increased retinal thickness and decreased intraretinal reflectivity, without a prominent round or oval intraretinal fluid space (Figure 1a). CME was defined as DME containing hyporeflective round or oval-shaped intraretinal cystoid areas bordered by hyperreflective septa (Figure 1b). CMD was defined as DME containing 600 µm and larger intraretinal cystoid spaces (Figure 1c). In the Arf et al.[7] classification, the presence of serous macular detachment, vitreomacular interface disease, and hard exudate is designated as subgroups a, b, and c, respectively. Although there was no image subclassification based on the presence of these pathological lesions in this study, images with these findings were also included. Eyes with additional retinal pathology, such as age-related macular degeneration, glaucoma, and images with signal quality worse than 20 (according to manufacturer's signal quality index, range 0-40) were excluded.

As a result, a total of 695 fovea-centered cross-sectional SD-OCT images were included and 205 were classified as DRE, 350 as CME, and 140 as CMD-type DME. In addition, 200 fovea-centered SD-OCT scans from 200 healthy controls were included as "normal" (Figure 1d). All images were resized to 512 x 512 pixels centered on the fovea using the crop function in Fiji (ImageJ, 1.53f; National Institute of Health, Bethesda, MD, USA). Metadata such as patient and device information were deleted from the images. Eighty percent of the images were parsed for training the ML model and 20% were allocated for testing.

This study has been approved by the Bezmialem Vakif University Faculty of Medicine Ethics Committee (decision no: 2022/30, date: 22.02.2022).

Training the Deep Learning Model

The Lobe program was downloaded from the website https://www.lobe.ai/ (Version 0.10.1130.5) free of charge and installed on a personal computer. After installation, a new project was created with four image labels named DRE, CMD, CME, and normal (Figure 2). To train the ML model, 164 DRE, 280 CME, and 112 CMD, and 160 normal images were imported into the appropriate image classes created in the application.

No additional data augmentation techniques were performed, as the current application automatically generated five random variations of the image (random modifications included brightness, contrast, saturation, hue, rotation, zoom, and JPEG encoding noise) during training.[12] The ResNet-50 V2 CNN was used for model architecture by selecting the "optimize for accuracy" option in the Project Settings menu. After selecting the CNN, the training phase was restarted, followed by model optimization with the built-in "model optimization" function for better real-world performance.

Performance Evaluation and Statistical Analysis

Twenty percent of the dataset, consisting of 41 DRE, 28 CMD, 70 CME, and 40 normal external test images allocated for testing, were imported one by one into the "Use" function of Lobe, and the model's prediction for each image was recorded (Figure 3). Predictions were not manually marked as "correct" or "incorrect" during testing.

Statistical analyses were performed using SPSS version 22 software package (IBM Corp., Armonk, NY, USA). The sensitivity and specificity of the model in recognizing any type of DME (DRE or CME or CMD vs. normal image) and in detecting individual types of DME were determined. In addition, the area under the curve (AUC) was calculated with receiver operating characteristic (ROC) curve analysis to determine the effectiveness of the model in image classification.

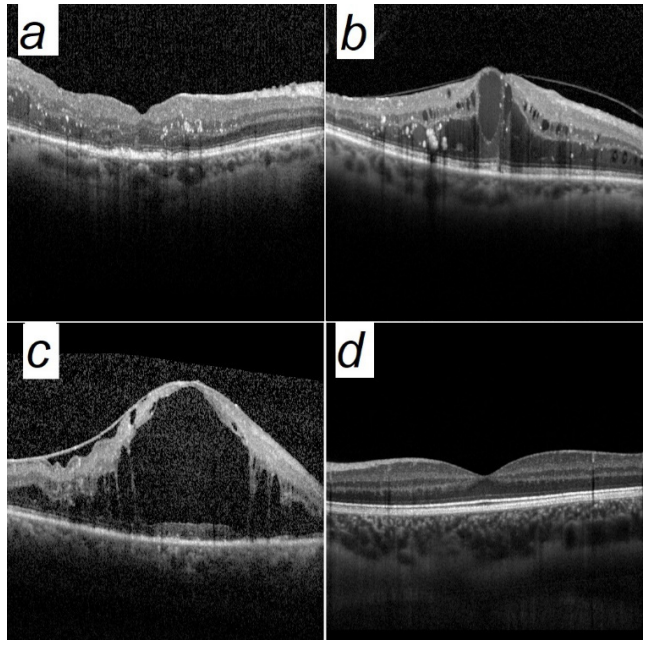

Figure 1. Samples of retinal spectral-domain optical coherence tomography (SD-OCT) scans from different classes included in the study. SD-OCT images of diabetic macular edema were classified into three types: diffuse retinal edema, defined as retinal thickening with reduced retinal hyperreflectivity and no cystoid spaces (a); cystoid macular edema, defined as retinal thickening with round or oval intraretinal spaces with a diameter less than 600 microns separated by hyperreflective septa (b); and cystoid macular degeneration, defined as intraretinal hyporeflective cystoid spaces with a diameter greater than 600 microns (c). SD-OCT images with no retinal pathology were classified as "normal" (d)

Results

Internal validation automatically performed using 145 internal images randomly selected from the imported images used for model training indicated that the developed model had prediction accuracy of 93.79% (98.74% of all imported images) in labeling. The effectiveness of the model was also evaluated with 41 DRE, 28 CMD, 70 CME, and 40 normal external test images. The predictions of the ML model in classifying DME types on external test images and the normalized confusion matrix based on the test data are shown in Figure 4.

Sensitivity, specificity, and AUC values for detecting DME regardless of type (any type of DME vs. normal) were calculated as 99.28%, 100%, and 0.996, respectively. Sensitivity, specificity, and AUC values for each DME type were calculated as 87.80%, 98.57%, and 0.936 for DRE; 96.43%, 99.29%, and 0.979 for CMD; and 95.71%, 95.41%, and 0.960 for CME, respectively. ROC curve analyses indicating the performance of the ML model in classifying DME types are shown in Figure 5. The presence of serous macular detachment, vitreomacular interface disease, and hard exudates in the training and testing datasets are also presented in Table 1.

Discussion

This study demonstrated that Lobe, a code-free ML application, could be used with high efficiency in the diagnosis and classification of DME from cross-sectional SD-OCT images. In addition, it showed that Lobe could provide satisfactory performance with a much smaller number of images compared to untrained deep learning (DL) models. This is an advantage of performing transfer learning using a pre-trained algorithm and automatically applying data augmentation to the dataset.

There are several studies in which ophthalmological images were classified by computer vision, a subfield of AI.[8,9,13,14,15,16,17,18,19] However, few studies have attempted to classify DME subtypes from OCT images. Alsaih et al.[18] developed a multi-stage ML model to identify the presence of retinal thickening (DRE in the new classification), hard exudates, intraretinal cystoid spaces (CME in the new classification), and subretinal fluid (serous macular detachment in new classification) using the volumetric SD-OCT scans of 16 patients. The generic pipeline they developed included pre-processing, feature detection, feature representation, and classification. Although this model appears to have a sequential structure that can perform the current DME classification, it may not be practical for physicians without prior coding knowledge. In addition, it differs from our study in that all images featuring diabetic retinopathy were obtained from only 16 patients and classic ML algorithms were used instead of the CNN that forms the structure in Lobe.

A method similar to that performed in our study was recently used by Wu et al.[19] The authors aimed to classify DRE, CMD, and serous macular detachment based on SD-OCT images using a VGG-16 CNN. Their model was developed with a large number of OCT images (12365 in total), yet shows little superiority over the DRE and CME classification in our study (AUC values 0.970 vs. 0.936 for DRE and 0.997 vs. 0.960 for CME, respectively). A large amount of data is required, especially during the development of DL models, and therefore the number of OCT images included in our study may seem insufficient.[20,21] Despite this, the DL model developed in our study resulted in acceptable accuracy with a relatively small number of images. The main reason for this may be the fact that Lobe utilizes transfer learning with pre-trained weights from the ImageNet, and automatically applies data augmentation techniques to the dataset. Thus, it was demonstrated that Lobe trained with a small number of

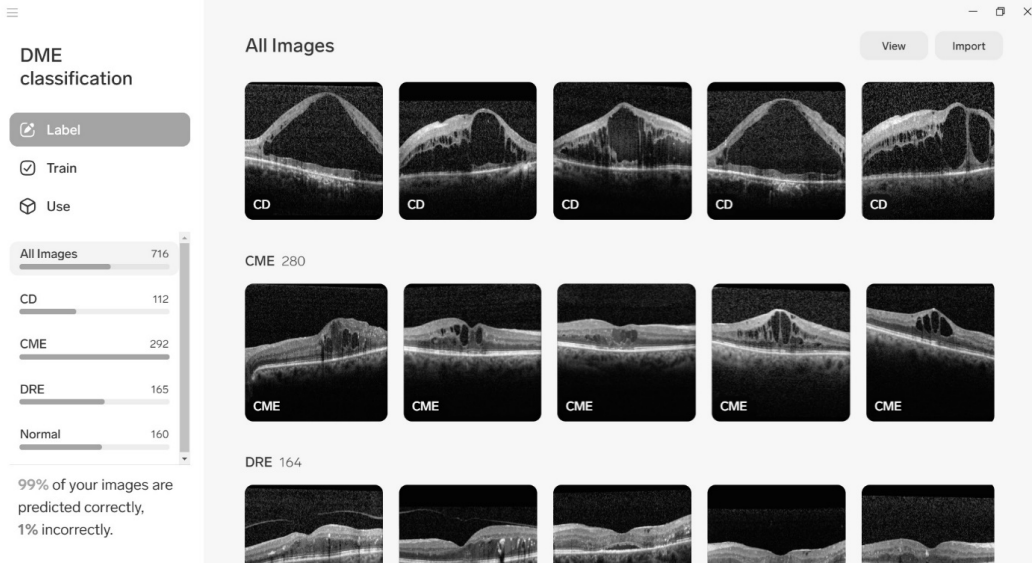

Figure 2. The "New Project" user interface (named "DME classification" in the current project) in the Lobe program. Spectral-domain optical coherence tomography images were labeled as diffuse retinal edema (DRE), cystoid macular edema (CME), cystoid macular degeneration (CD), and normal according to the classes defined after being imported

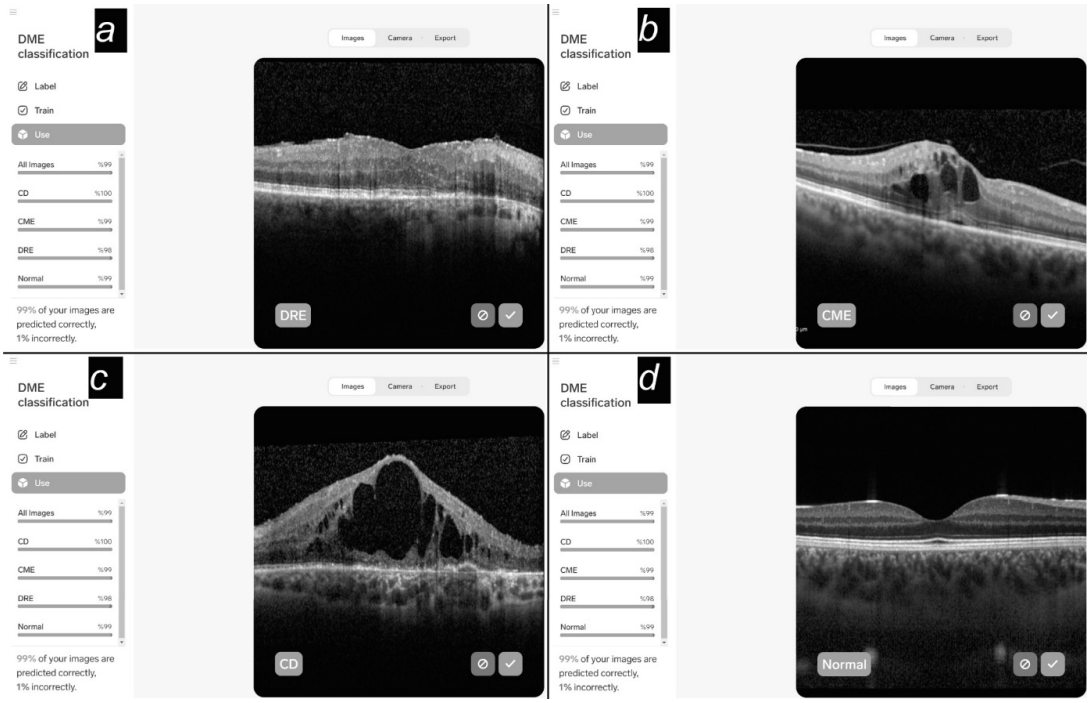

Figure 3. The accuracy of the developed model in predicting the labels was evaluated on external test images by the "Use" function. Model prediction on the sample external test images: (a) diffuse retinal edema (DRE), (b) cystoid macular edema (CME), (c) cystoid macular degeneration (labeled CD in the project), and (d) normal images

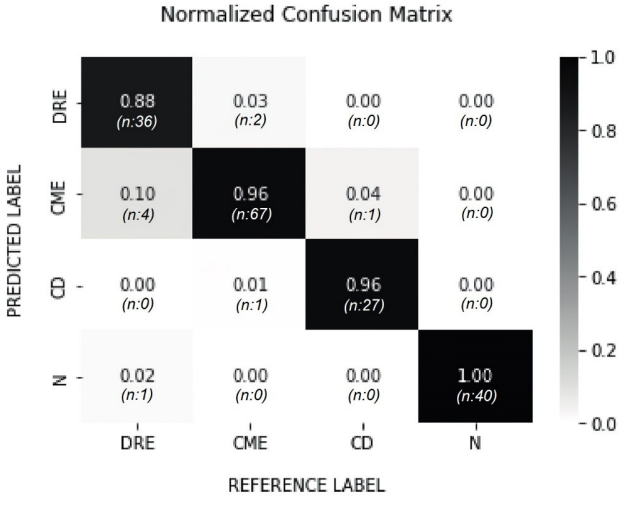

Figure 4. Normalized confusion matrix graph indicates the model had high accuracy in the prediction of diffuse retinal edema (DRE), cystoid macular edema (CME), cystoid macular degeneration (labeled CD in the project), and normal images

OCT images could be used effectively in DME classification and recognition, similar to DL-based models developed using large datasets. Furthermore, the built-in automatic data augmentation function in Lobe seems to be an added benefit, without the need for additional software/coding for data augmentation.

With increasing interest in AI and its widespread use in recent years, many companies have started to offer no-code ML platforms to serve users who do not have coding experience. The most detailed analysis of these platforms, which have different features and functions, was conducted recently by Korot et al.[11] Their study examined the performance of various code-free DL platforms in open-access datasets, as well as several features such as data security, usage fee, and model architecture. However, Lobe was not evaluated in that study. To the best of our knowledge, the clinical usage of Lobe has recently been evaluated in a few non-ophthalmological studies but not in the field of ophthalmology.[22] The cost-free availability of Lobe is an advantage for physicians seeking to gain experience in AI with image classification. In addition, running and training DL models entirely on a personal device, i.e., not having to share data with the cloud or web services, seems to be a feature that can satisfy users in terms of data security. Another remarkable feature of Lobe is that after the model is developed, it can be improved even while in use. The user can confirm the prediction made by the model for an uploaded image as correct or incorrect during the test phase of the model. Upon selecting "correct" or "reject" in the "use" tool, the image is saved automatically with the label that the user deems appropriate, allowing the model to improve after each test image.

Lobe includes two different CNN architectures and is selected automatically based on the size and complexity of the dataset, or manually based on user preference.[12] In this study, we preferred the ResNet-50 V2 CNN structure because we targeted high accuracy from the model. On the other hand, the user can also choose to use the MobileNet V2 to get

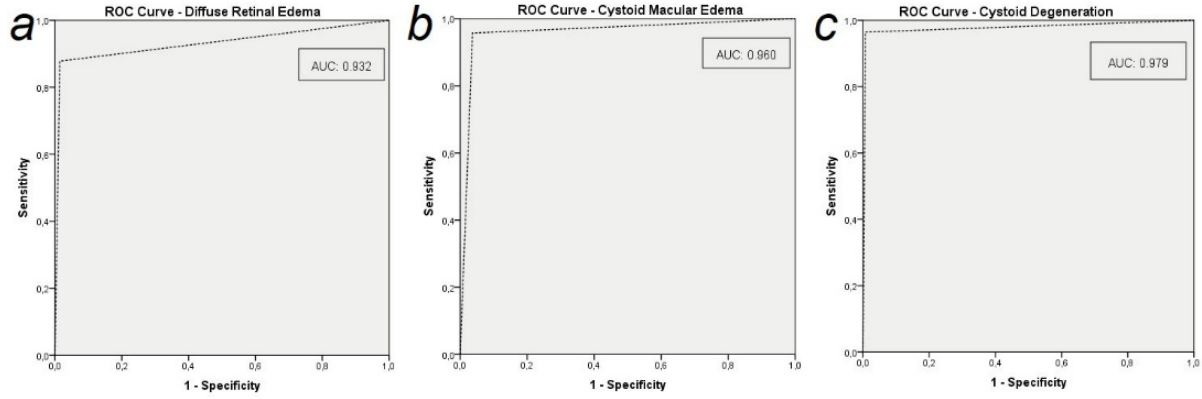

Figure 5. Receiver operating characteristic (ROC) curves and area under the ROC curves (AUC) indicate the diagnostic ability of the developed model for the types of diabetic macular edema: diffuse retinal edema (a), cystoid macular edema (b), and cystoid macular degeneration (c)

Table 1. The presence of serous macular detachment, vitreomacular interface disease, and hard exudate in the training and test datasets

	DRE		CME		CMD	
	Train (n=164)	**Test (n=41)**	**Train (n=280)**	**Test (n=70)**	**Train (n=112)**	**Test (n=28)**
SMD (%)	46 (28.05)	7 (17.07)	99 (35.36)	18 (25.71)	5 (4.46)	1 (3.57)
VMID (%)	31 (18.90)	9 (21.95)	20 (7.14)	4 (5.71)	19 (16.96)	6 (21.43)
HE (%)	75 (45.73)	19 (46.34)	138 (49.29)	17 (24.29)	19 (16.96)	3 (10.71)

SMD: Serous macular detachment, VMID: Vitreomacular interface disease, HE: Hard exudate, DRE: Diffuse retinal edema, CME: Cystoid macular edema, CMD: Cystoid macular degeneration

faster predictions at the cost of lower accuracy.[23,24] In addition, these developed models can be exported and used as a mobile application if desired. Although Lobe has many advantageous features and can successfully identify and classify DME in SD-OCT images, it lacks object detection or segmentation functions that would allow the identification of target structures in images, which limits its areas of application.

Study Limitations

The difference in the number of images between groups is a limitation of this study. However, in our retrospectively collected body of data, images with CME were frequently encountered, while images with CMD were less common. As reported by Arf et al.,[7] the frequency of CMD was lower than other types of DME. In addition, a larger data sample in DL/ML models increases the accuracy of the models. However, imbalance (over- or under-sampling) in datasets is a problem that limits the accuracy and reliability of the models. A size ratio of the smallest (minority) class (group) to the largest (majority) class (group) between 20% and 40% is considered a mild imbalance.[25] For this reason, datasets were created to attain high accuracy from the model without being imbalanced. Similar sample size differences between the groups are also seen in previous studies.[26]

Conclusion

Our study showed that Lobe, a free, no-code ML program, could be used effectively in DME detection and classification without the need for a large dataset by using pre-trained CNN architecture and automatic data augmentation. Advantageous features of the program are that it provides additional data security by being used on a personal device, the developed model can continue to be improved with every test image, and users have the option of selecting the CNN architecture. Thus, the Lobe program is an efficient and user-friendly option for physicians who do not have basic coding skills.

Ethics

Ethics Committee Approval: This study has been approved by the Bezmialem Vakif University Faculty of Medicine Ethics Committee (decision no: 2022/30, date: 22.02.2022).

Informed Consent: Obtained.

Peer-review: Externally peer-reviewed.

Authorship Contributions

Surgical and Medical Practices: H.Ö., A.K., Concept: F.K., H.Ö., A.K., Design: F.K., H.Ö., Data Collection or Processing: B.D., C.E.A., Analysis or Interpretation: H.Ö., A.K., Literature Search: F.K., B.D., C.E.A., Writing: F.K.

Conflict of Interest: No conflict of interest was declared by the authors.

Financial Disclosure: The authors declared that this study received no financial support.

References

1. Fujimoto JG, Drexler W. Introduction to OCT. In: Drexler W, Fujimoto JG, eds. Optical Coherence Tomography: Technology and Applications. 2nd ed. Cham; Springer; 2015:3-64.

2. Acón D, Wu L. Multimodal Imaging in Diabetic Macular Edema. Asia Pac J Ophthalmol (Phila). 2018;7:22-27.
3. Ruia S, Saxena S, Gemmy Cheung CM, Gilhotra JS, Lai TY. Spectral Domain Optical Coherence Tomography Features and Classification Systems for Diabetic Macular Edema: A Review. Asia Pac J Ophthalmol (Phila). 2016;5:360-367.
4. Otani T, Kishi S, Maruyama Y. Patterns of diabetic macular edema with optical coherence tomography. Am J Ophthalmol. 1999;127:688-693.
5. Panozzo G, Parolini B, Gusson E, Mercanti A, Pinackatt S, Bertoldo G, Pignatto S. Diabetic macular edema: an OCT-based classification. Semin Ophthalmol. 2004;19:13-20.
6. Kim BY, Smith SD, Kaiser PK. Optical coherence tomographic patterns of diabetic macular edema. Am J Ophthalmol. 2006;142:405-412.
7. Arf S, Sayman Muslubas I, Hocaoglu M, Ersoz MG, Ozdemir H, Karacorlu M. Spectral domain optical coherence tomography classification of diabetic macular edema: a new proposal to clinical practice. Graefes Arch Clin Exp Ophthalmol. 2020;258:1165-1172.
8. Ting DSW, Pasquale LR, Peng L, Campbell JP, Lee AY, Raman R, Tan GSW, Schmetterer L, Keane PA, Wong TY. Artificial intelligence and deep learning in ophthalmology. Br J Ophthalmol. 2019;103:167-175.
9. Schmidt-Erfurth U, Sadeghipour A, Gerendas BS, Waldstein SM, Bogunović H. Artificial intelligence in retina. Prog Retin Eye Res. 2018;67:1-29.
10. Faes L, Wagner SK, Fu DJ, Liu X, Korot E, Ledsam JR, Back T, Chopra R, Pontikos N, Kern C, Moraes G, Schmid MK, Sim D, Balaskas K, Bachmann LM, Denniston AK, Keane PA. Automated deep learning design for medical image classification by health-care professionals with no coding experience: a feasibility study. Lancet Digit Health. 2019;1:232-242.
11. Korot E, Guan Z, Ferraz D, Wagner SK, Zhang G, Liu X, Faes L, Pontikos N, Finlayson SG, Khalid H, Moraes G, Balaskas K, Denniston AK, Keane PA. Code-free deep learning for multi-modality medical image classification. Nat Mach Intell. 2021;3:288-298.
12. Lobe Help: What models are used? Available from: https://www.lobe.ai/docs/train/train. Access date: 01 May 2022
13. Hormel TT, Hwang TS, Bailey ST, Wilson DJ, Huang D, Jia Y. Artificial intelligence in OCT angiography. Prog Retin Eye Res. 2021;85:100965.
14. Ting DSJ, Foo VH, Yang LWY, Sia JT, Ang M, Lin H, Chodosh J, Mehta JS, Ting DSW. Artificial intelligence for anterior segment diseases: Emerging applications in ophthalmology. Br J Ophthalmol. 2021;105:158-168.
15. Li JO, Liu H, Ting DSJ, Jeon S, Chan RVP, Kim JE, Sim DA, Thomas PBM, Lin H, Chen Y, Sakomoto T, Loewenstein A, Lam DSC, Pasquale LR, Wong TY, Lam LA, Ting DSW. Digital technology, tele-medicine and artificial intelligence in ophthalmology: A global perspective. Prog Retin Eye Res. 2021;82:100900.
16. Reid JE, Eaton E. Artificial intelligence for pediatric ophthalmology. Curr Opin Ophthalmol. 2019;30:337-346.
17. Keskinbora K, Güven F. Artificial Intelligence and Ophthalmology. Turk J Ophthalmol. 2020;50:37-43.
18. Alsaih K, Lemaitre G, Rastgoo M, Massich J, Sidibé D, Meriaudeau F. Machine learning techniques for diabetic macular edema (DME) classification on SD-OCT images. Biomed Eng Online. 2017;16:68.
19. Wu Q, Zhang B, Hu Y, Liu B, Cao D, Yang D, et al. Detection of Morphologic Patterns of Diabetic Macular Edema Using A Deep Learning Approach Based on Optical Coherence Tomography Images. Retina. 2021;41:1110-1117.
20. Ting DSW, Lee AY, Wong TY. An Ophthalmologist's Guide to Deciphering Studies in Artificial Intelligence. Ophthalmology. 2019;126:1475-1479.
21. Soekhoe D, van der Putten P, Plaat A. On the Impact of Data Set Size in Transfer Learning Using Deep Neural Networks. In: Boström H, Knobbe A, Soares C, Papapetrou P, eds. Advances in Intelligent Data Analysis XV. Cham; Springer; 2010:50-60.
22. Richardson ML, Ojeda PI. A "Bumper-Car" Curriculum for Teaching Deep Learning to Radiology Residents. Acad Radiol. 2022;29:763-770.
23. Keras Applications. Available from: https://keras.io/api/applications/. Access date: 01 May 2022.
24. Sandler M, Howard A, Zhu M, Zhmoginov A, Chen LC. Mobilenetv2: Inverted residuals and linear bottlenecks. In: IEEE/CVF Conference on Computer Vision and Pattern Recognition; 2018:4510-4520.
25. Imbalanced Data. Available from: https://developers.google.com/machine-learning/data-prep/construct/sampling-splitting/imbalanced-data?hl=en. Access date: 31 March 2023.
26. Milea D, Najjar RP, Zhubo J, Ting D, Vasseneix C, Xu X, Aghsaei Fard M, Fonseca P, Vanikieti K, Lagrèze WA, La Morgia C, Cheung CY, Hamann S, Chiquet C, Sanda N, Yang H, Mejico LJ, Rougier M-B, Kho R, Thi Ha Chau T, Singhal S, Gohier P, Clermont-Vignal C, Cheng C-Y, Jonas JB, Yu-Wai-Man P, Fraser CL, Chen JJ, Ambika S, Miller NR, Liu Y, Newman NJ, Wong TY, Biousse V; BONSAI Group. Artificial Intelligence to Detect Papilledema from Ocular Fundus Photographs. N Engl J Med. 2020;382:1687-1695.

Invited Review

Management of Myopic Maculopathy: A Review

William J. Anderson*, Levent Akduman*, **

*Saint Louis University, Department of Ophthalmology, Saint Louis, United States of America
**Eye Care Partners and The Retina Center, Saint Louis, United States of America

Abstract

Myopia, including pathologic myopia, has seen a significant increase in prevalence in recent years. It is a significant cause of irreversible vision loss worldwide and prediction models demonstrate the substantial future impact on the population. With increased awareness and research, it is possible to prevent blindness on a large scale in the younger, productive age group affected by myopic maculopathy (MM). The vision-threatening manifestations of pathologic myopia include myopic choroidal neovascularization, macular atrophy, maculoschisis, macular hole, and retinal detachment. Myopic traction maculopathy (MTM) is a progressive manifestation of pathologic myopia and its treatment includes pars plana vitrectomy, macular buckle, or a combination. In this article we aim to review the diagnosis, clinical characteristics, and treatment of MM with an emphasis on recent developments in the surgical management of MTM. We discuss commercially available macular buckles, along with potential advantages to the use of macular buckle in MM. We review the new MTM staging system and its role in determining surgical management of these complex cases.

Keywords: Myopic maculopathy, macular buckle, myopic traction maculopathy, myopia, maculopathy

Cite this article as: Anderson WJ, Akduman L. Management of Myopic Maculopathy: A Review. Turk J Ophthalmol 2023;53:307-312

Address for Correspondence: Levent Akduman, Saint Louis University, Department of Ophthalmology; Eye Care Partners and The Retina Center, Saint Louis, United States of America
E-mail: akdumanlevent@gmail.com **ORCID-ID:** orcid.org/0000-0002-2543-154X
Received: 07.05.2023 **Accepted:** 24.07.2023

DOI: 10.4274/tjo.galenos.2023.59844

Introduction

Myopia, including pathologic myopia, has seen a significant increase in prevalence in recent years. Prediction models suggest that by 2050, about 50% of the global population will have myopia and nearly 10% will have high myopia.[1] Unfortunately, with current trends, it is predicted that 33.7 million people will experience vision impairments and 18.5 million people will become blind due to myopic maculopathy (MM).[2] The impacts will be especially felt in Asian countries, where myopia is more prevalent than in the United States.[3] This makes the management of myopia progression, particularly in childhood and adolescence, a topic of significant concern. In this article we will provide an overview of MM, with a focus on the latest trends in the surgical management of myopic traction maculopathy (MTM).

Definition of Myopia and Pathologic Myopia

Myopia is defined as a spherical equivalent of ≤-0.50 diopter (D), when ocular accommodation is relaxed.[4] Pathologic myopia occurs in eyes with an axial length ≥26.5 mm, refraction ≤-6.0 D, with concurrent structural changes observed in the retina.[4,5] MM refers to any anatomical changes that occur in the macula of myopic eyes, primarily attributed to elongation of the axial length. When these anatomical changes progress over time, the term "progressive myopic maculopathy" is used. However, it is worth noting that most eyes diagnosed with MM were not born with it. In reality, most cases of MM have already been progressing at varying rates, shapes, and forms throughout the individual's lifetime.

Epidemiology

The prevalence of MM varies among different ethnicities and populations. Rates have been reported between 1-4%, with higher rates of around 8-10% in Asian countries.[6,7,8,9] A recent meta-analysis revealed that myopic patients have an increased risk of MM, especially those with high myopia (<-6.00 D) (odds ratio: 845.08).[8] However, the study also found that moderate myopia (-3.00 to -6.00 D) (odds ratio: 72.74) and even low

myopia (-0.5 to -3.00 D) (odds ratio: 13.57) were associated with increased risk of MM.[8]

Natural Course

It is well known that higher diopters of myopia and increasing axial length are directly correlated with an increased risk of developing pathologic myopia in later years.[10] Although high axial length may not be the only explanation, it is the most obvious and associated factor in pathologic myopia (similar to elevated intraocular pressure in glaucoma). Although the rate of myopia progression can slow down or stop in adult years, studies have shown that pathologic myopia can develop and worsen later in life. In fact, one study reports that 40.6% of patients progressed significantly to visual impairment within 12.7 years after the age of 40.[11]

In a case series by Sonne et al.[12], eyes with MM had an increased axial length after cataract surgery, averaging 1.32 mm over 13 years after their surgeries, resulting in reduced vision from 20/30 to 20/200 during the follow-up period. The maculopathy presented as choroidal neovascularization (CNV), maculoschisis, or macular atrophy.

Clinical manifestations of MM (Table 1) present as a progressive disease and include tessellated fundus, lacquer cracks, macular atrophy, CNV, maculoschisis, macular hole, posterior staphyloma, and posterior pole retinal detachment.[5]

Prevention of Pathologic Myopia

Myopia progression is most rapid during childhood and adolescence, making this an ideal time to consider interventions to prevent high myopia. Spectacles, bifocal and multifocal contact lenses, orthokeratology lenses, and atropine have all been studied as potential interventions to slow myopia progression in childhood, with topical atropine showing the most promise in recent studies.[13,14,15,16] While the exact mechanism of atropine's effect on axial elongation is still unclear, it appears to be unrelated to accommodation effects. A recent meta-analysis demonstrated that low-dose 0.01% atropine is as effective as 1% atropine but with fewer side effects such as pupil dilation, loss of accommodation, and near vision blur.[17] Wei et al.[18] found that low-dose atropine resulted in a relative reduction of approximately 34% in myopia progression in children over a 1-year period. Low-dose atropine may also be preferred due to its relatively minimal rebound effect when treatment is stopped, and it is typically better tolerated by children compared to wearing contact lenses. Ongoing research is focused on developing interventions that can slow or halt the progression of myopia and prevents its pathologic consequences.

Table 1. Types of myopic maculopathy
Staphyloma
Macular atrophy
Lacquer cracks
Choroidal neovascularization, which may lead to disciform scar ("Fuchs spots")
Posterior pole retinal detachment

Manifestations of Myopic Maculopathy

Clinical characteristics of MM include tessellated fundus, lacquer cracks, and macular atrophy with later stages resulting in CNV and MTM. In 2015, Ohno-Matsui et al.[19] proposed an international classification system that classifies MM into categories with "+" signs indicative of features that may predispose to central vision loss (Table 2).

One of the initial clinical manifestations of MM is a tessellated fundus, which results from thinning of the retinal pigment epithelium (RPE) and reduced pigmentation. This leads to prominent choroidal vasculature, typically seen along the macula and arcades, and is associated with reduced choroidal thickness.[20] As the disease progresses, diffuse chorioretinal atrophy may develop, characterized by a yellowish-white appearance which usually first appears around the optic disc and macula. Patchy choroidal atrophy may also develop, with demarcated areas of gray-white lesions secondary to choriocapillaris dropout and subsequent RPE loss. While it is rare to experience central vision loss from chorioretinal atrophy in MM, it can occur in late stages of the disease.[19] Additionally, lacquer cracks are a common finding in the posterior fundus early in the disease course and are seen as yellow lines in a branching pattern that represent a rupture in the RPE, Bruch's membrane, choriocapillaris complex.[21] These cracks may result in subretinal hemorrhage, which can resolve without intervention. However, lacquer cracks are a known precursor to myopic CNV, which can be a more significant threat to vision. CNV may spontaneously regress, leading to atrophy and dark pigmented scars known as Fuchs spots from proliferating RPE cells surrounding the regressed CNV.

Posterior staphyloma, defined as an outpouching of the wall of the eye that has a radius of curvature less than the surrounding curvature of the wall of the eye, is commonly associated with MM, particularly at the posterior pole.[22] If present, it likely plays a role in the development of MTM due to progressive thinning and mechanical damage to the retina.[23]

Myopic Choroidal Neovascularization

Pathogenesis of myopic CNV

Myopic CNV is one of the most serious vision-threatening complications of pathologic myopia, affecting approximately 5-11% of patients and often resulting in sudden vision loss. Individuals with myopic CNV in one eye are at increased risk of developing CNV in the fellow eye, with a 35% chance over

Table 2. Classification of myopic maculopathy[18]	
Classification	**Clinical manifestations**
Category 0	No macular lesions
Category 1	Tessellated fundus
Category 2	Diffuse chorioretinal atrophy
Category 3	Patchy chorioretinal atrophy
Category 4	Macular atrophy
"Plus signs"	Lacquer cracks, choroidal neovascularization, Fuchs spots

an 8-year period demonstrated by Ohno-Matsui et al.[24] Myopic CNV typically arises from lacquer cracks and is classified as a type 2 CNV that enters from beneath Bruch's membrane as defects arise from the expanding scleral wall and subsequent thinning of the retina.

Management of myopic CNV

The current standard of care for myopic CNV is treatment with anti-vascular endothelial growth factor (anti-VEGF) agents. Bevacizumab (Avastin; Genentech Inc, San Francisco, CA, USA), ranibizumab (Lucentis; Genentech Inc), and aflibercept (Eylea; Regeneron, Tarrytown, NY, USA) have all shown short-term benefits in the management of myopic CNV.[25,26,27] In the RADIANCE trial, ranibizumab was found to have sustained improvement in best corrected visual acuity (BCVA) compared to photodynamic therapy at 12 months.[25] Aflibercept was also shown to be effective in the MYRROR study, which demonstrated a gain of 13.5 letters compared to a 3.9-letter gain in the sham control at 1-year follow up.[26] However, the use of anti-VEGF agents for myopic CNV should be considered judiciously, as several long-term studies have failed to show improvement in BCVA over a follow-up period of 5 years or more with bevacizumab, ranibizumab, and aflibercept.[27,28,29] This is due to the secondary chorioretinal atrophy which develops as a result of the CNV. There is some debate about whether anti-VEGF agents may worsen this atrophy by causing a degenerative effect on the RPE and choriocapillaris, which may be exacerbated in highly myopic eyes with an already extremely thin choroid.[30,31] It is important to note that myopic CNV behaves differently than CNV related to age-related macular degeneration, and these patients often require fewer injections to control the CNV.[5]

Recently, biosimilar agents have also been introduced into clinical practice. Of the anti-VEGF agents mentioned above, only ranibizumab (Lucentis 0.5 mg) and its biosimilar equivalents ranibizumab-nuna (Byooviz; Biogen, Cambridge, MA, USA) and ranibizumab-eqrn (Cimerlie; Coherus, Redwood City, CA, USA) are FDA-approved and on-label for treatment of myopic CNV.[32]

Myopic Traction Maculopathy

In 2004, Panozzo and Mercanti[33] introduced the term "myopic traction maculopathy" to describe various clinical changes associated with MM such as maculoschisis, retinal/foveal detachment, lamellar macular hole, and full thickness macular hole with or without retinal detachment. This led to the development of the MTM staging system (MSS) by Parolini et al.[34], which is currently the most widely used classification system for MTM. The MSS is based on optical coherence tomography (OCT) imaging and consists of four stages: Stage 1- inner/outer maculoschisis, Stage 2- predominantly outer maculoschisis, Stage 3- maculoschisis/macular detachment, and Stage 4- macular detachment. The foveal morphology is also described in stages: A- Normal foveal architecture, B- lamellar macular hole, and C- full-thickness macular hole.[35] A recent international validation study demonstrated good interobserver reliability of the new staging system.[34]

Pathogenesis of Myopic Traction Maculopathy

MTM and its sequelae can be seen as a progressive evolution of the same disease with multiple contributing factors. Incomplete posterior vitreous detachment, vitreomacular traction, and epiretinal membrane are pre-retinal factors that may exert centrifugal and tangential traction which contribute to the development of MTM.[36] Subretinal factors, such as progressive staphylomatous changes of the sclera, may also contribute to MTM by leading to retinal thinning and decreased blood supply, thereby weakening the adhesion forces between retinal layers. Forces perpendicular to the retinal plane, such as incomplete posterior vitreous detachment and progressive staphyloma, are more likely to contribute to progressive maculoschisis and Stage 1-4 MTM. On the other hand, tangential forces such as epiretinal membrane may be more responsible for the development of foveal changes and Stage A-C MTM. The evolution of MTM is a complex process with multiple overlapping factors contributing to the development and progression of the disease.

Management of Myopic Traction Maculopathy

The treatment of MTM can be addressed through either an ab interno or an ab externo approach. The timing and selection of surgical intervention depends on various factors such as the degree of visual impairment and the MSS classification. Typically, ab interno surgery is more effective in addressing pathology related to tangential centrifugal forces on the retina, while ab externo surgery may be more effective in addressing pathology secondary to perpendicular centrifugal forces. In severe cases of MTM, a combination or stepwise approach may be required to manage both components.

Macular Buckle

In the 1930s, the ab externo approach was first attempted by reinforcing the posterior sclera with materials such as fascia lata and donor sclera.[37,38] Schepens et al.[39] developed the first macular buckle technique in 1957, but it did not become common practice. Recently, there has been a renewed interest in macular buckling for MTM management. Several types of macular buckles have been developed and improved over time. Currently, commercially available macular buckles include the AJL macular buckle, T-shaped buckle, ando plombe, and adjustable macular buckle, although none are available in the United States.

Tanaka et al.[40] published a case series in 2005 on a T-shaped rod silicone plastic exoplant reinforced with titanium, which showed promising results. Parolini et al.[41] developed an L-shaped macular buckle using titanium and a soft sponge material which indents the macula and is sutured to the anterior sclera. This was further developed to utilize two optic fibers positioned in the head of the buckle to assist with macular buckle positioning at the fovea.

The Akduman Myopia Support device (Figure 1) is a recently developed titanium macular buckle with several unique features that seem to make it advantageous.[42] Its concave supportive plate helps preserve the natural contour of the globe, possibly avoiding long-term foveal changes and any inhibition of the retina and choroidal circulation due to the indentation.[42]

Furthermore, its fixed stiffness and size create a fixed final axial length regardless of initial axial length unless adjusted for pseudophakic eyes where a rather limited indentation is desired. A recent case report demonstrated successful resolution of maculoschisis with improvement in refraction by 7.25 D.[42] This patient, whose preoperative OCT, postoperative OCT, and postoperative fundus photos are seen in Figure 2, had a reduction in axial length from 28.77 mm to 26.31 mm and also exhibited remarkable improvement in vision.[43] The surgery of this case can be reviewed at: https://eyetube.net/videos/titanium-macular-buckle-placement. The Akduman Myopia Support device was also reported to successfully close a recurrent MM hole.[42]

Recent developments in devices and surgical techniques have increased success rates and decreased complications with macular buckling. While intraoperative OCT is not yet widely available, it could be a valuable adjunct in macular buckle surgery. Given the increasing prevalence of MTM, it is important to be familiar with these techniques.

Vitrectomy

The ab-interno approach involves pars plana vitrectomy (PPV), with or without internal limiting membrane (ILM) peeling, and typically a gas tamponade. Vitrectomy in MM can be successful but has been associated with a high rate of recurrent retinal detachment, failure to close macular hole, and may induce iatrogenic macular holes during surgery. More recent studies have shown that ILM peeling and ILM flap improve success rates of macular hole closure in eyes with MTM.[44,45,46]

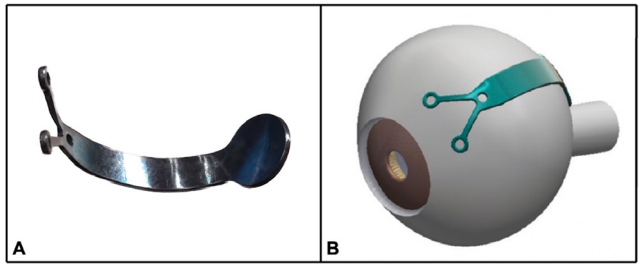

Figure 1. The Akduman Titanium Macular Buckle (A) and schematic representation of its position on the eye (B)

Surgical Decision Making

The choice of whether to use PPV, macular buckle, or a combination of both in the management of MTM depends on various factors. Parolini et al.[47] recently proposed new management guidelines for MTM based on the MSS in a retrospective review of the outcomes of PPV, macular buckle, or combined PPV and macular buckle in over 150 eyes with different stages of MTM. PPV was found to better address tangential centrifugal retina forces whereas macular buckle better addressed perpendicular centrifugal forces.

Early-stage maculoschisis can often be observed if vision is preserved and no significant epiretinal membrane is present. However, if mild maculoschisis is associated with worsening foveal pathology (lamellar macular hole, full-thickness macular hole), or epiretinal membrane, then PPV with ILM peeling or ILM flap and gas tamponade has high success rates in addressing these tangential forces. As maculoschisis and perpendicular forces worsen (Stages 2, 3, 4), then macular buckle becomes the preferred treatment. For Stages 2, 3, 4 (except those with full-thickness macular hole), macular buckle should be the initial treatment and PPV may be supplemented as a second surgery if foveal pathology progresses or does not resolve. If a full-thickness macular hole is present initially with Stage 2 or worse MTM, then a combination approach of PPV and macular buckle will likely be necessary to address both anterior/posterior and tangential forces.[47] Figure 3 provides an example of this combined surgical approach in Stage 4C MTM successfully managed with PPV, ILM peeling, and macular buckle by Parolini et al.[47]

As macular buckle techniques and devices continue to improve, it is expected to be utilized more frequently to address MTM. Macular buckle also addresses the underlying cause of progressive MTM, which is the increasing axial length of the eye. Additionally, it does not carry the risk of cataract progression, is reversible, and can also improve refraction in patients that likely are extremely near-sighted.

Conclusion

With increased awareness and research, it is possible to prevent blindness on a large scale in the younger, productive age group affected by MM. The vision-threatening manifestations of pathologic myopia include myopic CNV, macular atrophy,

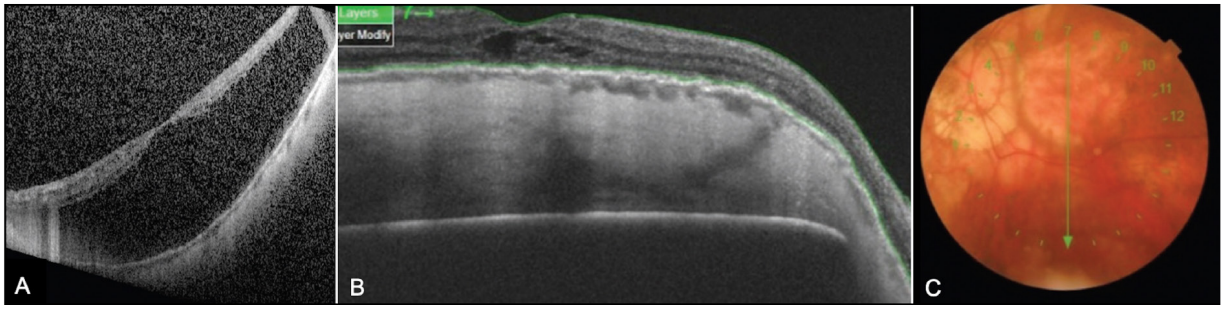

Figure 2. Preoperative optical coherence tomography image of a patient who underwent Akduman Titanium Macular Buckle placement (A). Postoperative photo demonstrates the indentation helping resolve the posterior pole retinal detachment reducing the axial length. No vitrectomy was performed (B). Postoperative fundus photo after Akduman Titanium Macular Buckle was placed with adequate indentation in the macula (C) (image courtesy of Retina Today)

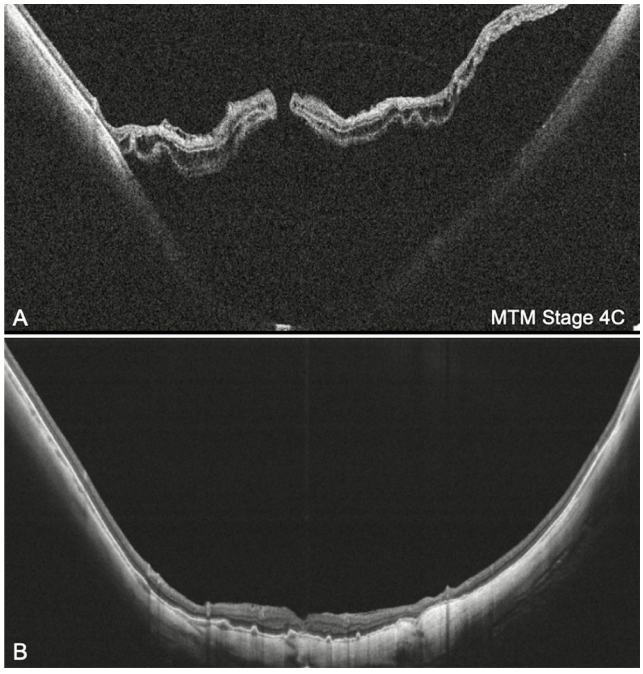

Figure 3. Severe myopic traction maculopathy Stage 4C with macular retinal detachment and full-thickness macular hole (A). Optical coherence tomography image after pars plana vitrectomy with internal limiting membrane peeling and macular buckle surgery performed by Parolini et al.[47] (B) (images courtesy of Barbara Parolini, MD)

maculoschisis, macular hole, and retinal detachment. While anti-VEGF therapy can improve short-term BCVA in myopic CNV, more studies are needed to assess its long-term benefits. MTM is a progressive manifestation of pathologic myopia and its treatment includes PPV, macular buckle, or a combination of both. The recently proposed MTM MSS provides a framework for approaching the surgical management of these cases. However, effectively treating vision-threatening manifestations of pathologic myopia such as CNV and MTM remains challenging. This highlights the importance of treating high axial length, the underlying cause of these pathologies, with myopia control in the early years and devices such as macular buckle to directly address axial length progression, which can ultimately prevent or delay vision loss.

Ethics

Peer-review: Externally and internally peer-reviewed.

Authorship Contributions

Surgical and Medical Practices: L.A., W.J.A., Concept: L.A., Design: L.A., Analysis or Interpretation: L.A., W.J.A., Literature Search: W.J.A., L.A., Writing: W.J.A., L.A.

Conflict of Interest: No conflict of interest was declared by the authors.

Financial Disclosure: The authors declared that this study received no financial support.

References

1. Holden BA, Fricke TR, Wilson DA, Jong M, Naidoo KS, Sankaridurg P, Wong TY, Naduvilath TJ, Resnikoff S. Global Prevalence of Myopia and High Myopia and Temporal Trends from 2000 through 2050. Ophthalmology. 2016;123:1036-1042.
2. Fricke TR, Jong M, Naidoo KS, Sankaridurg P, Naduvilath TJ, Ho SM, Wong TY, Resnikoff S. Global prevalence of visual impairment associated with myopic macular degeneration and temporal trends from 2000 through 2050: systematic review, meta-analysis and modelling. Br J Ophthalmol. 2018;102:855-862.
3. Naidoo KS, Fricke TR, Frick KD, Jong M, Naduvilath TJ, Resnikoff S, Sankaridurg P. Potential Lost Productivity Resulting from the Global Burden of Myopia: Systematic Review, Meta-analysis, and Modeling. Ophthalmology. 2019;126:338-346.
4. Flitcroft DI, He M, Jonas JB, Jong M, Naidoo K, Ohno-Matsui K, Rahi J, Resnikoff S, Vitale S, Yannuzzi L. IMI - Defining and Classifying Myopia: A Proposed Set of Standards for Clinical and Epidemiologic Studies. Invest Ophthalmol Vis Sci. 2019;60:20-30.
5. Silva R. Myopic maculopathy: a review. Ophthalmologica. 2012;228:197-213.
6. Liu HH, Xu L, Wang YX, Wang S, You QS, Jonas JB. Prevalence and progression of myopic retinopathy in Chinese adults: the Beijing Eye Study. Ophthalmology. 2010;117:1763-1768.
7. Choudhury F, Meuer SM, Klein R, Wang D, Torres M, Jiang X, McKean-Cowdin R, Varma R; Chinese American Eye Study Group. Prevalence and Characteristics of Myopic Degeneration in an Adult Chinese American Population: The Chinese American Eye Study. Am J Ophthalmol. 2018;187:34-42.
8. Haarman AEG, Enthoven CA, Tideman JWL, Tedja MS, Verhoeven VJM, Klaver CCW. The Complications of Myopia: A Review and Meta-Analysis. Invest Ophthalmol Vis Sci. 2020;61:49.
9. Wong TY, Ferreira A, Hughes R, Carter G, Mitchell P. Epidemiology and disease burden of pathologic myopia and myopic choroidal neovascularization: an evidence-based systematic review. Am J Ophthalmol. 2014;157:9-25.
10. Hashimoto S, Yasuda M, Fujiwara K, Ueda E, Hata J, Hirakawa Y, Ninomiya T, Sonoda KH. Association between Axial Length and Myopic Maculopathy: The Hisayama Study. Ophthalmol Retina. 2019;3:867-873.
11. Hayashi K, Ohno-Matsui K, Shimada N, Moriyama M, Kojima A, Hayashi W, Yasuzumi K, Nagaoka N, Saka N, Yoshida T, Tokoro T, Mochizuki M. Long-term pattern of progression of myopic maculopathy: a natural history study. Ophthalmology. 2010;117:1595-1611.
12. Sonne S, Akduman YC, Meyer C, Saxena S. Elongation of Axial Length in Older Patients with Degenerative Myopia. Investig Ophthalmol Vis Sci. 2022;63:3773.
13. Tay SA, Farzavandi S, Tan D. Interventions to Reduce Myopia Progression in Children. Strabismus. 2017;25:23-32.
14. Ruiz-Pomeda A, Pérez-Sánchez B, Valls I, Prieto-Garrido FL, Gutiérrez-Ortega R, Villa-Collar C. MiSight Assessment Study Spain (MASS). A 2-year randomized clinical trial. Graefes Arch Clin Exp Ophthalmol. 2018;256:1011-1021.
15. Hiraoka T. Myopia Control With Orthokeratology: A Review. Eye Contact Lens. 2022;48:100-104.
16. Chua WH, Balakrishnan V, Chan YH, Tong L, Ling Y, Quah BL, Tan D. Atropine for the treatment of childhood myopia. Ophthalmology. 2006;113:2285-2291.
17. Gong Q, Janowski M, Luo M, Wei H, Chen B, Yang G, Liu L. Efficacy and Adverse Effects of Atropine in Childhood Myopia: A Meta-analysis. JAMA Ophthalmol. 2017;135:624-630.
18. Wei S, Li SM, An W, Du J, Liang X, Sun Y, Zhang D, Tian J, Wang N. Safety and Efficacy of Low-Dose Atropine Eyedrops for the Treatment of Myopia Progression in Chinese Children: A Randomized Clinical Trial. JAMA Ophthalmol. 2020;138:1178-1184.
19. Ohno-Matsui K, Kawasaki R, Jonas JB, Cheung CM, Saw SM, Verhoeven VJ, Klaver CC, Moriyama M, Shinohara K, Kawasaki Y, Yamazaki M, Meuer S, Ishibashi T, Yasuda M, Yamashita H, Sugano A, Wang JJ, Mitchell P, Wong TY; META-analysis for Pathologic Myopia (META-PM) Study Group.

International photographic classification and grading system for myopic maculopathy. Am J Ophthalmol. 2015;159:877-883.
20. Yan YN, Wang YX, Yang Y, Xu L, Xu J, Wang Q, Yang X, Yang JY, Zhou WJ, Wei WB, Jonas JB. Long-term Progression and Risk Factors of Fundus Tessellation in the Beijing Eye Study. Sci Rep. 2018;8:10625.
21. Klein RM, Green S. The development of lacquer cracks in pathologic myopia. Am J Ophthalmol. 1988;106:282-285.
22. Spaide RF, Ohno-Matsui K, Yannuzzi LA. Pathologic myopia. Springer; 2014:17-376.
23. Oie Y, Ikuno Y, Fujikado T, Tano Y. Relation of posterior staphyloma in highly myopic eyes with macular hole and retinal detachment. Jpn J Ophthalmol. 2005;49:530-532.
24. Ohno-Matsui K, Yoshida T, Futagami S, Yasuzumi K, Shimada N, Kojima A, Tokoro T, Mochizuki M. Patchy atrophy and lacquer cracks predispose to the development of choroidal neovascularisation in pathological myopia. Br J Ophthalmol. 2003;87:570-573.
25. Wolf S, Balciuniene VJ, Laganovska G, Menchini U, Ohno-Matsui K, Sharma T, Wong TY, Silva R, Pilz S, Gekkieva M; RADIANCE Study Group. RADIANCE: a randomized controlled study of ranibizumab in patients with choroidal neovascularization secondary to pathologic myopia. Ophthalmology. 2014;121:682-692.
26. Ikuno Y, Ohno-Matsui K, Wong TY, Korobelnik JF, Vitti R, Li T, Stemper B, Asmus F, Zeitz O, Ishibashi T; MYRROR Investigators. Intravitreal Aflibercept Injection in Patients with Myopic Choroidal Neovascularization: The MYRROR Study. Ophthalmology. 2015;122:1220-1227.
27. Kasahara K, Moriyama M, Morohoshi K, Yoshida T, Simada N, Nagaoka N, Yokoi T, Shinohara K, Kaneko Y, Suga M, Ohno-Matsui K. Six-Year Outcomes of Intravitreal Bevacizumab for Choroidal Neovascularization in Patients with Pathologic Myopia. Retina. 2017;37:1055-1064.
28. Onishi Y, Yokoi T, Kasahara K, Yoshida T, Nagaoka N, Shinohara K, Kaneko Y, Suga M, Uramoto K, Ohno-Tanaka A, Ohno-Matsui K. Five-Year Outcomes of Intravitreal Ranibizumab for Choroidal Neovascularization in Patients with Pathologic Myopia. Retina. 2019;39:1289-1298.
29. Ruiz-Moreno JM, Montero JA, Araiz J, Arias L, García-Layana A, Carneiro A, Figueroa MS, Silva R. Intravitreal Anti-Vascular Endothelial Growth Factor Therapy for Choroidal Neovascularization Secondary to Pathologic Myopia: Six Years Outcome. Retina. 2015;35:2450-2456.
30. J Julien S, Biesemeier A, Taubitz T, Schraermeyer U. Different effects of intravitreally injected ranibizumab and aflibercept on retinal and choroidal tissues of monkey eyes. Br J Ophthalmol. 2014;98:813-825.
31. Ahn SJ, Park KH, Woo SJ. Subfoveal Choroidal Thickness Changes Following Anti-Vascular Endothelial Growth Factor Therapy in Myopic Choroidal Neovascularization. Invest Ophthalmol Vis Sci. 2015;56:5794-5800.
32. Tufail A, Narendran N, Patel PJ, Sivaprasad S, Amoaku W, Browning AC, Osoba O, Gale R, George S, Lotery AJ, Majid M, McKibbin M, Menon G, Andrews C, Brittain C, Osborne A, Yang Y. Ranibizumab in myopic choroidal neovascularization: the 12-month results from the REPAIR study. Ophthalmology y. 2013;120:1944-1945.
33. Panozzo G, Mercanti A. Optical coherence tomography findings in myopic traction maculopathy. Arch Ophthalmol. 2004;122:1455-1460.
34. Parolini B, Arevalo JF, Hassan T, Kaiser P, Rezaei KA, Singh R, Sakamoto T, Rocha J, Frisina R. International Validation of Myopic Traction Maculopathy Staging System. Ophthalmic Surg Lasers Imaging Retina. 2023;54:153-157.
35. Parolini B, Palmieri M, Finzi A, Besozzi G, Lucente A, Nava U, Pinackatt S, Adelman R, Frisina R. The new Myopic Traction Maculopathy Staging System. Eur J Ophthalmol. 2021;31:1299-1312.
36. Parolini B, Palmieri M, Finzi A, Besozzi G, Frisina R. Myopic Traction Maculopathy: A New Perspective on Classification and Management. Asia Pac J Ophthalmol (Phila). 2021;10:49-59.
37. Borley WE, Snyder AA. Surgical treatment of high myopia; the combined lamellar scleral resection with scleral reinforcement using donor eye. Trans Am Acad Ophthalmol Otolaryngol. 1958;62:801-802.
38. Curtin BJ. Scleral support of the posterior sclera. II. Clinical results. Am J Ophthalmol. 1961;52:853-862.
39. Schepens CL, Okamura ID, Brockhurst RJ. The scleral buckling procedures. I. Surgical techniques and management. AMA Arch Ophthalmol. 1957;58:797-811.
40. Tanaka T, Ando F, Usui M. Episcleral macular buckling by semirigid shaped-rod exoplant for recurrent retinal detachment with macular hole in highly myopic eyes. Retina. 2005;25:147-151.
41. Parolini B, Frisina R, Pinackatt S, Gasparotti R, Gatti E, Baldi A, Penzani R, Lucente A, Semeraro F. Indications and Results of a New L-Shaped Macular Buckle to Support a Posterior Staphyloma in High Myopia. Retina. 2015;35:2469-2482.
42. Akduman L. A Titanium Macular Buckle Implant Designed for an Easy Placement in Myopic Macular Holes. Retin Cases Brief Rep. 2022.
43. Akduman L, Serhat E, Artunay O. Macular Buckling for Myopia: A Novel Approach. Retina Today. 2023. https://retinatoday.com/articles/2023-mar/macular-buckling-for-myopia-a-novel-approach.
44. Sasaki H, Shiono A, Kogo J, Yomoda R, Munemasa Y, Syoda M, Otake H, Kurihara H, Kitaoka Y, Takagi H. Inverted internal limiting membrane flap technique as a useful procedure for macular hole-associated retinal detachment in highly myopic eyes. Eye (Lond). 2017;31:545-550.
45. Yuan J, Zhang LL, Lu YJ, Han MY, Yu AH, Cai XJ. Vitrectomy with internal limiting membrane peeling versus inverted internal limiting membrane flap technique for macular hole-induced retinal detachment: a systematic review of literature and meta-analysis. BMC Ophthalmol. 2017;17:219.
46. Kinoshita T, Onoda Y, Maeno T. Long-term surgical outcomes of the inverted internal limiting membrane flap technique in highly myopic macular hole retinal detachment. Graefes Arch Clin Exp Ophthalmol. 2017;255:1101-1106.
47. Parolini B, Palmieri M, Finzi A, Frisina R. Proposal for the management of myopic traction maculopathy based on the new MTM staging system. Eur J Ophthalmol. 2021;31:3265-3276.

Epithelial Inoculation After Small-Incision Lenticule Extraction (SMILE): A Case Report

Sibel Ahmet, Ahmet Kırgız, Fevziye Öndeş Yılmaz, Mehmet Özgür Çubuk, Nilay Kandemir Beşek

University of Health Sciences Türkiye, Beyoğlu Eye Training and Research Hospital, Clinic of Ophthalmology, İstanbul, Türkiye

Abstract

Epithelial ingrowth is a rare condition that is generally seen after laser *in situ* keratomileusis (LASIK) and has been reported in the literature in a small number of cases after small-incision lenticule extraction (SMILE) surgery. "Epithelial inoculation" should also be considered in patients presenting with decreased vision and an appearance similar to epithelial ingrowth in the early period after SMILE surgery. A 23-year-old woman presented to our clinic with a request for refractive surgery. Her manifest refractions were -7.50 -1.00 x 180° in the right eye and -7.25 -1.00 x 150° in the left eye, and best corrected distance visual acuity was 10/10 in both eyes. The SMILE procedure was performed with the Visumax femtosecond laser (Carl Zeiss Meditec AG). Slit-lamp examination at postoperative 1 week revealed a small grayish-white intrastromal opacity resembling epithelial ingrowth in the central optic axis of the right eye. Irrigation of the interface was performed with balanced salt solution using an irrigation cannula and the epithelial cluster was removed. The patient remained clinically stable 6 months after surgery and has experienced no recurrence. When epithelial inoculation is observed early after SMILE surgery, immediate irrigation of the interface appears to be an effective and safe treatment.

Keywords: Astigmatism, epithelial ingrowth, epithelial inoculation, LASIK, myopia, SMILE

Introduction

Small-incision lenticule extraction (SMILE) surgery has been used in the surgical treatment of refractive errors such as myopia and myopic astigmatism since 2008. Flapless removal of an intrastromal lenticule with SMILE has led to a paradigm shift in which the complications of traditional flap-based ablation methods can be avoided.[1,2] Epithelial ingrowth, a flap-related complication, is common after laser *in situ* keratomileusis (LASIK).[3] In contrast to LASIK, a small lateral incision ranging from 3 to 5 mm is made to remove the lenticule created in SMILE, so it is expected that interface epithelial ingrowth will be less likely.[4] However, in SMILE, epithelial cells can still be seeded into the interface by surgical instruments and epithelial cell proliferation can follow, leading to an ingrowth-like appearance. The result can be corneal irregularity and decreased vision, especially if the affected area is close to the visual axis.[5]

In this case report, we present a case of epithelial inoculation following SMILE surgery that was managed with interface irrigation.

Case Report

A 23-year-old female patient presented to our clinic with a request for refractive surgery. Her manifest refraction values were -7.50 -1.00 x 180° and -7.25 -1.00 x 150° in the right and left eyes, respectively. Best corrected distance visual acuity (BCVA) was 10/10 in both eyes. Central corneal thickness was 557 µm in the right and 548 µm in the left eye. Ocular and systemic histories were unremarkable. Ophthalmological examinations including corneal topography were normal in both eyes. Emmetropia was targeted and bilateral SMILE was planned for the patient.

The SMILE procedure was performed with the Visumax femtosecond laser (Carl Zeiss Meditec AG, Jena, Germany) under topical anesthesia (0.5% proparacaine hydrochloride; Alcaine;

Cite this article as: Ahmet S, Kırgız A, Öndeş Yılmaz F, Çubuk MÖ, Kandemir Beşek N. Epithelial Inoculation After Small-Incision Lenticule Extraction (SMILE): A Case Report. Turk J Ophthalmol 2023;53:313-317

Address for Correspondence: Sibel Ahmet, University of Health Sciences Türkiye, Beyoğlu Eye Training and Research Hospital, Clinic of Ophthalmology, İstanbul, Türkiye

E-mail: dr.sibelahmet@gmail.com **ORCID-ID:** orcid.org/0000-0002-1842-4077

Received: 02.10.2022 **Accepted:** 06.05.2023

DOI: 10.4274/tjo.galenos.2023.14825

Alcon Laboratories, Inc, Fort Worth, TX, USA; one drop in each eye). The cap diameter was 7.8 mm, with an intended thickness of 120 µm, and the optical zone in both eyes was 6.5 mm. Superotemporal lateral incisions 3 mm long were made in both eyes for lenticule extraction. The repetition rate was 500 kHz, and the pulse energy was 140 NJ. Both ocular areas were prepared for surgery. After proper centralization and corneal contact, incisions were made with the laser system without any complications. A Duckworth & Kent double-ended dissector with a bullet-shaped tip was used to enter the interface. Although there was no evidence of loose epithelium or corneal dystrophy on preoperative examination, penetration under the epithelium was observed even though the tip of the dissector was directed towards the interfacial area. After several unsuccessful attempts, it was possible to enter the interface without an epithelial defect and perform a proper dissection of the lenticule. The procedure was uneventful for the left eye.

In both eyes, the interface was irrigated with balanced salt solution (BSS) and the side cut was dried with a sponge. After this stage, the interface was checked in both eyes with the slit lamp of the device and there was nothing noticeable. We do not routinely use postoperative bandage contact lenses in our SMILE cases. Although there was no epithelial defect in the side cut area, we used them prophylactically in both eyes for epithelial ingrowth due to loose epithelium in this case.

On the same day, half an hour after the procedure, the interfaces of both eyes were checked by slit-lamp biomicroscopy. The interfaces of both eyes were transparent and no suspicious findings were observed.

The patient was treated topically with 0.5% moxifloxacin (Moxai; Abdi Ibrahim, Istanbul, Türkiye), loteprednol etabonate 0.5% (Lotemax; Bausch & Lomb, Florida, USA), and preservative-free artificial tears 4 times daily for 1 week postoperatively.

Uncorrected distance visual acuity (UDVA) was 6/10 in the right eye and 8/10 in the left eye on the first postoperative day. After removal of the bandage contact lenses, slit lamp examination of both eyes showed no epithelial defect in the lateral incision areas and the interfaces were clear.

At postoperative 1 week, UDVA was 2/10 in the right and 10/10 in the left eye. No results could be obtained from autorefractometer measurements in the right eye. Biomicroscopic examination revealed a small grayish-white intrastromal opacity similar to epithelial growth in the central corneal interface in the optic axis of the right eye which was not associated with the lateral incision. The opacity was also detectable with Cirrus HD (Carl Zeiss Meditec AG) optical coherence tomography (OCT) B-scan, and corneal topographic examination revealed a central irregularity immediately above the area of opacity (Figure 1). In order to determine the cause, the surgical recording was reviewed several times with the surgical team on the Visumax device and there was no manipulation that could lead to an epithelial defect. However, during the interfacial penetration phase, the patient's epithelium appeared to loosen when the dissector tip unexpectedly penetrated under the epithelium. Although precautions were taken by irrigating the interface and placing bandage contact lenses, it was concluded that a few invisible epithelial cells were introduced to the interface and multiplied there after repeated penetrations under the epithelium before entering the interface.

Since the lesion was on the optical axis and UDVA was affected, interface irrigation was performed with a diagnosis of "epithelial inoculation" due to repeated manipulation of loose epithelium. After dissection of the interface with the spoon tip of a double-ended dissector, the interface was irrigated with BSS by an irrigation cannula. During irrigation, it was observed that the epithelial cluster became mobile easily and detached from the interface (Figure 2). After making sure that there was no epithelial residue at the interface, the anterior surface of the cornea was rubbed towards the side cut with the back of the irrigation cannula to drain the fluid from the interface. The side

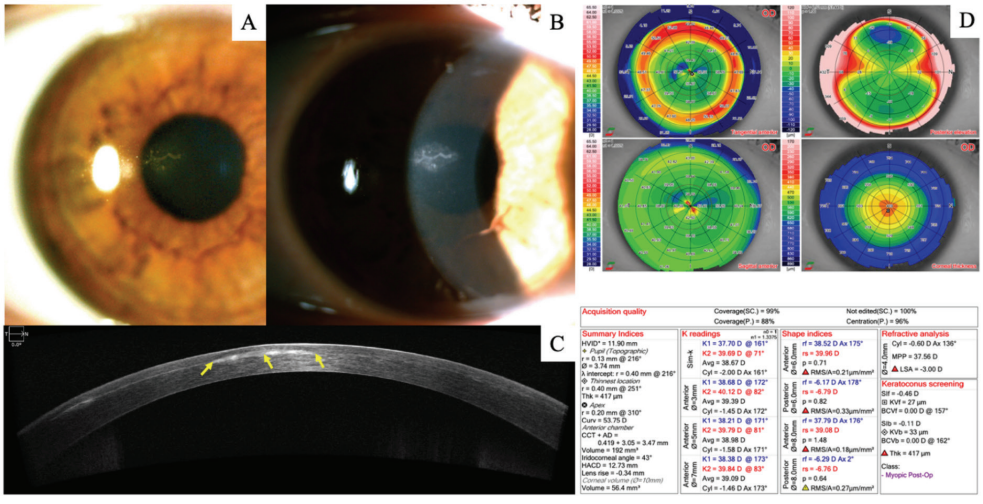

Figure 1. The right eye at postoperative 1 week. A, B) Irregularly circumscribed grayish-white opacities similar to epithelial ingrowth at the interface in the optical axis were observed on slit-lamp examination. C) Anterior segment optical coherence tomography showed increased hyperreflectivity at the interface limited to the central cornea (yellow arrows). D) Corneal steepening above the inoculation area and an irregular astigmatism-like appearance were observed on corneal topography

cut was dried with a cotton-tipped sponge. After irrigation, the patient was treated with topical 0.5% moxifloxacin (Moxai; Abdi Ibrahim, Istanbul, Türkiye), dexamethasone (Dexasine SE; LIBA, Kaysersberg, France), and preservative-free artificial tears 8 times a day for 1 day. The steroid and antibiotic drops were gradually tapered over 1 month. Treatment with artificial tears 4 times a day was planned for the following 6 months.

One day after interface irrigation, UDVA was 5/10 and CDVA was 10/10 (-1.00 -0.75 x 180°) in the right eye. On slit-lamp examination, the interface was hazy and smooth. A more regular map was observed on topography, while OCT imaging of the interface revealed no trace of hyperreflectivity due to epithelial deposition (Figure 3).

One month after refractive surgery, UDVA was 10/10 in both eyes. On slit-lamp examination, the interface was clear and smooth and a more regular corneal map was observed on topography of the right eye compared to the first postoperative day. On OCT imaging of the right eye, there was still no trace of hyperreflectivity due to epithelial deposition at the interface (Figure 4).

Discussion

Epithelium at the interface is frequently encountered as a postoperative complication in the form of epithelial ingrowth after femto-LASIK surgery.[6] Since SMILE does not require a corneal flap like LASIK, epithelial ingrowth is a rare postoperative complication.[7] The possible causes of epithelial cell migration to the interface during SMILE are varied: a) frequent instillation of topical anesthetic drops, resulting in a loose epithelium-like state, b) migration of corneal epithelium from the lateral incision to the interface, c) disruption of the epithelium close to the incision site and seeding of disrupted epithelial cells via severe and repetitive surgical manipulations,[5] and d) migration of epithelial cells to the interface through a fistula formed between the interface and epithelium by a vertical epithelial gas breakthrough.[8,9] Each of these may be the cause or multiple causes may coexist.

Loose epithelium that is not detected in the preoperative biomicroscopic evaluation may be encountered intraoperatively. During entry into the interface through the side cut, the dissector may be directed under the epithelium due to loose epithelium and surgical manipulations may increase during the operation. Therefore, with epithelial cells detached from the loose epithelium, interfacial inoculation can take place through a side incision. In the present case, while intending to enter the interface, the dissector went under the epithelium due to the presence of loose epithelium. Then, although the

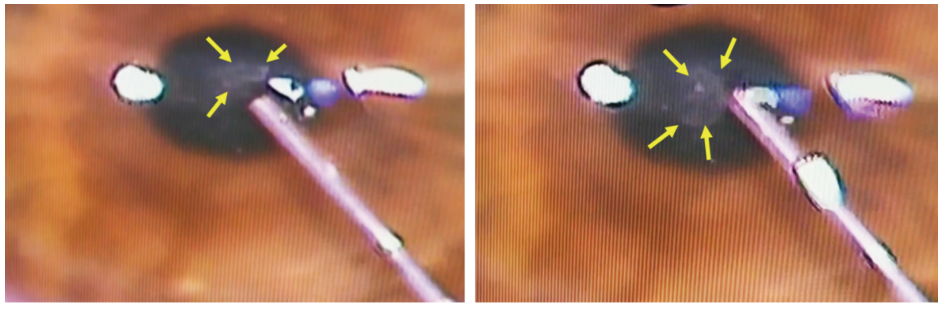

Figure 2. The interface was irrigated with balanced salt solution using an irrigation cannula. The gray epithelial accumulation became mobile and detached from the cornea as the interface was irrigated. Yellow arrows indicate the epithelial inoculation margins

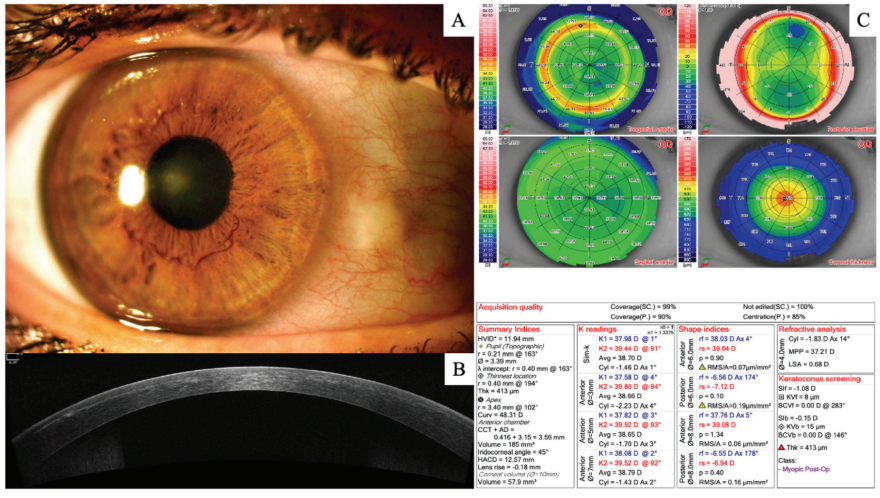

Figure 3. The right eye 1 day after interface irrigation. A) The epithelial ingrowth-like appearance disappeared, with only a slight haze remaining. B) Anterior segment optical coherence tomography imaging showed no hyperreflectivity. C) Corneal irregularity was significantly decreased on topography

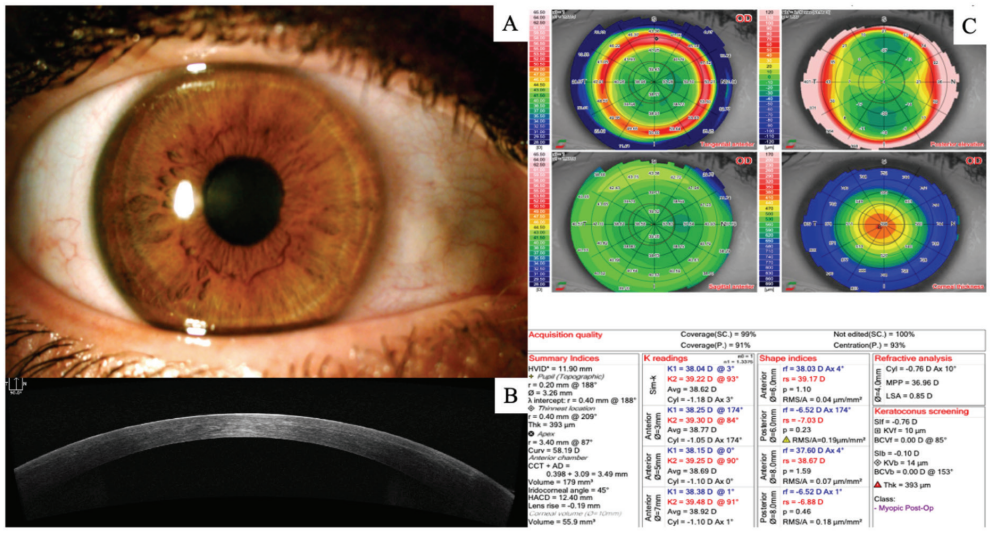

Figure 4. The right eye at postoperative 1 month. A) Slit-lamp examination showed the cornea is completely clear. B) Anterior segment optical coherence tomography imaging and C) corneal topography were completely normal

surgery proceeded correctly, the epithelial cells detached from this loose epithelium around the side cut were planted at the interface during lenticule dissection. The fact that the epithelial accumulation was distant from the incision site and not associated with the side cut supports the diagnosis of epithelial inoculation rather than ingrowth.

It is a common approach to observe epithelial ingrowth seen after LASIK without treatment. If the visual axis is affected, the surface becomes irregular, visual acuity is reduced, or stromal melting is observed, a more aggressive approach is required. Many treatment options have been described for epithelial ingrowth. The flap can be lifted and mechanically debrided, and adjuvant treatments such as mitomycin C or alcohol can be used. In addition, phototherapeutic keratectomy can be performed on the residual stromal bed after flap removal. Following these methods, the flap can be closed with sutures or tissue glue to prevent recurrence.[10] Although epithelial ingrowth is less common in SMILE, certain complications that affect the optical axis or reduce vision require treatment. Compared to LASIK, the epithelial infiltration area is relatively smaller in SMILE and therefore less aggressive methods may be sufficient.[5] Intervention is necessary when the optical axis is affected because it leads to an irregular ocular surface and reduced visual acuity. The treatment decision depends on the size of the epithelial ingrowth area, its connection with the side cut, and its distance from the side cut. In our case, the epithelial debris was easily detached and removed from the interface by irrigation and was not connected to the side cut, facts strongly suggestive of epithelial inoculation rather than ingrowth. Prompt action was taken as the condition was interfering with the optical axis and creating topographic irregularity. After irrigating the interface, a dramatic increase in visual acuity was observed which confirmed that our diagnosis and intervention were appropriate.

In conclusion, in the presence of loose epithelium that was not detected in the preoperative examination, as in our case, or when access is repeatedly attempted during the procedure, the interface should always be checked immediately after surgery with the slit lamp of the device or biomicroscope, and the patient should be followed closely after surgery. When epithelial inoculation occurs after SMILE, treatment is planned depending on factors such as the location of epithelial cells and the amount of epithelial proliferation, necrosis, or progression at the inoculation site. If epithelial inoculation is in the optic axis, interfacial irrigation and scraping may improve visual acuity and reduce topographically irregular astigmatism. As epithelial inoculation is observed early after SMILE surgery, immediate irrigation of the interface appears to be an effective and safe treatment.[5]

Ethics

Informed Consent: Obtained.

Peer-review: Externally peer-reviewed.

Authorship Contributions

Surgical and Medical Practices: A.K., F.Ö.Y., Concept: N.K.B., Design: M.Ö.Ç., Data Collection or Processing: S.A., Analysis or Interpretation: A.K., Literature Search: S.A., Writing: S.A.

Conflict of Interest: No conflict of interest was declared by the authors.

Financial Disclosure: The authors declared that this study received no financial support.

References

1. Sekundo W, Kunert KS, Blum M. Small incision corneal refractive surgery using the small incision lenticule extraction (SMILE) procedure for the correction of myopia and myopic astigmatism: results of a 6 month prospective study. Br J Ophthalmol. 2011;95:335-339.
2. Tăbăcaru B, Stanca S, Mocanu V, Zemba M, Stanca HT, Munteanu M. Intraoperative flap-related complications in FemtoLASIK surgeries performed

with Visumax® femtosecond laser: A ten-year Romanian experience. Exp Ther Med. 2020;20:2529-2535.
3. Sahay P, Bafna RK, Reddy JC, Vajpayee RB, Sharma N. Complications of laser-assisted *in situ* keratomileusis. Indian J Ophthalmol. 2021;69:1658-1669.
4. Shah R, Shah S, Sengupta S. Results of small incision lenticule extraction: All-in-one femtosecond laser refractive surgery. J Cataract Refract Surg. 2011;37:127-137.
5. Piccinini P, Vida RS, Piccinini R, Maiore I, Archer TJ, Carp GI, Reinstein DZ. Epithelial implantation treatment after small-incision lenticule extraction. J Cataract Refract Surg. 2020;46:636-640.
6. Li S Le, Chen J, Zhang HY, Li T, Lu Y. Treatment of epithelial ingrowth after laser in situ keratomileusis. Int J Ophthalmol. 2010;10:1224-1225.
7. Kamiya K, Takahashi M, Shoji N, Naruse S. Two cases of epithelial ingrowth after small incision lenticule extraction. Am J Ophthalmol Case Rep. 2020;19:100819.
8. de Rojas Silva MV, Tobío Ruibal A. New mechanism for epithelial ingrowth after small incision lenticule extraction: Vertical epithelial gas breakthrough. Eur J Ophthalmol. 2023;33:78-83.
9. Tok OY, Tok L, Atay IM, Argun TC, Demirci N, Gunes A. Toxic keratopathy associated with abuse of topical anesthetics and amniotic membrane transplantation for treatment. Int J Ophthalmol. 2015;8:938-944.
10. Fagerholm P, Molander N, Podskochy A, Sundelin S. Epithelial ingrowth after LASIK treatment with scraping and phototherapeutic keratectomy. Acta Ophthalmol Scand. 2004;82:707-713.

Tractional Retinal Detachment Related to Hemoglobin C Trait Retinopathy: A Case Report

Xavier Garrell-Salat, Claudia Garcia-Arumi, Yann Bertolani, Sandra Banderas García, Paul Buck, Jose Garcia-Arumi

Hospital Universitari Vall d'Hebron, Department of Ophthalmology, Barcelona, Spain

Abstract

Hemoglobin C (HbC) disease is an uncommon disease that is generally considered benign, causing only occasionally painless hematuria, osteomyelitis, and dental abnormalities. Ocular manifestations have rarely been described in these patients. Here we report a novel ophthalmological manifestation of the disease. A 20-year-old woman presented with progressive visual loss in her right eye due to tractional retinal detachment. The left eye was apparently normal, but wide-field fluorescence angiography showed mild peripheral ischemia with multiple vascular abnormalities. Vitrectomy was performed and the systemic workup revealed the presence of hemoglobinopathy C in heterozygous form. HbC disease can be sight-threating due to retinal proliferation, similar to sickle cell retinopathy. Patients affected with this disease should undergo regular surveillance. Ultra-wide angiography is a helpful examination to detect peripheral ischemia in the earlier stages.

Keywords: Hemoglobin C trait, sickle cell retinopathy, retinal detachment, tractional retinal detachment, case report

Introduction

Sickle cell retinopathy is a retinal disease that consists of multiple vascular phenomena that have been well described, including peripheral vascular obliteration, sea-fan neovascularization, and hemorrhages. These findings are a consequence of vaso-occlusion in the peripheral retina and have been associated with a variety of hemoglobinopathies such as sickle cell anemia and sickle-C disease.

Similar findings have been described in other hemoglobinopathies, such as hemoglobin C (HbC) disease, which can be present either in a homozygous or heterozygous state. Homozygous HbC disease is uncommon and most patients are asymptomatic, although it may cause moderate hemolytic anemia, splenomegaly, and microspherocytes.[1] Heterozygous HbC disease is more common, being present in 2-3% of the African-American population and 17-28% of the black population in West Africa.[2] Although this entity has traditionally been considered benign, only occasionally causing painless hematuria, osteomyelitis, and dental abnormalities, some reports have described a proliferative retinopathy in these patients.[3,4] We now describe an extreme case of tractional retinal detachment in a 20-year-old patient affected by heterozygous HbC disease.

Case Report

A 20-year-old female patient who was a native of Ghana residing in Barcelona for the last 3 years consulted the emergency department complaining of progressive visual impairment in her right eye for the last 4 months. She reported no personal medical history or ocular disease. Her visual acuity was hand motions in the right eye and Snellen 20/20 in the left eye. The anterior segment showed mild anterior chamber reaction and abundant cells in the anterior vitreous in her right eye. The left eye was completely normal. Intraocular pressure was 10 mmHg and 18 mmHg, respectively.

Cite this article as: Garrell-Salat X, Garcia-Arumi C, Bertolani Y, García SB, Buck P, Garcia-Arumi J. Tractional Retinal Detachment Related to Hemoglobin C Trait Retinopathy: A Case Report. Turk J Ophthalmol 2023;53:318-321

Address for Correspondence: Xavier Garrell-Salat, Hospital Universitari Vall d'Hebron, Department of Ophthalmology, Barcelona, Spain
E-mail: xaviergarrellsalat@gmail.com **ORCID-ID:** orcid.org/0000-0002-9947-1149
Received: 18.02.2023 **Accepted:** 15.06.2023

DOI: 10.4274/tjo.galenos.2023.48672

Fundoscopy of the right eye was difficult due to abundant vitreous haze but revealed a tractional retinal detachment in the posterior pole that extended beyond the vascular arcades, with an important area of fibrovascular proliferation in the superior temporal arch with sickle-shaped retinal folds towards the periphery and subretinal fibrotic tracts. In the lower region, two areas of proliferation with sickle-shaped folds were identified. In addition, a marked peripheral vascular attenuation was observed. Fluorescein angiography revealed vascular attenuation and peripheral vascular loops, showcasing severe peripheral ischemia. Increased contrast uptake without clear contrast leakage was observed in the area of fibrovascular proliferation (Figure 1). Fundoscopy of the left eye was apparently normal, but a detailed study of fluorescein angiography images showed mild peripheral ischemia with vascular abnormalities (Figure 2).

It was decided to perform vitreoretinal surgery in the right eye. A 23-gauge pars plana vitrectomy was performed with hyaloid dissection (induced posterior vitreous detachment). Traction zones were dissected with the vitreotome and the vitreoretinal proliferation was released with bimanual technique. Perfluorocarbon was injected, draining subretinal fluid and flattening the macula and lower retina. Traction persisted in the superior retina, so a superior retinotomy was performed from the 11 to 1 clock hours, after which the entire retina was flattened. Endolaser was applied around the superior retinotomy and silicone oil exchange was performed.

A complete workup study was initiated to identify the etiology of the case. Various entities were considered in the differential diagnosis, including sickle cell retinopathy, familial exudative vitreoretinopathy, peripheral vasculitis, and retinopathy of prematurity. Given the characteristics of the patient and the high probability of sickle cell retinopathy, a study of hemoglobinopathies was performed and revealed the presence of heterozygous HbC (38.5%), but no hemoglobin S (HbSC). The hematology department adopted a watch-and-see approach due to the benign nature of hemoglobinopathy C in heterozygous form.

After two years of follow-up, the retina remained attached under silicone oil and vision improved from hand motions to counting fingers at 50 cm in the patient's right eye. Furthermore, follow-up optical coherence tomography scans showed an important destructuring of the inner and outer layers of the retina, given the chronicity of the retinal detachment at presentation (Figure 3).

Discussion

HbC is a variant of normal hemoglobin A caused by the substitution of a single glutamic amino acid at position 6 on the β chain to a lysine. It is similar to HbSC, in which there is a substitution of glutamic acid in the same position by valine. Unlike in sickle cell disease, HbC does not polymerize under conditions of low oxygen tension, so it does not cause the same elongation of the erythrocyte's cell membrane producing the characteristic sickle shape. However, HbC can form precipitates in the form of crystals inside the erythrocytes, increasing their rigidity. This can lead to hyperviscosity and decreased red blood cell life span. Nevertheless, the vaso-occlusive crises seen in sickle cell disease do not happen in HbC disease, unless it is combined with HbSC.

Retinal ischemic phenomena related to the HbC trait have been described very rarely. Most reports have described peripheral vascular abnormalities including obliteration and vascular loops. There are also cases of sea-fan neovascularization similar to the retinopathy caused by sickle cell anaemia.[3,4] Welch and Goldberg[5] examined the ocular fundus of nine patients with HbC and found that three of them had retinal vascular changes such as venous tortuosity and obliteration of peripheral capillaries, suggesting that these findings might not be that rare. No ocular findings in homozygous HbC disease have been reported to date.

This case is the first to report a tractional retinal detachment related to the HbC trait. It is of particular interest that we could observe two different stages of the same disease in this patient: a more advanced stage with severe peripheral ischemia and tractional retinal detachment in the right eye versus an earlier phase with mild peripheral ischemia and secondary vascular anomalies in the left eye.

We believe the role of wide-field fluorescence angiography in this case should be highlighted. It is a relatively new

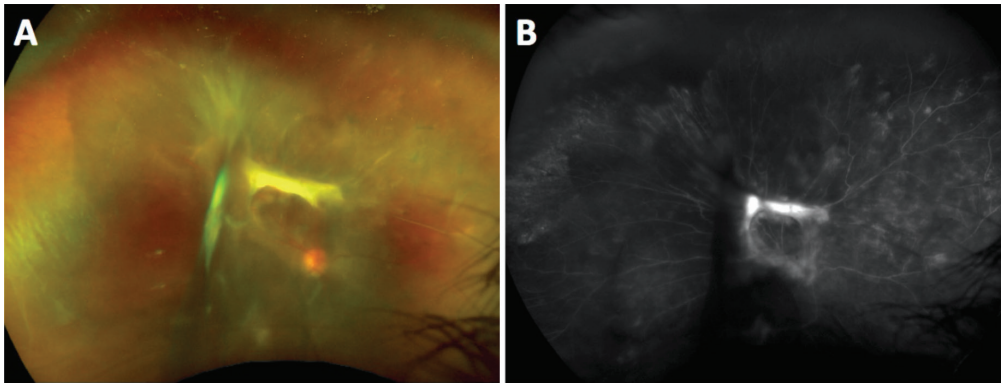

Figure 1. Wide-field retinography (A) of the right eye shows the presentation of the tractional retinal detachment, with prominent fibrovascular proliferations along the vascular arcades. Wide-field angiography (B) of the right eye shows marked ischemia and peripheral vascular attenuation

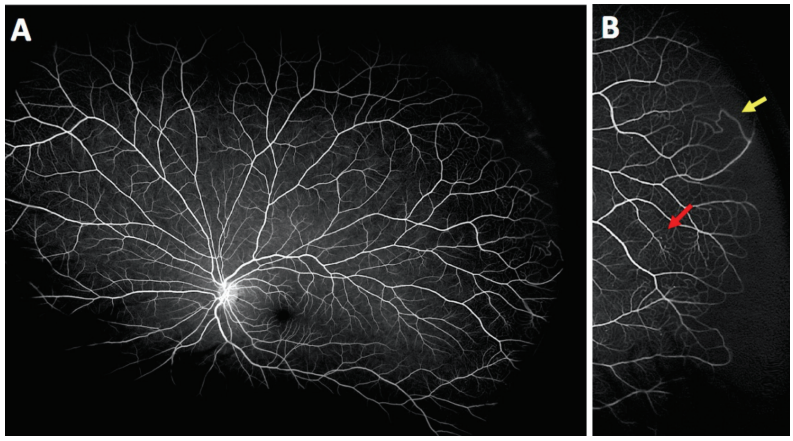

Figure 2. Wide-field angiography of the left eye (A) and a detailed view of the periphery (B) showing peripheral ischemia and vascular abnormalities, including vascular loops and telangiectasias (yellow arrow) and microaneurysms (red arrow)

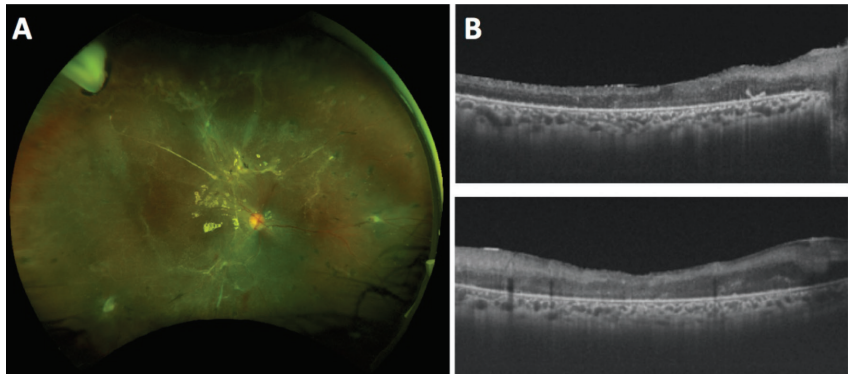

Figure 3. Wide-field retinography (A) and optical coherence tomography (OCT) (B) after surgery. The retina remains flattened with silicone oil as a tamponade, but marked atrophy can be seen on OCT, which indicates poor visual function and prognosis

technology that permits the study of vascular changes in the extreme periphery, such as in retinopathy of prematurity, sickle cell retinopathy, or peripheral vasculitis.[6,7,8] These changes may be missed during routine fundoscopy, whereas ultra-wide field fluorescein angiography permits a better study of this area.

In conclusion, proliferative retinopathy may be present not only in association with sickle cell disease, but also in other hemoglobinopathies in which there is no sickling. These hemoglobinopathies, such as the HbC trait, can be sight-threatening despite being generally considered a benign disease. The use of ultra-wide field fluorescein angiography may reveal a higher prevalence of this retinopathy than previously reported.

Ethics

Informed Consent: Obtained.

Peer-review: Externally and internally peer-reviewed.

Authorship Contributions

Surgical and Medical Practices: X.G-S., C.G-A., S.B.G., J.G-A., Concept: X.G-S., C.G-A., S.B.G., J.G-A., Design: X.G-S., C.G-A., Data Collection or Processing: X.G-S., Y.B., Analysis or Interpretation: X.G-S., Y.B., Literature Search: X.G-S., Y.B., Writing: X.G-S., C.G-A., Y.B., S.B.G., P.B., J.G-A.

Conflict of Interest: No conflict of interest was declared by the authors.

Financial Disclosure: The authors declared that this study received no financial support.

References

1. Ouzzif Z, El Maataoui A, Oukhedda N, Messaoudi N, Mikdam M, Abdellatifi M, Doghmi K. Hemoglobinosis C in Morocco : A report of 111 cas. Tunis Med. 2017;95:229-233.
2. Myerson RM, Harrison E, Lohmuller HW. Incidence and significance of abnormal hemoglobins; report of a series of 1,000 hospitalized Negro veterans. Am J Med. 1959;26:543-546.
3. Moschandreou M, Galinos S, Valenzuela R, Constantaras AA, Goldberg MF, Adams J 3rd. Retinopathy in hemoglobin C trait (AC hemoglobinopathy). Am J Ophthalmol. 1974;77:465-471.
4. Hingorani M, Bentley CR, Jackson H, Betancourt F, Arya R, Aclimandos WA, Bird AC. Retinopathy in haemoglobin C trait. Eye (Lond). 1996;10:338-342.
5. Welch RB, Goldberg MF. Sickle - cell hemoglobin and its relation to fundus abnormality. Arch Ophtalmol. 1966;75:353-362.

6. Mao J, Shao Y, Lao J, Yu X, Chen Y, Zhang C, Li H, Shen L. Ultra-wide-field imaging and intravenous fundus fluorescein angiography in infants with retinopathy of prematurity. Retina. 2020;40:2357-2365.
7. Alabduljalil T, Cheung CS, VandenHoven C, Mackeen LD, Kirby-Allen M, Kertes PJ, Lam WC. Retinal ultra-wide-field colour imaging versus dilated fundus examination to screen for sickle cell retinopathy. Br J Ophthalmol. 2021;105:1121-1126.
8. Kumar V, Chandra P, Kumar A. Ultra-wide-field angiography in the management of Eales disease. Indian J Ophthalnol. 2016;64:504-507.

Letter to the Editor Re: Bacillary Layer Detachment in Acute Vogt-Koyanagi-Harada Disease

Nazima Ali, Rachael Niederer, Aliyah Thotathil

University of Auckland, Department of Ophthalmology, Auckland, New Zealand

Keywords

Vogt-Koyanagi-Harada disease, bacillary layer detachment, visual outcome

Dear Editor,

We read with interest the recent paper by Ataş et al.[1] on bacillary layer detachment (BLD) in acute Vogt-Koyanagi-Harada (VKH) disease. We would like to share our experience in the Department of Ophthalmology of Te Whatu Ora in Auckland, New Zealand. Continuous variables are reported as median (interquartile range [IQR]) and categorical variables as number and percentage. Statistical analysis was performed on STATA (version 15; StataCorp LLC, College Station, TX).

We examined a series of 100 eyes (50 patients) with VKH diagnosed according to the revised diagnostic criteria proposed by the First International Workshop on VKH disease.[2] The median age was 42.0 years (IQR: 32.6-52.3 years) and 31 were female (62.0%). Median vision at presentation was 20/50 (IQR: 20/30-20/112). An initial optical coherence tomography (OCT) scan was available for 94 eyes. BLD was observed in 27 eyes (28.7%). Mean subretinal fluid height was 299 µm and a significant difference was observed between those with BLD (mean 741 µm) and without BLD (mean 120 µm) ($p<0.001$).

Patients with BLD also had poorer presenting vision (median 20/100 vs. 20/30, $p<0.001$). Median time to resolution of BLD was 29 days (IQR: 14-48 days) and the overall mean time to resolution of subretinal fluid (for the entire group) was 25 days (IQR: 16-47.5 days). The median follow-up duration for our cohort was 3.6 years (IQR: 1.6-8.8 years). Final visual acuity was 20/25 (IQR: 20/20-20/40). No significant difference was observed in final visual acuity between patients with and without BLD. Central choroidal thickness (CCT) was only available in 36 eyes. Median CCT was 373 µm (IQR: 306-498 µm). No significant difference was observed in those with and without BLD ($p=0.564$).

BLD has been described in multiple other ocular pathologies besides VKH, such as posterior scleritis, exudative age-related macular degeneration, ocular toxoplasmosis, and acute posterior multiple placoid pigment epitheliopathy.[3] The similarity

Cite this article as: Ali N, Niederer R, Thotathil A. Letter to the Editor Re: Bacillary Layer Detachment in Acute Vogt-Koyanagi-Harada Disease. Turk J Ophthalmol 2023;53:322-323

Address for Correspondence: Nazima Ali, University of Auckland, Department of Ophthalmology, Auckland, New Zealand
E-mail: nazima83@yahoo.com.sg **ORCID-ID:** orcid.org/0000-0002-7130-7910
Received: 02.04.2023 **Accepted:** 26.08.2023

DOI: 10.4274/tjo.galenos.2023.37739

between all these diseases is the primary involvement of the choroid and retinal pigment epithelium either because of pachychoroid disease, choroidal inflammation, or infiltration.

In BLD there is an intraretinal split at the photoreceptor inner segment myoid level, proximal to the external limiting membrane. It has been hypothesized that acute fluid shifts in the posterior pole force the fluid into the neuroretina via hydrostatic pressure, thus splitting the photoreceptors due to shearing forces.[4] The adhesion between photoreceptors and RPE cells may be disrupted by the accumulation of subretinal fibrin which increases the likelihood of fluid shift, leading to BLD due to hydrostatic pressure.[5] The suspended hyperreflective particles in the fluid within BLD, which are not commonly found in subretinal fluid, most likely represent inflammatory products, including fibrin, as well as photoreceptor debris.

Despite BLD being a common tomographic finding in eyes with acute VKH with poorer presenting visual acuity, it appears not to have a negative effect on the final visual outcome. Durmaz Engin and Saatci[4] reported that BLD is predominantly non-vision threatening and often exhibits spontaneous regression or rapid improvement with treatment. Several studies showed rapid restoration of the outer retinal architecture leading to good visual gain after resolution of fluid.[5,6]

Chronicity of the disease, severity of the anterior segment inflammation, and the number of recurrent episodes of inflammation increase the risk of late complications such as choroidal neovascular membrane, glaucoma, or cataract.[7] Read et al.[7] found that a greater number of complications, older age at onset, and worse visual acuity at presentation were associated with worse final visual acuity.

In conclusion, our observations support those of Ataş et al.[1] in demonstrating good visual outcome despite the presence of BLD. Further studies will be beneficial to examine other OCT features that are associated with poorer prognosis, increased complications (such as choroidal neovascular membrane), or recurrent disease.

Ethics

Peer-review: Internally peer-reviewed.

Authorship Contributions

Surgical and Medical Practices: N.A., R.N., Concept: R.N., Design: N.A., R.N., Data Collection or Processing: A.T., Analysis or Interpretation: N.A., R.N., Literature Search: N.A., A.T., Writing: N.A., R.N.

Conflict of Interest: No conflict of interest was declared by the authors

Financial Disclosure: The authors declared that this study received no financial support.

References

1. Ataş F, Kaya M, Saatci AO. Bacillary Layer Detachment in Acute Vogt-Koyanagi-Harada Disease. Turk J Ophthalmol. 2022;52:400-404.
2. Read RW, Holland GN, Rao NA, Tabbara KF, Ohno S, Arellanes-Garcia L, Pivetti-Pezzi P, Tesla HH, Usui M. Revised diagnostic criteria for Vogt–Koyanagi– Harada disease: report of an international committee on nomenclature. Am J Ophthalmol. 2001;131:647-652.
3. Mehta N, Chong J, Tsui E, Duncan JL, Curcio CA, Freund KB, Modi Y. Presumed foveal bacillary layer detachment in a patient with toxoplasmosis chorioretinitis and pachychoroid disease. Retin Cases Brief Rep. 2021;15:391-398.
4. Durmaz Engin C, Saatci AO. The revival of an old term with optical coherence tomography: Bacillary layer detachment. Eur Eye Res. 2022;2:180-188.
5. Cicinelli MV, Giuffré C, Marchese A, Jampol LM, Introini U, Miserocchi E, Bandello F, Modorati GM. The Bacillary Detachment in Posterior Segment Ocular Diseases. Ophthalmol Retina. 2020;4:454-456.
6. Ramtohul P, Engelbert M, Malclès A, Engelbert M, Malclès A, Gigon E, Miserocchi E, Modorati G, Cunha de Souza E, Besirli CG, Curcio CA Freund KB. Bacillary layer detachment: multimodal imaging and histologic evidence of a novel optical coherence tomography terminology: literature review and proposed theory. Retina. 2021;41:2193-2207.
7. Read RW, Rechodouni A, Butani N, Johnston R, Labree LD, Smith RE, Rao NA. Complications and prognostic factors in Vogt-Koyanagi-Harada disease. Am J Ophthalmol. 2001;131:599-606.